# CHARACTERIZING CHEMICAL TRANSPORT OF OZONE AND FINE PARTICLES IN THE GREAT LAKES REGION

by

Scott N. Spak

A dissertation submitted in partial fulfillment of

the requirements for the degree of

Doctor of Philosophy

(Atmospheric & Oceanic Sciences)

at the

UNIVERSITY OF WISCONSIN-MADISON

2009

**Abstract**

CHARACTERIZING CHEMICAL TRANSPORT OF OZONE AND FINE PARTICLES IN THE GREAT LAKES REGION

Scott N. Spak

Under the supervision of Assistant Professor Tracey Holloway

At the University of Wisconsin-Madison

This dissertation presents a science framework relevant to evaluating impacts of land use policy scenarios, energy technologies, and climate on urban and regional air quality. Emerging from collaboration with urban planners, this work provides a means for employing atmospheric chemical transport modeling to understand environmental ramifications of long-term, spatially disaggregated changes in population and automobile emissions at the census tract level, and to assess the sensitivity of these changes to densification strategies. Toward these goals, the framework is used to evaluate model skill in resolving contemporary characteristics of ozone ($O_3$) and speciated fine particles ($PM_{2.5}$) in the Great Lakes region of North America, and to quantitatively explore meteorological processes that bring about observed features of these pollutants in the region.

The Great Lakes was chosen due to a population concentrated in sprawling metropolitan areas, consistently high and widespread pollutant burdens, and seasonal effects of the lakes on the atmosphere. In annual simulation at 36 km resolution, the

Community Multiscale Air Quality model is evaluated using speciated $PM_{2.5}$ measurements taken at regulatory monitoring networks orientated to sample urban, rural, and remote areas. Performance relative to ad-hoc regional modeling goals and prior studies is average to excellent for most species throughout the year. Both pollution episodes and seasonality are captured. The Great Lakes affect pollution seasonality: strong winds advect aerosols around the deep marine boundary layer to lower surface $PM_{2.5}$ in fall and winter, while $O_3$ over the lakes is enhanced throughout the year, driven by temperature in the cool seasons and lake breeze circulation in spring and summer.

Simulations confirm observational evidence that rural and small-city sources are responsible for most regional $PM_{2.5}$. Sensitivities to urban and rural reductions are of comparable magnitude on a percentage basis. Higher horizontal resolution is necessary to capture changes in urban-suburban-rural pollution gradients, given the non-linear $O_3$ response to emissions changes in $NO_x$-limited urban environments (where vehicle $NO_x$ reductions increase $O_3$) vs. VOC-limited rural environments (where reductions decrease $O_3$). Densification scenarios produce small-scale responses. $O_3$ response in the suburbs is of opposite sign to $O_3$ response in urban cores, while emissions reductions consistently reduce $PM_{2.5}$.

# Table of Contents

# Chapter 1. Introduction

The Laurentian Great Lakes of North American contain 95% of the surface fresh water in the United States and host as nearby residents about 10% of the U.S. population and 30% of the Canadian population. On the U.S. side, more than 65% of this population resides in the 11 largest metropolitan areas in the region, each with more than 500,000 people. These population centers contribute high levels of anthropogenic emissions, which interact with the complex meteorology associated with the large lakes, such that the highest regionally dispersed concentrations of aerosol nitrate ($NO_3^-$), sulfate ($SO_4^{2-}$), and fine particles ($PM_{2.5}$) in North America are found in the region. Lake effect meteorology further influences summertime formation and transport of ozone ($O_3$) to such a degree that nearly all lakeshore counties along Lake Michigan are in violation of the National Ambient Air Quality Standard (NAAQS) for $O_3$ [*USEPA*, 2008] (Figure 1-1). Many urban counties are also in exceedance of the NAAQS for $PM_{2.5}$ (Figure 1-2.) The Great Lakes region thus offers an excellent study area for examining the impact of lake-effect processes on regional atmospheric chemical transport and air quality. Understanding the chemical and meteorological processes controlling these pollutants allows for more efficient policy design for emissions regulations, improved air quality forecasting, and broader understanding of atmospheric chemical processes in coastal environments.

Yet the study of air pollution in the Great Lakes region has been highly asymmetric with regard to both the species of interest, the season, and the methods employed. The impacts of Great Lakes meteorology on the chemical transport of $O_3$ in its peak summer season have been thoroughly documented in numerous field campaigns [e*Dye et al.*, 1995; *Lennartson and Schwartz*, 2002; *Eschel and Bernstein*, 2006; *Hastie et al.*, 1999] and numerical modeling studies [*Sillman et al.*, 1993;*Fast and Heilman*, 2003, 2005], but the influences of the Lakes on the complete annual seasonality of $O_3$ have never been described in the peer-reviewed literature.

More than 40 sites in the region conduct routine observations of aerosol speciation, several hundred sites monitor aerosol mass concentrations, and numerous measurement and chemical mass balance source apportionment studies [*Lee et al.*, 2003; *Rao et al.*, 2003; *Kerr et al.,* 2004, *Sheesley et al.*, 2004; *Kim et al.*, 2005, 2007; *Buzcu-Guven et al.,* 2007, *Rizzo and Scheff*, 2007; *Zhao and Hopke*, 2006; *Zhao et al.*, 2007] have characterized aerosols and their sources in great detail. However, with the exception of regulatory modeling [e.g. *Baker*, 2006, 2007] that is rarely compiled into reports, the region has never been the focus of an aerosol chemical transport model (CTM) study; merely included in larger domains in global and regional modeling [e.g. *Karydis et al.*, 2007]. Moreover, the impacts of lake effect meteorology on aerosols have not been explored, with the exception of a single episodic tracer study [*Harris and Kotamarthi,* 2005] over Chicago and southern Lake Michigan. A consistent regional characterization of chemical transport and a better understanding of the transport processes that lead to

observed conditions would fill in these gaps in the knowledge base and integrate the results from studies of isolated episodes, chemical species, and locations into a cohesive body of knowledge.

One important outcome of better characterizing air pollution in the Great Lakes region, and the extent to which it is influenced by lake effect meteorology, is that it can provide a point of reference from which to estimate potential future air quality conditions, and how they response to long-term changes local activities, technology, global climate, intercontinental pollution transport. Given the importance of $O_3$ and fine particles on human health, their roles as climate forcing agents, and the close links between human economic activities and pollutant emissions, projections of future air pollution at the regional scale, informed by a characterization of the present state, would be very valuable for long-range planning. However, regional projections to date, in the Great Lakes region and elsewhere, and typically focused exclusively on $O_3$ [*Hogrefe et al.*, 2004; *Leung et al.*, 2005; *Kunkel et al.*, 2007; *Steiner et al.*, 2006; *Tao et al.*, 2007] have been limited to assessments of linear changes in emissions, maintaining the same relative profiles of emitting activities and emitted species, or to the application of national-level scenarios designed for use in global climate modeling.

These simplifications are also reflected in the emissions inventories that feed present-day chemical transport modeling activities. Despite current horizontal CTM resolutions of 1 km to 40 km, emissions in the U.S., where such data is collected and

estimated more regularly and more rigorously than anywhere else, is only reported at the county level at best. Area source emissions are often estimated at the state level and allocated to counties through a top-down modeling process, with county-level estimates then disaggregated by population or other surrogate information. This approach has met the needs of national regulatory modeling [e.g. *USEPA*, 2005] and in air quality forecasting [*Mathur et al*., 2008] to date, as most populous counties are roughly the size of a 36 km x 36 km gridcell. State and regional planning modeling at 12 km has highlighted deficiencies in this coarse spatial scale, and led the Midwest Regional Planning Office to develop their own systems for estimating emissions in certain sectors where higher-resolution data are available [*LADCO*, 2007].

Uncertainties in emissions [*Frost et al*, 2006; *Hudman et al*., 2008] currently contribute errors—whether biases or offsetting errors—that obscure the true performance of CTMs in simulating real-world processes for even if the chemistry and physics are correct, errors in the location, timing, or speciation of emissions lead to errors in chemical transport simulation. Therefore, both science and policy analysis would be better served by the implementation of consistent bottom-up methods for estimating area source emissions, capable of describing current conditions and projecting spatial and temporal changes related to emitting activities. This would clearly be a "best practice" for regional modeling, but is not yet standard practice due to the absence of proven methodologies, leading the U.S. EPA in 2004 to fund eight research and development nprojects for developing methods related to "Regional Development, Population Trend,

and Technology Change Impacts on Future Air Pollution Emissions" under the Science to Achieve Results program. In one of these studies, *Projecting the Impact of Land Use and Transportation on Future Air Quality in the Upper Midwestern United States (PLUTO)*, we set out to develop a modeling system capable of generating "bottom-up" census tract-level emissions projections linking land use policy to driving patterns. We integrated a census-tract level land use and vehicle travel modeling framework and a mobile source emissions model, which we then used to evaluate the sensitivity of future primary pollutant emissions and resultant $O_3$ and $PM_{2.5}$ changes to different land development and population migration scenarios in six states in the Great Lakes region.

For my doctoral research, **I have sought to improve our understanding of atmospheric chemical transport of ozone and aerosols in the Great Lakes region, and to explore the use of novel techniques for identifying potential impacts of changes in global climate and regional land use on regional climate and air quality**. This dissertation is presented in four core chapters, each representing an independent experiment or a cohesive group of experiments. The work described was conducted in collaboration with colleagues at the University of Wisconsin-Madison, Columbia University, the Georgia Institute of Technology, the University of Illinois at Urbana-Champaign, NASA Goddard Institute for Space Sciences, and Texas Tech University.

The central goal of this dissertation is to use document the present state of atmospheric chemistry of the Great Lakes region, to quantitatively explore processes that

give rise to it, and to identify the system's response to potential changes. The only way to address all of these questions with a single consistent approach is through numerical modeling, so this dissertation relies heavily on modeling as the primary tool for inquiry. In Chapter 2, I discuss the challenges in modeling regional-scale chemical transport, and explain the choices I have made in considering these challenges and constructing a modeling platform suitable for use in answering my research questions. I describe in detail the model configuration the sources and processing of all input data.

I characterize the current state of chemical transport in the region in Chapter 3. In identifying the seasonality and spatial distribution of speciated aerosols, I conduct a chemical transport model performance evaluation focused exclusively on conditions in this region, introducing new methods of time-series analysis for evaluating the representation of model processes in addition to concentrations. This chapter is currently in press at the *Journal of Geophysical-Atmospheres*.

With this knowledge on the state of the atmospheric system and the ability of my modeling system to represent it, Chapter 4 uses chemical transport modeling to identify influences of lake effect meteorology on the seasonality of $O_3$ and fine particles in the Great Lakes region.

In Chapter 5, I leverage the results of Chapters 3 and 4 to model the impacts of a series of fixed and scenario-based emissions perturbations on air pollution in six states in

the Upper Midwest. In the process, I also explore the impacts of spatial resolution on CTM modeling of linear and non-linear physical and chemical processes, which had often been dismissed in prior studies.

Chapter 6 presents novel methods for analyzing potential future changes in climate and air quality. This chapter includes excerpts from two papers published in *Journal of Geophysical-Atmospheres* [*Spak et al.*, 2007 and *Holloway et al.*, 2008]. both of which employ statistical downscaling in support of integrated assessments of climate, air quality, and human health. The first seeks to assess uncertainty in statistically and dynamically modeled regional and local climate response to global climate change. The second applies statistical downscaling to assess climate change impacts on $O_3$, and was conducted alongside a CTM study as part of the Chicago Climate Impacts Report (http://www.chicagoclimateaction.org/pages/research___reports/48.php), which formed the scientific basis for the City of Chicago Climate Action Plan. These experiments provide additional measures of confidence in the ability of the dynamical models I employed to adequately simulate potential states of the atmospheric system, such that they are not merely "tuned" to observed states.

I summarize the overall results of this dissertation in the concluding chapter, emphasizing policy-relevant findings. I also reflect on the unique methodological requirements that arise when conducting regional climate and air quality modeling in long-term policy analysis and integrated assessment, explore their strengths and

limitations in this capacity, and suggest new standards for best practices based on my experiences.

**References**

Baker, K. (2006), Photochemical Model Performance for PM2.5 Sulfate, Nitrate, Ammonium, and pre-cursor species SO2, HNO3, and NH3 at Background Monitor Locations in the Central and Eastern United States, Presentation to the 5th annual CMAS Conference, Research Triangle Park, NC, 16 October 2006.

Baker, K. (2007), Source Apportionment Results for PM2.5 and Regional Haze at Receptors in the Great Lakes Region. Lake Michigan Air Directors Consortium, Des Plaines, Illinois.

Buzcu-Guven, B., S.G. Brown, A. Frankel, H.J. Hafner, and P.T. Roberts (2007), Analysis and apportionment of organic carbon and fine particulate matter sources at multiple sites in the Midwestern United States, *J. Air Waste Manag. Assoc.*, 57(5), 606-619.

Dye, T.S., P.T. Roberts, and M.E. Korc (1995), Observations of Transport Processes for Ozone and Ozone Precursors during the 1991 Lake Michigan Ozone Study, *J. Appl. Met.*, 34(8), 1877–1889, doi: 10.1175/1520-0450(1995)034<1877:OOTPFO>2.0.CO;2.

Fast, J.D., and W.E. Heilman (2003), The Effect of Lake Temperatures and Emissions on Ozone Exposure in the Western Great Lakes Region, *J. Appl. Meteor.*, 42, 1197–1217, doi: 10.1175/1520-0450(2003)042<1197:TEOLTA>2.0.CO;2.

Fast, J.D., and W.E. Heilman (2005), Simulated sensitivity of seasonal ozone exposure in the Great Lakes region to changes in anthropogenic emissions in the presence of interannual variability, *Atmos. Environ.*, 39, 5291-5306, doi:10.1016/j.atmosenv.2005.05.032.

Frost, G.J., S. A. McKeen, M. Trainer, T.B. Ryerson, J.A. Neuman, J.M. Roberts, A. Swanson, J.S. Holloway, D.T. Sueper, T. Fortin, D.D. Parrish, F.C. Fehsenfeld, F. Flocke, S.E. Peckham, G.A. Grell, D. Kowal, J. Cartwright, N. Auerbach, and T. Habermann (2006), Effects of changing power plant NOx emissions on ozone in the eastern United States: Proof of concept, *J. Geophys. Res.*, 111, D12306, doi:10.1029/2005JD006354.

Harris, L., and V.R. Kotamarthi (2005), The Characteristics of the Chicago Lake Breeze and Its Effects on Trace Particle Transport: Results from an Episodic Event Simulation, J. *Appl. Met.*, 44(11), 1637–1654, doi: 10.1175/JAM2301.1.

Hastie D.R., J. Narayan, C. Schiller, H. Niki, P.B. Shepson, D.M.L. Sills, P.A. Taylor, W.J. Moroz, J.W. Drummond, N. Reid, R. Taylor; P.B. Roussel, and O.T. Melo (1999), Observational Evidence for the Impact of the Lake Breeze Circulation on Ozone Concentrations in Southern Ontario, *Atmos. Environ.*, 33, 323-335.

Holloway, T., S.N. Spak, D.J. Barker, M.P. Bretl, K. Hayhoe, J. Van Dorn, D. Wuebbles (2008), Change in Ozone Air Pollution over Chicago associated with Global Climate Change, *J. Geophys. Res*, in press, doi:10.1029/2007JD009775.

Hudman, R.C., L. T. Murray, D. J. Jacob, D. B. Millet, S. Turquety, S. Wu, D. R. Blake, A. H. Goldstein, J. Holloway, and G. W. Sachse (2008), Biogenic versus anthropogenic sources of CO in the United States, *Geophys. Res. Lett.*, 35, L04801, doi:10.1029/2007GL032393.

Karydis, V. A., A. P. Tsimpidi, and S. N. Pandis (2007), Evaluation of a three-dimensional chemical transport model (PMCAMx) in the eastern United States for all four seasons*, J. Geophys. Res.*, 112, D14211, doi:10.1029/2006JD007890.

Kerr .SC., J.J. Schauer, and B. Rodger (2004), Regional haze in Wisconsin: sources and the spatial distribution, *J. Env. Eng. Sci.,* 3(3), 213-222, doi: 10.1139/S04-003.

Kim, E., P.K. Hopke, D.M Kenski, and M. Koerber (2005), Sources of fine particles in a rural Midwestern area, *Environ. Sci. Tech.*, 39, 4953-4960, doi: 10.1021/es04907749.

Kim, M., S.R. Deshpande, and K.C. Crist (2007), Source apportionment of fine particulate matter (PM2.5) at a rural Ohio River Valley site, *Atmos. Environ.*, 41, 9231–9243, doi:10.1016/j.atmosenv.2007.07.061.

Kunkel, K. E., H.-C. Huang, X.-Z. Liang, J.-T Lin, D. Wuebbles, Z. Tao, A. Williams, M. Caughey, J. Zhu, and K. Hayhoe (2007), Sensitivity of future ozone concentrations in the Northeast U.S. to regional climate change, *Mitigation and Adaptation Strategies for Global Change*.

LADCO (2007), 2005 Base M3/Round 5 Emissions Report. Lake Michigan Air Directors Consortium, Des Plaines, Illinois.

Lee, P.K.H., J.R. Brook, E. Dabek-Zlotorzynska, and S.A. Mabury (2003), Identification of the major sources contributing to PM2.5 observed in Toronto, *Environ. Sci. Tech.*, 37(21), 4831-4840, doi: 10.1021/es026473i S0013-936X(02)06473-8.

Lennartson, G.J., and M.D. Schwartz (2002), The lake breeze-ground-level ozone connection in eastern Wisconsin: a climatological perspective, *Int. J. Climatol.*, 22(11), 1347-1364, doi: 10.1002/joc.802.

Leung, L. R. and W. I. Gustafson Jr. (2005), Potential regional climate change and implications to U.S. air quality, *Geophys. Res. Lett.*, 32, L16711, doi:10.1029/2005GL022911.

Mathur, R., S. Yu, D. Kang, and K.L. Schere (2008), Assessment of the wintertime performance of developmental particulate matter forecasts with the Eta-Community Multiscale Air Quality modeling system, *J. Geophys. Res.*, 113(D2), D02303, doi:10.1029/2007JD008580.

Rao, V., N. Frank, A. Rush, and F. Dimmick (2003), Chemical speciation of PM2.5 in urban and rural areas in national air quality and emissions trends report. /http://www.epa.gov/air/airtrends/aqtrnd03S.

Rizzo, M.J., and P.A, Scheff (2007), Fine particulate source apportionment using data from the USEPA speciation trends network in Chicago, Illinois: Comparison of two source apportionment models, *Atmos. Environ.*, 41(29), 6276-6288, doi:10.1016/j.atmosenv.2007.03.055

Sheesley, R. J., J. J. Schauer, E. Bean, and D. Kenski (2004), Trends in Secondary Organic Aerosol at a Remote Site in Michigan's Upper Peninsula, *Env. Sci. Tech.*, 38, 6491-6500, doi: 10.1021/es049104q.

Sillman, S., P. J. Samson, and J. M. Masters (1993), Ozone Production in Urban Plumes Transported Over Water: Photochemical Model and Case Studies in the Northeastern and Midwestern United States, *J. Geophys. Res.*, 98:12687-12699.

Spak, S.N., T. Holloway, B. Lynn, R. Goldberg (2007), A Comparison of Statistical and Dynamical Downscaling for Surface Temperature in North America, *J. Geophys. Res.*,, 112, D08101, doi:10.1029/2005JD006712.

Steiner, A. L., S. Tonse, R. C. Cohen, A. H. Goldstein, and R. A. Harley (2006), Influence of future climate and emissions on regional air quality in California, *J. Geophys. Res.*, 111, D18303, doi:10.1029/2005JD006935.

Tao, Z., A. Williams, H.-C. Huang, M. Caughey, and X.-Z. Liang (2007), Sensitivity of U.S. surface ozone to future emissions and climate changes, *Geophys. Res. Lett.*, 34, L08811, doi:10.1029/2007GL029455,.

US EPA (2008), Nonattainment Areas Map - Criteria Air Pollutants, effective date of nonattainment designations June 2008, available at http://www.epa.gov/air/data/nonat.html?us~USA~United%20States.

Zhao, W.X., P.K. Hopke, and L.M. Zhou (2007), Spatial distribution of source locations for particulate nitrate and sulfate in the upper-midwestern United States, *Atmos. Environ.*, 41(9), 1831-1847, doi: 10.1016/j.atmosenv.2006.10.060.

Zhao, W.X., and P.K. Hopke (2006), Source investigation for ambient PM2.5 in Indianapolis, IN, *Aerosol Sci. Tech.*, 40(10), 898-909, doi:10.1080/02786820500380297.

## Figures

### Figure 1-1. Counties in Nonattainment for the U.S. 8-hour Ozone Standard, 2008

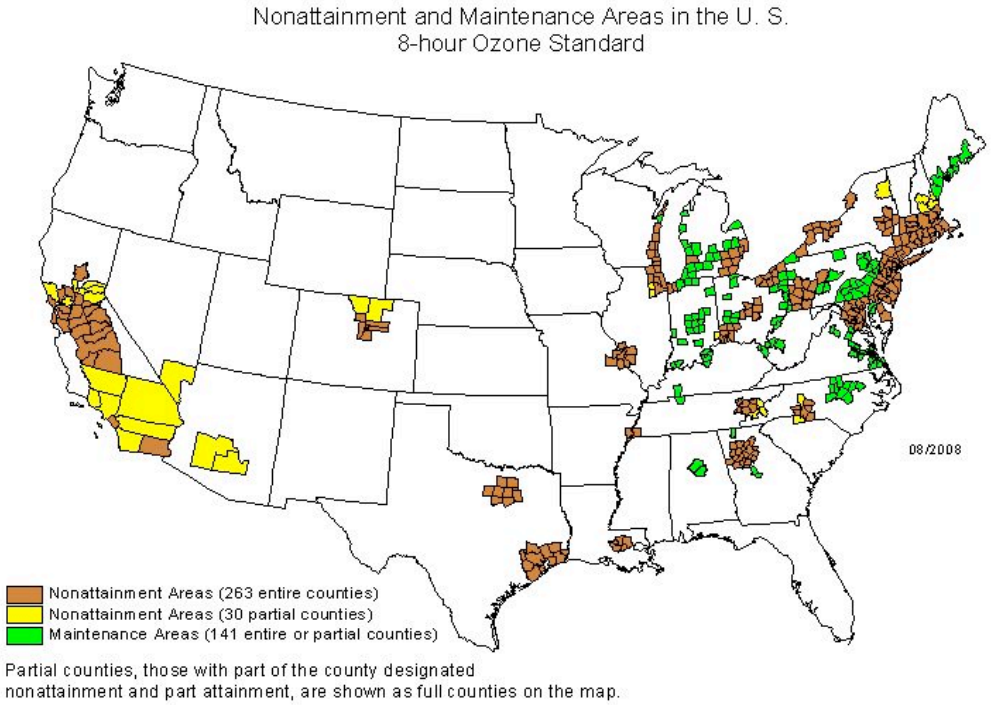

**Figure 1-2. Counties in Nonattainment for the U.S. $PM_{2.5}$ Standard, 2008**

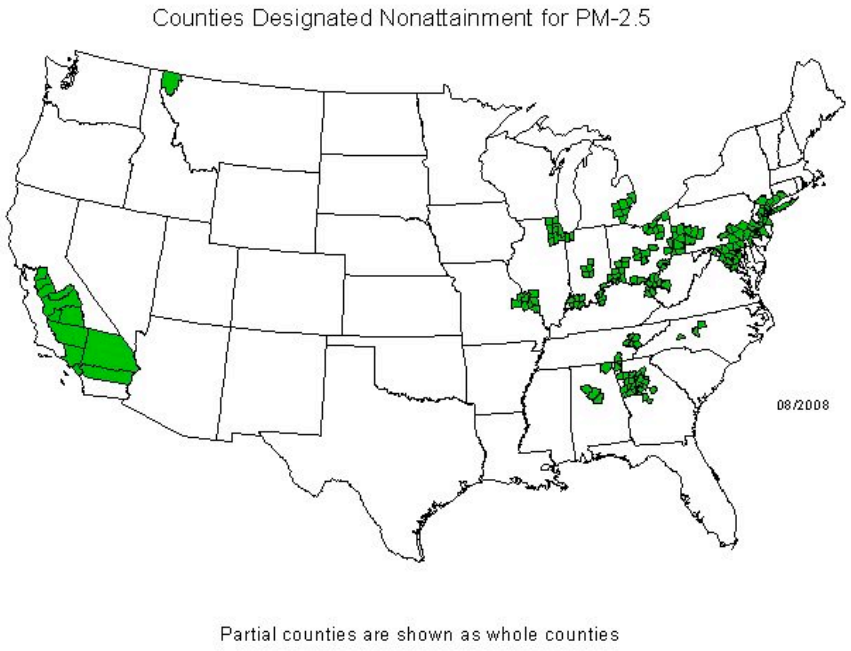

# Chapter 2. Methods and Data

## 2.1. Introduction

The many strengths of chemical transport models align well with my experimental needs. Model output from a CTM provides a full three dimensional analysis of all relevant atmospheric conditions and every modeled species, transcending the limited spatial "fetch" of in-situ observations and the temporal and technological limitations of remote sensing. Despite rapid improvements [e.g. *Kim et al.*, 2007; *Liu et al.*, 2007, remote sensing instruments cannot yet identify aerosol speciation, and instruments and techniques capable of retrieving vertical profiles of gas-phase species and aerosol physical properties are rarely available on the same platform. Thus, at present, remote sensing is limited to the identification of the state of certain species at certain places and times. In contrast, CTMs provide not only the full atmospheric state and its evolution, but can be also identify—through online process analysis, adjoint models, or forward sensitivity calculations—the conditions that influence the state and evolution of any part of the system at any place and time. Most importantly, while observational networks are capable of identifying important chemical transport processes [e.g. *Sickles and Shadwick*, 2007], CTMs provide the only process-based means for evaluating the impacts of potential future changes in emissions on atmospheric composition. Therefore, for identifying the sensitivity of pollution problems to widespread changes in technology-specific emissions control technologies or changes in

the patterns of economic activities and land use that lead to anthropogenic emissions demands the use of CTMs.

However, taking advantage of the strengths of CTMs is a challenging process, because adequately modeling the full state of regional atmospheric chemical transport in polluted environments with reactive constituents and complex local climatic influences—as in the Great Lakes region—requires pairing a "good" model with "good" data.

We note that there are many questions in atmospheric chemical transport that can be approached with simple dispersion modeling of inert tracer species, such as the cross-tropopause exchange of $O_3$ [e.g. *Büker et al.*, 2005], or the spatial extent of primary particle polluion due to emissions from large urban areas [e.g. *Lawrence et al.*, 2007]. However, an appropriate model of atmospheric chemical transport for tropospheric $O_3$ and speciated aerosols in polluted environments must incorporate all of the chemical species, chemical and photolytic reactions, microphysics, and transport and removal processes that define the system being studied. In other words, it must simulate the full interactive chemical state of the atmosphere. It must adequately resolve or parameterize these interactions at relevant spatial and temporal scales; in the case of regional chemical transport, spatial scales of 1-50 km at time steps of no more than 10 minutes. To meet these needs while remaining affordable, a CTM must implement a vast array of empirical and derived rate constants in simplified chemical mechanisms and still provide results

that are consistent with the observed state of the atmosphere in any place, at any time. At this stage in the maturity of the sciences, this remains a challenge, because many chemical and microphysical interactions remain unknown or not yet consistently quantified with a complete theoretical mechanism that describes both the results of chamber experiments, observations in the field [*Ma et al.*, 2008]. Moreover, even where observed processes are well understood, the spatial scales relevant to regional chemical transport—both the chemical reactions and the dynamics of the atmosphere—are in a "gray area" between the synoptic and local scales, where neither the bulk parameterizations of global-scale models nor the precise mechanistic calculations of chamber experiments and large eddy simulations are completely effective. Instead, the regional scale is subject to many messy real-world meteorological phenomena, such as convective fronts, cloud bands, and land-sea breezes, as well as complications that are distinct to chemical transport, such as providing realistic mixing and reaction within grid cells of 10 - 1000 $km^2$ that are nowhere near instantaneously well-mixed in the real world.

Even if a "good" model is constructed, its effective application is dependent on the quality of a large volume and wide variety of required input data. Accurate representation of environmental conditions and transport at regional scales requires hourly or better model meteorology on the native model grid from a regional climate model initialized and constrained by yet another forecast model or observational analysis. As chemical transport is highly sensitive to initial conditions for weeks into a simulation,

an estimate of the initial 3D state of every modeled chemical species must be provided from an analysis, prior modeling results, or a climatological average. Unless the CTM run covers the entire globe, boundary conditions must be supplied for transport into the study domain—again, from other models, analyses, or climatologies. Incoming solar radiation and photolysis constants must also be calculated, and are dependent on stratospheric $O_3$ and sulfate concentrations, yet more estimates from other models or satellite retrievals.

Finally, the greatest hurdle in providing "good data" for input to a CTM is in generating emissions. Not only are emissions estimates the most important modeling input, responsible for the first-order signal in the concentrations of trace gases and particles in the troposphere, they are also the most complicated, and most dependent on data and methods from outside the realm of the sciences. Emissions inventories of all relevant species and their precursors from all emissions sources in the study domain must be compiled and allocated in space and time to the model grid.

For large point sources in most parts of the world, this is straightforward: the location of the point source is known, the height of any smokestacks are known, emissions rates are directly reported or easily estimated from reported activities (e.g. fuel use), and the reported inventory need only be converted to the model speciation, allocated in time, and placed in the appropriate grid cell, with the vertical layer determined by the stack height and the stability of the atmosphere in the model meteorology.

However, for the vast majority of emissions categories—biogenic, dust, automobiles, and other natural and anthropogenic area sources—there are no such directly measured and reported emissions rates, and both emissions rates and their spatial and temporal distribution must be estimated from other available information. Satellite land cover classification has improved spatial allocation, particularly for biogenic sources, but in many areas of the world, the dearth of emissions data is crippling, and limits the effective spatial resolution of models to the 1° x 1° scales at which national-level inventories (e.g. *Streets et al*. [2003]) can be constructed. In the U.S., EPA uses a consistent methodology to compile a comprehensive National Emissions Inventory (NEI) every 3 years, with county-level emissions estimates for all area sources and facility-based inventories for large point sources. However, since most U.S. counties are larger than one CTM gridcell, area emissions must be allocated to the model grid based on other available knowledge about where the emitting activities might occur; for example, distributing mobile emissions along highways, agricultural emissions equally over all the farmland in a county, or weighting VOC emissions from grilling meat by Census population data. In the absence of a total surveillance society with direct monitoring of all emissions at their source, the uncertainty in area source emissions rates and their geographic distribution are major sources of uncertainty in the modeling of regional air pollution, particularly near urban areas.

**2.2. Model Description**

*2.2.1. Model Selection Rationale*

We employ the Community Multiscale Air Quality model (CMAQ) as the primary tool for studying chemical transport in the Great Lakes region. Developed by the U.S. EPA and descended from earlier models such as the Urban Airshed Model dating back to the late 1970s, CMAQ has a number of unique properties that combine to qualify it as the most suitable model for this study. First, stemming from its near-exclusive use by EPA and regional planning offices, CMAQ is the most widely-used CTM for public-sector policy analysis and academic research in North America. While several CTMs are officially approved by EPA, CMAQ has become established over the past decade as the primary tool for use in evaluating proposed federal policies, especially after the 1998 release of the "Finding of Significant Contribution and Rulemaking for Certain States in the Ozone Transport Assessment Group Region for Purposes of Reducing Regional Transport of Ozone," commonly known as the "NOx SIP Call." The NOx SIP Call required states to demonstrate that their proposed State Implementation Plans (SIPs) were adequate for addressing state contribution to regional transport of NOx and its role as a precursor to $O_3$, with a focus on large stationary sources of NOx emissions. CMAQ has since been used by EPA to demonstrate the efficacy of proposed administrative decrees including the Clean Air Interstate Rule (CAIR), Clean Air Mercury Rule (CAMR), and Clean Air Visibility Rule, as well as by states and regional planning groups in SIP evaluation for both the NOx SIP Call and compliance with NAAQS. Over time, CMAQ has also found extensive use in academic research on regional air pollution, as it

represents a community-based model with a codified mechanism for including user-driven development and improvements in new releases and ensuring their compatibility in a cohesive modeling system. As a result, CMAQ is currently the "state of the science" model for the study of regional scale atmospheric chemical transport.

Unlike most other regional CTMs developed by independent research groups, CMAQ is fully supported by EPA, making it the only CTM with funded development and support staff. Among a class of models where public availability, regular training, active development, and full documentation beyond a README file are all relatively rare, this support, combined with CMAQ's active user base, might make it an attractive choice for regional air quality analysis even if other models exhibited superior performance.

Regardless of its extensive use and infrastructure, does CMAQ qualify as a "good" model? In my view, yes. Key strengths include the treatment of relevant processes, adequately simulating them at the spatial and temporal scales of interest, and doing so with affordable runtime requirements. Model performance has been evaluated more extensively than any other CTM in the world (this year alone, there have been 29 studies published evaluating CMAQ's predictive ability, e.g. *Yu et al.*, 2008), and evaluation has been conducted regularly for new releases of the software and as new emissions data have become available [e.g. *Appel et al.*, 2008]. As described extensively in results and references in Chapter 3, CMAQ is known to simulate both $O_3$ and $PM_{2.5}$

with little bias over the continental United States. There are always limitations in every model, of course, and CMAQ is the representation of atmospheric chemical transport that meets the criteria of a "good model" with the fewest scientific and operational limitations among available CTMs.

*2.2.2. Model configuration*

We employ the most recent CMAQ release (v4.6) [*Byun and Schere*, 2006] using the Carbon Bond IV (CB-IV) lumped gas phase chemical mechanism [*Gery et al.*, 1989], the CMAQ AE3 aerosol module, RADM aqueous chemistry [*Chang et al.*, 1987], advection by the piecewise parabolic method, and eddy diffusion. This is a standard configuration for research and regulatory use, with known performance and numerical stability in extended multi-month application. I did not employ the "bleeding edge" configuration with most recent update to this chemical mechanism (CB05), the newest iteration of the aerosol module (AE4), and new advection schemes, as this combination had yet to be thoroughly described and evaluated, and I encountered nonphysical errors in photochemistry in test simulations. Moreover, the use of a relatively standard configuration allows for the most direct comparison to prior peer-reviewed modeling studies.

As it is currently impractical and computationally inefficient to explicitly model the thousands of chemical species and tens of thousands of their known and suspected

interactions in polluted atmospheres [*Bloss et al.*, 2005] in a chemical transport model in seasonal or annual studies, chemical mechanisms are employed to aggregate species and reduce the number of modeled reactions. This simplification is typically accomplished through mathematical lumping of equations, molecular lumping of species with similar chemical structures, or structural lumping of compounds with similar chemical activity. I chose to use the CB-IV chemical mechanism, designed to represent gas phase interactions at the regional scale. The primary alternative in CMAQ, the SAPRC-99 mechanism [*Carter*, 2000] developed from observations and smog chamber experiments by California's Statewide Air Pollution Research Center, is meant to represent gas phase chemistry at the urban scale in polluted environments, and tends to produce more $O_3$ than CB-IV [*Lin et al.*, 2008] and other mechanisms.

The CB-IV scheme combines explicit chemistry, structural surrogate approximations, and lumped speciation to simulate urban and regional photochemistry. The mechanism consists of 36 species in 93 reactions, including 11 photolytic reactions. Inorganic species, carbonyls, ethene, isoprene, and formaldehyde are modeled explicitly, while peroxy radicals and organics are lumped by the dominant functional carbon bond, e.g. paraffins, olefins, and aromatics. Each higher-order reactive VOC species is represented as a combination of paraffin, olefin, toluene, and xylene. This lumping strategy allows for explicit treatment of the species that are present in the highest concentrations in the atmosphere, while efficiently including all the highly reactive trace species and their great impact per mole.

The CMAQ AE3 aerosol module employed consists of aerosol microphysics [*Binkowski and Roselle*, 2003] and the ISORROPIA (v1.7) aerosol equilibrium model [*Nenes et al.*, 1998], in which partitioning between gas and aerosol phases is a function of temperature and relative humidity, distinct for each species. CMAQ employs a trimodal size distribution with lognormal Aitken, aggregation, and coarse modes. Speciated aerosols in the model do not grow to the coarse mode, and all coarse mode particles are treated as chemically inert. The use of a modal rather than sectional treatment for aerosols, the lack of speciation in the coarse mode, and the lack of mass transfer between fine and coarse mode aerosols are all drastic simplifications, but each assumption halves the number of modeled aerosol species required, with geometric reductions in runtime.

The secondary organic aerosol (SOA) scheme, based on the Secondary Organic Aerosol Model (SORGAM) [*Schell et al.*, 2001], accounts for SOA formation from the oxidation of alkenes, cresol, high-yield aromatics, low-yield aromatics, and monoterpenes, which form ten lumped, idealized semi-volatile gaseous SOA precursors that can subsequently condense onto particles. As implemented for CB-IV gas phase chemistry, SOA reactions are fully reversible—gaseous precursors can condense and evaporate—but SOA production from alkanes, olefins, and isoprene is not simulated. Given recent attention to SOA and advances in understanding the heterogeneous chemistry and physics involved [e.g. *Stanier et al.*, 2008], the employed SOA mechanism

is limited and outdated, but no more recent SOA mechanisms are currently available in the standard public releases of any regional scale CTM.

CMAQ simulates transport and removal processes, including advection, turbulent diffusion, and wet and dry deposition. Distinct dry deposition velocities are calculated for each species according to the surface exchange aerodynamic method [*Pleim et al.*, 2001], which uses surface resistance, canopy resistance, and stomatal resistance to compute the likelihood of deposition of each modeled gaseous and aerosol species based on its molecular properties. While advection and turbulent dispersion are well understood, and most CTMs implement them with nearly identical equations, the complications in their implementation in regional-scale models are thoughtfully considered in CMAQ. The minimum value for eddy diffusivity (Kz) is particularly important for determining nighttime concentrations, through the representation of vertical mixing. If Kzmin—the parameterization for the minimum simulated rate of eddy diffusion—is too low, ventilation is reduced, and unrealistically high concentrations of primary species are simulated in urban areas with high emissions. On the other hand, using a high $Kz_{min}$ value would lead to overpredictions of $O_3$ at night in more rural areas, as too much $O_3$-rich air is brought down from aloft. To allow mixing to better respond to the land-use characteristics, I employed a minimum diffusivity option that considers the fraction of urban area within each grid cell, and adjust the $Kz_{min}$ value according to:

$$Kz_{min} = (0.5 * (1.0 - F_{urban})) + (2.0 * F_{urban})$$

where "$F_{urban}$" is the fraction of urban area in the grid cell (0.0 - 1.0) from 1 km x 1 km USGS land cover classification. Using this formula, $Kz_{min}$ varies from 0.5 $m^2/s$ (in grid cells with no urban areas) and 2.0 $m^2/s$ (in grid cells that are considered 100% urban).

We ran CMAQ calculating chemistry every 90 seconds, with transport every 15 minutes, to produce hourly output of instantaneous and hourly average three dimensional concentration fields and hourly wet and dry deposition values. I interpolated input meteorology to CMAQ's terrain-following sigma-pressure vertical coordinate system to represent the troposphere and lower stratosphere in 14 vertical layers, with higher resolution and greater fidelity to the host climate model in the near-surface layers in order to fully resolve boundary layer phenomena.

The configuration above was employed for all CMAQ experiments contributing to this dissertation, ensuring a consistent representation of the atmosphere as spatial scale, domain, and model inputs varied.

## 2.3. Data

### *2.3.1. Model inputs*

#### 2.3.1.1. Meteorology

Meteorology inputs are produced by the Pennsylvania State University/National Center for Atmospheric Research mesoscale meteorological model (MM5) described by *Grell et al*. [1995] and its successor, the Weather Research and Forecasting Model (WRF) v3. MM5 and WRF are both nonhydrostatic Eulerian models, meaning the models calculate geophysical fluid dynamics and cloud physics without assuming hydrostatic equilibrium, a requirement when resolving regional scale atmospheric phenomena. The horizontal grid uses an Arakawa C-grid staggering scheme, which helps to minimize error and supports higher grid resolution. These models are used extensively in operational weather and chemical weather forecasting and in regional climate simulation, and are at present the only meteorological models that provide input to current versions of CMAQ.

For all 36 km simulations in Chapters 3, 4, and 5, MM5 (v3.6.1) output for 2002 was provided by the Lake Michigan Air Directors Consortium (LADCO) [*Baker*, 2004] over a continental United States domain on a 36 km x 36 km horizontal grid with 34 vertical levels. This meteorology data set provides a strong foundation for chemical transport in CMAQ, as it has been used extensively in regulatory air quality modeling by LADCO and state agencies, has been extensively evaluated, and has been employed in several CTM evaluations over the Eastern U.S. Model evaluation [*Abraczinskas et al.,* 2004*; Olerud and Simms,* 2004*; Baker et al*., 2005] indicated good performance for temperature, humidity, precipitation, and wind speed, with lower levels of agreement on wind direction. An MM5 study in the same region [*Zhong et al*., 2005] found that the

model captures the general development and evolution of boundary layer inversions and lake–land breezes, although with errors in their strength and timing.

MM5 output was processed for CMAQ using the Meteorology Chemistry Interface Processor (MCIP) v3.2. For all 12 km simulations shown in Chapter 5, I ran the WRF-ARW model for 2002 in a 2-way nested mode between that 36 km x 36 km domain and a smaller 12 km x 12 km domain covering the Great Lakes region. The model was nudged closer to input model analyses every 3 hours. This data was prepared for CMAQ using MCIP 3.4, for which I served as a beta tester, as earlier versions were incompatible with WRF output.

2.3.1.2. Photolysis rates

Clear sky photolysis rates were calculated using CMAQ's dedicated preprocessor, JPROC. JPROC employs temperature profiles from the U.S. Standard Atmosphere (*NOAA*, 1976), and a profile of the aerosol extinction coefficients, (*Elterman et al.*, 1969). JPROC uses this information in a simple forward radiative transfer model to calculate the actinic flux (photons $cm^2$/min) needed for calculating photolysis rates. JPROC calculates the actinic flux for clear-sky conditions (no clouds present), and CMAQ then attenuates for cloudiness based on estimates of cloud water path from modeled cloud fraction and cloud top and bottom heights when clouds are present. JPROC computes the rate for each photolysis reaction at 10º latitude bands, each model

layer altitude, and several zenith angles. CMAQ interpolates the data generated by JPROC to individual grid cells, and adjusts for the presence of clouds.

2.3.1.3. Initial Conditions

For the continental-scale 36 km simulation in Chapters 3 and 4, initial three dimensional chemistry fields were generated from a set of time-independent vertical concentration profiles from the Regional Acid Deposition Model, Version 2 (RADM2) (*Stockwell et al.*, 1990), which represent clean climatological atmospheric conditions in the Northern Hemisphere. Model runs were initialized and then allowed to spin-up more realistic concentrations for 10 days before data was collected.

For regional 36 km and 12 km simulations over the Great Lakes in Chapter 5, initial conditions were generated from CMAQ concentration results from that first 36 km continental scale run.

2.3.1.4. Boundary Conditions

Boundary conditions for the continental 36 km CMAQ domain were extracted from 2002 monthly mean concentration fields from the Model of Ozone and Related Tracers (MOZART) [*Horowitz et al.*, 2003], a global CTM, incorporating aerosol physics described by *Tie et al.* [2001, 2005]. MOZART was run with 2002 reanalyzed meteorology from National Centers for Environmental Prediction Global Reanalysis

[*Kalnay et al.*, 1996]. Fourteen gaseous and aerosol species with atmospheric lifetimes sufficient for intercontinental transport were taken from MOZART, including $O_3$; $SO_4^{2-}$; $NH_4^+$; $NO_3^-$; carbon monoxide (CO); elemental carbon (EC); organic carbon (OC); nitrogen dioxide ($NO_2$); sulfur dioxide ($SO_2$); ethane ($C_2H_6$); propane ($C_3H_8$); acetone ($CH_3COCH_3$), butane ($C_4H_{10}$); and peroxyacetylnitrite (PAN) ($C_2H_3NO_5$). I developed a chemical mechanism conversion between the two models and, before using MOZART boundary conditions in CMAQ for this dissertation, I employed them in CMAQ over East Asia. In *Holloway et al.* [2008], a post-analysis of Phase 2 of the Model Intercomparison Project for Asia, I conducted sensitivity testing of regional chemical transport modeling to changes in MOZART global boundary conditions for these species, and compiled observations for the evaluation of global and regional CTMs.

For regional 36 km and 12 km simulations over the Great Lakes in Chapter 5, boundary conditions were generated from CMAQ concentrations output from the continental run.

2.3.1.5. Emissions Inventory

Emissions estimates for CMAQ were developed using the Sparse Matrix Operating Kernel for Emissions (SMOKE) [*Houyoux et al.*, 2000]. The data sets processed with SMOKE (v2.1) were obtained from EPA's 2001-based Platform, Version 1 [*US EPA*, 2005a]. This inventory is based on the 1999 NEI, with growth factors applied by Source Classification Code, and augmented with national inventories for Canada

(2000) and Mexico (1999). It is designed to be a comprehensive estimate of all emissions of criteria pollutants and their precursors from all anthropogenic emissions sources, estimated for each point source and at the county level for area sources. This NEI was used by EPA for analyses of the Clean Air Interstate Rule, Clean Air Visibility Rule (CAIR), and Clear Skies Legislation. The 2001 NEI was the most recent complete national inventory publicly available at the time my work began. This emissions inventory represents the seasonality of aerosol and precursor emissions, but does not include day-specific emissions for 2002 for any anthropogenic sources. Fire emissions from wildfires, prescribed burns, and agricultural fires were estimated using 1996-2001 averages. Biogenic emissions were calculated from modeled meteorology using BEIS3 (v3.12). Spatial allocation of emissions was conducted using spatial surrogate techniques and ancillary data distributed by EPA with the 2001 modeling platform, which I processed for the CMAQ grids using the Multimedia Integrated Modeling System.

This NEI has numerous advantages and disadvantages. It is a current standard inventory for federal policy modeling, which allows for direct comparison of CMAQ results with modeled impacts of CAIR and other point source-directed regulatory measures. It has also been extensively documented [USEPA 2005b] and evaluated for 2001 [USEPA, 2005c]. While all assumptions are thoroughly documented and quite reasonable, since it is a national inventory, the NEI's area source emissions are all calculated in a top-down method that takes reported state-level and, where available, county-level activity data and then disaggregates it to counties based on a set of 65

surrogate spatial datasets, such as census population and USGS land use classification. For example, for mobile source emissions, county-level travel estimates of travel rates for 12 roadway types (each with distinct average speeds) from the Federal Highway Administration, states, counties, municipalities, and tribes are combined with state-level vehicle fleet statistics and allocated to 33 roadway types and 28 vehicle classifications. The National Mobile Emissions Model (NMIM) then generates unique emissions factors for each vehicle-roadway combination for one representative county in each state using 1 climatological profile per state. NMIM allocates vehicle-roadway combinations by clustering all counties in the state according to the number of miles of roadway miles in the county of each roadway type, and then multiplies by the county-specific travel estimate to generate a county-level emissions inventory. This top-down method is practical, but does not take into account differences in local travel patterns at scales below the county level.

Emissions of most primary aerosols and aerosol precursors in the Great Lakes region exhibit limited seasonality, as represented in NEI 2001. Regional aggregate monthly emissions of reactive aerosol precursors ($SO_y$ and $NO_y$) and primary fine (the sum of all directly emitted $PM_{2.5}$ species) and coarse mode (unspeciated) aerosols in the region all vary within a range of less than 12% between the highest and lowest months, with $SO_y$ (2.1%) especially invariant. At the 36 km scale, the average gridcell varies by less than 20% over the course of the year. The top 5% of emitting gridcells are even more invariant, with less than 8% range. Elemental carbon emissions exhibit much greater

monthly range (33%), with a summer maximum and winter minimum. Ammonia emissions peak in April and June in concert with the planting seasons for the region's two largest commodity crops, soybeans and corn. Thus, with the exception of EC and $NH_4^+$, seasonal cycles in aerosol concentrations are due primarily to changes in regional atmospheric conditions, rather than to temporal changes in emissions. Unless emissions estimates are greatly in error, this implies that seasonality in modeled aerosol concentrations—especially $NO_3^-$ and $SO_4^{2-}$—is due to modeled chemical and thermodynamic processes.

2.3.1.6. Emissions Scenarios

*2.3.1.6.1. Fixed Emissions Scenarios*

These NEI emissions served as the "base case" for several emissions scenarios employed in Chapter 5. In one set of scenarios, we perturbed urban anthropogenic emissions by +/- 20% to identify the sensitivity of $O_3$ and $PM_{2.5}$ to potential changes in urban emissions activities. This choice of perturbation was selected to produce a discernible change in emissions, without incurring extensive non-linear errors associated with large changes. Although somewhat arbitrary, the 20% change has been adopted for consistency with ongoing global and regional studies by the UN Task Force on the Hemispheric Transport of Air Pollution [*LRTAP*, 2007]. We then kept urban emissions constant according to the NEI, but removed all anthropogenic emissions outside of urban

areas in order to estimate the contributions of emissions from rural areas and small cities to $O_3$ and $PM_{2.5}$ across the region, and their contribution to pollution in urban areas.

*2.3.1.6.2. Bottom-Up Mobile Emissions Scenarios*

In another set of simulations in Chapter 5, we used the NEI for all emissions sectors except on-road motor vehicle emissions. For these, we substituted a set of emissions scenarios I generated in collaboration with urban and regional planning researchers at the University of Wisconsin-Madison and the Georgia Institute of Technology. In this EPA-sponsored project, entitled *Projecting the Impact of Land Use and Transportation on Future Air Quality in the Upper Midwestern United States (PLUTO)*, we combined a census-tract level land use and vehicle travel modeling framework with a mobile source emissions model to evaluate the sensitivity of future primary pollutant emissions to different land development and population migration scenarios across the Upper Midwestern U.S.

We associate future emissions with land development and vehicle fleet hybridization scenarios by integrating four different modeling components: (1) a set of tract-level demographic, socioeconomic and land use projections based on alternative growth assumptions; (2) a household vehicle trip modeling framework, linking average household vehicle miles of travel (VMT) to projected tract-level characteristics; (3) a mobile source emissions model developed by the EPA for regulated air pollutants; and (4) the development of a set of fleet-level fuel economy and VMT adjustment factors,

based on the complete transformation of the light vehicle fleet from internal combustion-only to hybrid-electric vehicles by 2050. A brief description of these elements follows below. A more detailed description of the first three modeling components is described in *Stone et al*. [2007], and results are described in *Stone et al*. [2007, 2008].

"Business-as-Usual" Development Scenario (BAU). The BAU scenario assumes that future population and land use trends throughout the study region will be consistent with historical change. To derive this scenario, we extrapolated county populations to 2050 using multiple time-series regression models based on decennial census counts and annual intercensal estimates for the years 1970 through 2000, and post-censal estimates for the years 2001 through 2004. For each county we selected the projection with the lowest mean absolute percent deviation from the historic trend, extended to include independent projections for the years 2005 through 2030 [*Woods & Poole Economics Inc*., 2005]. We then allocated future county population to tracts via constant-share apportionment, holding the 2000 county-to-tract population ratio constant. Each census tract was assigned a neighborhood type: "urban," "suburban," or "rural," based on a combination of its projected contextual density (focal density, measured in persons per square mile in the individual tract and its surrounding tracts within a set radius) and the projected contextual density of the tract's nearest regional center. We assume that tract-level employment and household income will follow historic and projected sub-regional, and use regression-based methods similar to those used for population. We assume that changes in household vehicle ownership will track changes in neighborhood type over

time. Specifically, we assigned each tract with one of three possible vehicle ownership rates, corresponding to the average number of vehicles per household across all urban, suburban and rural tracts, respectively, in each Metropolitan Statistical Area (MSA) in 2000.

"Smart-Growth" Development Scenario 1 (SG1). In this scenario, as described in *Stone et al*. [2007], we assume that the total population of each MSA in 2050 is the same as under BAU, but that new population added in each decade is reallocated away from rural to suburban and urban census tracts in response to the widespread adoption of growth management policies, such as urban growth boundaries (UGBs) and transit-oriented development. Specifically, we adjusted the proportion of projected BAU population growth occurring in each of the three neighborhood types to match historical development trends in Portland, Oregon, a metropolitan area with a widely recognized comprehensive growth management program. Between the 1980 Census (one year after the establishment of an UGB) and the 2000 Census, the proportion of Portland's population residing in urban and suburban census tracts increased at a significantly higher rate than Midwestern MSAs on average, while the proportion of the population residing in rural census tracts increased by a significantly lower rate than within Midwestern MSAs. While the relative contribution of Portland's growth management policies to its increased urbanization during this period is difficult to separate from the effects of other attributes, Portland nevertheless provides a real, empirical basis for modeling the effects of compact urban growth on air quality under what has arguably been, at least in a U.S.

context, the most ideal of conditions. Projected income and employment are assumed the same under SG1 as BAU, reflecting historic and projected sub-regional trends. As with the BAU scenario, household vehicle ownership is linked to changes in neighborhood type over time.

"Smart-Growth" Development Scenario 2" (SG2). Under the SG2 scenario, a larger percentage of new MSA population growth is reallocated from rural to suburban and urban census tracts than occurs under the Portland-based SG1 scenario. Starting in the base year of 2000, all new population growth per MSA is directed to urban and suburban tracts only, with 10% of this growth directed to urban tracts and the remaining 90% directed to suburban census tracts in 2010. The urban allocation then increases by 10 percentage points per decade, rising to 50% of all new population growth in 2050. Relative to the SG1 scenario, SG2 results in higher urban populations and greater mean densities per MSA, as well as a larger number of "super-urban" tracts (i.e., tracts with densities of 10,000 people per square mile and higher). Income and employment values were assumed, once again, to be the same as BAU, reflecting historic and projected sub-regional trends, while household vehicle ownership is again linked to changes in neighborhood type, with each tract assigned the average number of vehicles per household that occurred across all tracts in each MSA sharing that neighborhood type in 2000.

Hybrid-Electric Vehicle Fleet Scenario (HEV). In this scenario we assume that 100 percent of the study region's stock vehicle fleet will be comprised of HEVs by 2050, but that the fleet will otherwise remain unchanged from 2000 in terms of its relative composition of different vehicle size classes. As with our alternative land use development scenarios, we also assume that tract-level fleet composition is the same as region-wide fleet composition, such that every tract has the same relative make-up of size classes. This enables us to derive and apply a single HEV emissions adjustment factor – a multiplier representing the proportion of VMT under base-case technology that would be equivalent, in terms of gasoline consumption and vehicle emissions, to 100 percent of VMT under the HEV scenario.

In order to compare land use changes with realistic assumptions of HEV market penetration , we assume that stock fleet fuel economy will increase from 19.5 MPG in 2000 to 25.6 MPG in 2050, which we projected via a time-series regression of the *EIA* [2007] thirty-year "base-case" forecast of U.S. stock fleet fuel economy. We developed our HEV emissions adjustment factor based on an EIA study on the potential impacts of alternative technology futures on energy consumption over a fifty-year time horizon [*Birky et al.*, 2001]. This study predicted that a complete hybridization of the U.S. stock light vehicle fleet would result in an average stock fleet fuel economy of 33.0 MPG in 2050 – representing a 29 percent increase over our technology base-case.

Vehicle Activity Modeling. As described in *Stone et al.* [2007], the core of our approach is a vehicle activity modeling framework for associating future land use and demographic change with vehicle travel. We extend a "transferability" framework, developed by researchers at the Oak Ridge National Laboratory (ORNL) to support the derivation of tract-level travel statistics from the 1995 Nationwide Personal Transportation Survey (NPTS), and use it to project future VMT based on a small set of demographic variables.

Developed in 2001, the NPTS transferability framework supports the estimation of VMT at the census tract level in response to three census variables: median household income, vehicle ownership, and employment rate, plus the neighborhood type classification discussed above. Identified in the transportation literature as significant predictors of vehicle travel [*Bento et al.*, 2005; *Heanue*, 1998; *Holzclaw et al.*, 2002], these variables can be used to identify clusters of census tracts hypothesized to share similar travel characteristics. Once tracts are grouped into these homogenous clusters, average daily VMT per household is derived from NPTS responses in each cluster and used to estimate tract-level VMT based on the number of households per tract (*Reuscher et al.*, 2002). For this study, we added an additional cluster, which included all census tracts with a contextual population density of 10,000 or more people per square mile.

We use this framework to project 2050 VMT based on our BAU, SG1 and SG2 projections of the four variables used to construct the clusters. We assume that as these

characteristics of a tract change over time, its average household VMT will change correspondingly. This framework allows VMT estimation to be conducted at the census tract level across scales that more completely capture pollution formation and transport processes. Furthermore, the framework predicts vehicle travel quite accurately. *Reuscher et al.* [2002] compared VMT estimated using the transferability framework and observed travel data obtained through three independent travel surveys conducted in New York, Massachusetts, and Oklahoma, finding the transferability framework to estimate VMT at the metropolitan and state levels with a mean error rate of approximately 3.1%.

Vehicle Emissions Modeling. We used the *USEPA* [2006] MOBILE6 emissions factor model to estimate monthly profiles of vehicle emissions factors for carbon monoxide (CO), NOx, $PM_{2.5}$, VOCs from exhaust and evaporation, sulfur dioxide ($SO_2$) and ammonia ($NH_3$) associated with our alternative BAU, SG1, and SG2 projected VMT. MOBILE6 calculates average emissions factors in grams per mile for each pollutant based on input parameters detailing the composite characteristics of the vehicle fleet, engine mode of operation (coldstart, hotstart, or stabilized operating modes), a set of climate variables, and mean travel speeds, among other variables.

For this work, I developed all climate inputs. In order to complement the spatially-resolved VMT estimates without generating 432,000 unique climate profiles to resolve all tracts and roadway types, I performed spatial clustering on 1990-2000 climatological monthly mean values of minimum and maximum temperature, relative

humidity, pressure, and cloud cover from the 0.5º x 0.5º gridded CRU TS 2.1 [*Mitchell and Jones*, 2004] to identify 10 sub-regions that were covariant for all four variables. I then assigned each sub-region the value of the gridcell containing its greatest number of registered vehicles, in order to best represent the conditions under which the majority of emissions took place.

These average emissions factors were then multiplied by the tract-level VMT projections to derive daily mean emissions of each regulated pollutant for each tract for each month.

### 2.3.2. Observations

As observations of atmospheric chemistry in the region were not used to condition the CMAQ simulations in any way, in-situ observations provide a completely independent means of evaluating CMAQ results. Although isolated ad-hoc point-based observations from field campaigns were available at certain places and times, I chose to employ observations from the region's routine monitoring networks in order to focus on the region-wide performance throughout the entire simulation. These observations, including their sources, methods, and monthly characteristics are described in detail in Chapter 3.

We have made every effort to employ the best available input data and modeling assumptions to provide a strong foundation for process studies and policy analysis. Model configuration, emissions, meteorological inputs and boundary conditions were selected to provide the best representation of regional chemical transport of $O_3$ and speciated $PM_{2.5}$ from publicly available, rigorously evaluated data; to allow for ready comparison with prior studies; and to serve as a platform for applying a novel bottom-up census tract level mobile emissions modeling framework to evaluate potential impacts of urban land use policies on air quality.

**References**

Abraczinskas, M., D.T. Olerud, and A.P. Sims (2004), Characterizing annual meteorological modeling performance for visibility improvement strategy modeling in the southeastern U.S., paper presented at 13th AMS Joint Conference on Applications of Air Pollution Meteorology with the Air and Waste Management Association, Am. Meteorol. Soc., Vancouver, B.C., Canada.

Appel, K.W. P.V. Bhave, A.B. Gilliland, G. Sarwar, S.J. Roselle (2008), Evaluation of the community multiscale air quality (CMAQ) model version 4.5: Sensitivities impacting model performance; Part II--particulate matter, *Atmos. Environ.*, 42, 6057-6066, 10.1016/j.atmosenv.2008.03.036

Baker, K. (2004), Midwest Regional Planning Organization Modeling Protocol. Lake Michigan Air Directors Consortium/Midwest Regional Planning Organization, Des Plaines, IL.

Baker, K., M. Johnson, S. King, and W. Ji (2005), Meteorological Modeling Performance Summary For Application to PM2.5/Haze/Ozone Modeling Projects. Lake Michigan Air Directors Consortium/Midwest Regional Planning Organization, Des Plaines, IL.

Bento, A. M., Cropper, M. L., Mobarak, A. M., & Vinha, K. (2005), The effects of urban spatial structure on travel demand in the United States. *Review of Economics and Statistics*, 87(3), 466–478.

Binkowski, F.S., and S.J. Roselle (2003), Models-3 Community Multiscale Air Quality (CMAQ) model aerosol component: 1: Model description, *J. Geophys. Res.*, 108(D6), 4183, doi:10.1029/2001JD001409.

Birky, A., et al. (2001), Future U.S. Highway Energy Use: A Fifty Year Perspective. Draft Report, Prepared for Office of Transportation Technologies, Energy Efficiency and Renewable Energy, U.S Department of Energy, 2001.

Bloss, C., Wagner, V., Jenkin, M. E., Volkamer, R., Bloss, W. J., Lee, J. D., Heard, D. E., Wirtz, K., Martin-Reviejo, M., Rea, G., Wenger, J. C., and Pilling, M. J. (2005), Development of a detailed chemical mechanism (MCMv3.1) for the atmospheric oxidation of aromatic hydrocarbons, *Atmos. Chem. Phys.*, 5, 641-664.

Büker, M. L., M. H. Hitchman, G. J. Tripoli, R. B. Pierce, E. V. Browell, and M. A. Avery, 2005, Resolution dependence of cross-tropopause ozone transport over East Asia. *J. Geophys. Res.*,110, D03107.

Byun D. W., and K. L. Schere (2006), Review of the governing equations, computational algorithms, and other components of the Models-3 Community Multiscale Air Quality (CMAQ) modeling system, *Appl. Mech. Rev.*, 59, 51–77, doi:10.1115/1.2128636.

Carter, W.P.L. (2000). Documentation of the SAPRC-99 Chemical Mechanism for VOC Reactivity Assessment. Final Report to California Air Resources Board Contract No. 92-329, and 95-308. May 2000.

Elterman, L., R. Wexler, and D. T. Chang (1969), Features of tropospheric and stratospheric dust. *Appl. Optics*, 8, 893–903.

Gery, MW., G.Z. Whitten, J.P. Killus, and M.C. Dodge (1989), A Photochemical Kinetics Mechanism For Urban And Regional Scale Computer Modeling, *J. Geophys. Res.*, 94 (D10), 12925-12956.

Grell, G. A., J. Dudhia, and D. R. Stauffer (1995), A description of the Fifth-Generation Penn State/NCAR Mesoscale Model (MM5), NCAR/TN-398+STR, Natl. Cent. for Atmos. Res., Boulder, Colo. (Available at http://www.mmm.ucar.edu/mm5/documents/mm5-desc-doc.html)

EIA (2007), Annual Energy Outlook 2007 with Projections to 2030. Report #:DOE/EIA-0383(2007). U.S. Energy Information Agency, Washington, D.C. (Available at http://www.eia.doe.gov/oiaf/archive/aeo07/issues.html).

Heanue, K. (1998), Highway capacity and induced travel: Issues, evidence and implications. *Transportation Research Circular*, 481, 33–45.

Holloway, T., T. Sakurai, Z. Han, S. Ehlers, S.N. Spak, L.W. Horowitz, G.R. Carmichael, D. Streets, Y. Hozumi, H. Ueda, S.U. Park, C. Fung, M. Kajino, N. Thongboonchoo, M. Engardt, C. Bennet, H. Hayami, K. Sartelet, Z. Wang, K. Matsuda, M. Amann (2008), Impact of Global Emissions on Regional Air Quality in Asia. *Atmospheric Environment*, 42, 3543–3561, doi:10.1016/j.atmosenv.2007.10.022.

Holzclaw, J., Clear, R., Dittmar, H., Goldstein, D., & Haas, P. (2002), Location efficiency: Neighborhood and socio-economic characteristics determine auto ownership and use—studies in Chicago, Los Angeles and San Francisco. *Transportation Planning and Technology*, 25(1), 1–27. 1552, 120–125.

Horowitz, L.W., S. Walters, D.L. Mauzerall, L.K. Emmons, P.J. Rasch, C. Granier, X. Tie, J.-F. Lamarque, M.G. Shultz, G.S. Tyndall, J.J. Orlando, and G.P. Brasseur (2003), A global simulation of tropospheric ozone and related tracers: Description and evaluation of MOZART, version 2, *J. Geophys. Res.*, 108(D24), 4784, doi:10.1029/2002JD002853.

Houyoux, M.R., J.M. Vukovich, C.J. Coats Jr., N.J.M. Wheeler, and P. Kasibhatla (2000), Emission inventory development and processing for the seasonal model for regional air quality, *J. Geophys. Res.,* 105 (D7), 9079–9090.

Kalnay, E., M. Kanamitsu, R. Kistler, W. Collins, D. Deaven, L. Gandin, M. Iredell, S. Saha, G. White, J. Woollen, Y. Zhu, M. Chelliah, W. Ebisuzaki, W. Higgins, J. Janowiak, K. C. Mo, C. Ropelewski, J. Wang, A. Leetmaa, R. Reynolds, R. Jenne, and D. Joseph (1996), The NCEP/NCAR 40-Year Reanalysis Project, *Bull. Amer. Meteor. Soc.*, 77, 437-471, doi: 10.1175/1520-0477(1996)077<0437:TNYRP>2.0.CO;2.

Kim, J., J. Lee, H. C. Lee, A. Higurashi, T. Takemura, and C. H. Song (2007), Consistency of the aerosol type classification from satellite remote sensing during the Atmospheric Brown Cloud–East Asia Regional Experiment campaign, *J. Geophys. Res.*, 112, D22S33, doi:10.1029/2006JD008201.

Lawrence, M. G., Butler, T. M., Steinkamp, J., Gurjar, B. R., and Lelieveld, J.: Regional pollution potentials of megacities and other major population centers, *Atmos. Chem. Phys.,* 7, 3969-3987, 2007.

Lin, M., T. Oki, M. Bentsson, T. Holloway, D.G. Streets, and S. Kanae (2008), Long-range transport of acidifying substance in East Asia-Part I: Model evaluation, Atmos. *Environ.*, in review.

Liu, Y.; P. Koutrakis, R Kahn (2007), Estimating fine particulate matter component concentrations and size distributions using satellite-retrieved fractional aerosol

optical depth: Part 1 - Method development, *Journal Of The Air & Waste Management Association*, 57 (11): 1351-1359.

LRTAP (2007), Hemispheric Transport Of Air Pollution 2007. United Nations *Report*: Air Pollution Studies No. 16. ISSN 1014-4625, ISBN 978-92-1-116984-3.

Ma, Y., A.T. Russell, G. Marston (2008), Mechanisms for the formation of secondary organic aerosol components from the gas-phase ozonolysis of α–pinene, Phys. Chem. Chem. *Phys.,* 10, 4294-4312, doi: 10.1039/b803283a.

Mitchell, T.D, and P.D. Jones (2004), An improved method of constructing a database of monthly climate observations and associated high-resolution grids, *Int. J. Climatol.*, **25** (6), 693-712, doi: 10.1002/joc.1181.

National Oceanic and Atmospheric Administration (1976), *U.S. Standard Atmosphere*, U.S. Government Printing Office, Washington, DC, NOAA-S/T76-1562.

Nenes A., S.N. Pandis, and C. Pilinis (1998). ISORROPIA: A new thermodynamic equilibrium model for multiphase multicomponent inorganic aerosols, *Aquat. Geoch.*, 4(1), 123-152, doi:10.1023/A:1009604003981.

Olerud, D., and A. Sims (2004), MM5 2002 modeling in support of VISTAS (Visibility Improvement—State and Tribal Association), Baron Adv. Meteorol. Syst. , LLC, Research Triangle Park, N.C. (Available at http://www.baronams.com/projects/VISTAS)

Pleim, J. E., A. Xiu, P. L. Finkelstein, and T. L. Otte, 2001: A coupled land-surface and dry deposition model and comparison to field measurements of surface heat, moisture, and ozone fluxes, *Water Air Soil Pollut. Focus*, 1, 243–252.

Reuscher, T., R. Schmoyer, and P. Hu (2002). Transferability of Nationwide Personal Transportation Survey data to regional and local scales. *Transportation Research Record*, 1817, 25-32.

Schell, B., I.J. Ackermann, H. Hass, F.S. Binkowski, and A. Ebel (2001), Modeling the formation of secondary organic aerosol within a comprehensive air quality model system, *J. Geophys. Res.*, 106, 28275-28293, doi:10.1029/2001JD000384.

Sickles, J.E., and D.S. Shadwick (2007), Seasonal and regional air quality and atmospheric deposition in the eastern United States, *J. Geophys Res.*, 112(D17), D17302, doi: 10.1029/2006JD008356.

Stanier, C.O.; N. Donahue, N, S.N. Pandis (2008), Parameterization of secondary organic aerosol mass fractions from smog chamber data, *Atmos. Environ.*, 42, 2276-2299 , doi: 10.1016/j.atmosenv.2007.12.042

Stockwell, W. R., P. Middleton, J. S. Chang, and X. Tang (1990), The second generation regional acid deposition model chemical mechanism for regional air quality modeling. *J. Geophys. Res.*, 95, 16 343–16 367.

Stone, B., A. Mednick, T. Holloway, and S.N. Spak (2007), Is Compact Growth Good For Air Quality? Journal of the American Planning Association, 73:4, 404-418. doi: 10.1080/01944360708978521.

Stone, B., A. Mednick, T. Holloway, and S.N. Spak (2008), Climate Change Mitigation through Smart Growth Development and Vehicle Fleet Hybridization (*Environmental Science & Technology*, in review).

Streets, D. G., et al. (2003), An inventory of gaseous and primary aerosol emissions in Asia in the year 2000, *J. Geophys. Res.*, *108*(D21), 8809, doi:10.1029/2002JD003093.

Tie, X., G.P. Brasseur, L.K. Emmons, L.W. Horrowitz, and D. Kinnison (2001), Effects of aerosols on tropospheric oxidants: A global model study. *J. Geophys. Res.*, 106, 22, 931-22, 964.

Tie, X., S. Madronich, S. Walters, D.P. Edwards, P. Ginoux, N. Mahowald, R. Zhang, C. Lou, and G. Brasseur (2005), Assessment of the global impact of aerosols on troposheric oxidants. *J. Geophys. Res.,* 100 (D03204), doi:10.1029/2004JD005359.

US EPA (2005a), Clean Air Interstate Rule Emissions Inventory Technical Support Document, *Docket* OAR-2003-0053-2047, U.S. Environmental Protection Agency, Research Triangle Park, N.C.

US EPA (2005b), Technical Support Document for the Final Clean Air Interstate Rule--Air Quality Modeling, *Docket* OAR-2003-0053-2151, U.S. Environmental Protection Agency, Research Triangle Park, N.C.

US EPA (2005c), CMAQ Model Performance Evaluation for 2001, *Docket* OAR-2003-0053-1716, U.S. Environmental Protection Agency, Research Triangle Park, N.C.

Woods & Poole Economics (2005), Complete economic and demographic data source (CEDDS) 2005. Washington, DC: Woods and Poole Economics, Incorporated.

Yu, S., R. Mathur, K. Schere, D. Kang, J. Pleim, J. Young, D. Tong, G. Pouliot, S. A. McKeen, and S. T. Rao (2008), Evaluation of real-time PM2.5 forecasts and

process analysis for PM2.5 formation over the eastern United States using the Eta-CMAQ forecast model during the 2004 ICARTT study, *J. Geophys. Res.*, 113, D06204, doi:10.1029/2007JD009226.

Zhong, S., H.J. In, X. Bian, J. Charney, W. Heilman, and B. Potter (2005), Evaluation of Real-Time High-Resolution MM5 Predictions over the Great Lakes Region. *Wea. Forecasting*, 20, 63–81, doi: 10.1175/WAF-834.1.

# Chapter 3. The Present State of Aerosols and Ozone in the Great Lakes Region

From: Scott N. Spak and Tracey Holloway (2009), Seasonality of Speciated Aerosol Transport over the Great Lakes Region, *J. Geophys. Res.*, in press.

## 3.1. Introduction

The Great Lakes, with their large volume and high heat capacity, have a dramatic influence on regional climate and air quality. The response of tropospheric $O_3$ to lake effect meteorology is pronounced, with maximum, summertime ground-level $O_3$ concentrations often located in the center of southern Lake Michigan and over Lake Erie. This above-lake build-up, and subsequent outflow to adjacent coastal areas, has been explained by the shallow, stable marine boundary layer and light southerly winds above the lake, which trap emissions close to the lake surface, enhancing photochemistry and directing polluted air back onshore [*Lyons and Cole*, 1976; *Wolff et al.*, 1977; *Sillman et al.*, 1993; *Dye et al.*, 1995; *Hanna and Chang*, 1994; *Eshel and Bernstein*, 2006]. Here, we examine the degree to which a chemical transport model (CTM) is able to adequately simulate speciated aerosols (PM) in this important region. Whereas $O_3$ is only a summertime problem, PM is a year-round pollutant in the Upper Midwestern U.S. and southern Canada, affected by summer photochemistry, winter storm systems, and seasonal patterns in emissions. Evaluating the degree to which a CTM can capture species-by-species seasonality, variability, and spatial patterns is a first step toward understanding how individual processes contribute to regional PM pollution.

Studies to date have shown that about 80% of $PM_{2.5}$ in the region is secondary, formed through condensation and chemical reactions among precursor gases [*Lee et al.*, 2003; *Rao et al.*, 2003; *Kerr et al.,* 2004]. In particular, secondary $SO_4^{2-}$, $NO_3^-$, ammonium ($NH_4^+$), and organic mass (OM) dominate in both urban and rural areas. On an annual basis, particulate levels in urban areas tend to be 30% higher than in rural areas, with the urban excess due mostly to carbonaceous aerosols [*Rao et al.*, 2003]. Multiple studies have attributed aerosol mass around the Great Lakes to emissions from motor vehicles as well as regionally dispersed secondary $SO_4^{2-}$ and $NO_3^-$ [*Lee et al.*, 2003; *Sheesley et al.*, 2004; *Kim et al.*, 2005, 2007; *Buzcu-Guven et al.,* 2007, *Rizzo and Scheff*, 2007; *Zhao and Hopke*, 2006; *Zhao et al.*, 2007]. On average, natural sources account for approximately 25% of observed aerosol mass, with 6% of observed $PM_{2,5}$ mass contributed by salt and soil [*Kim et al.*, 2005; *Malm et al.*, 2004]. The less volatile oxidation products of biogenic emissions from forests and croplands contribute about 20% to OM at background sites [*Malm et al.*, 2004], and up to 100% in remote forested areas of the region [*Sheesely et al.*, 2004].

The Great Lakes region has been included in larger spatial domains in numerous chemical transport modeling studies, particularly for model evaluation, but it has not been the focus of regional model aerosol studies to date. *Mebust et al.* [2003] established that summertime aerosol performance in the Community Multiscale Air Quality model (CMAQ) with a reactive aerosol module performed best for summertime $SO_4^{2-}$, with a

negative bias for $PM_{2.5}$ and its other components. In a model intercomparison between CMAQ and CAMx, *Tesche et al.* [2006] found that model bias for speciated aerosols was generally high in the winter and low in the summer, and that model performance was nearly identical on 12 km and 36 km grid systems in both models. *Gégo et al.* [2006] find that CMAQ better simulates longer-term weekly fluctuations in $SO_4^{2-}$ and $NO_3^-$ concentrations than day-to-day variability. *Phillips and Finkelstein* [2006] found that CMAQ was particularly skillful in simulating annual and summertime patterns in $SO_4^{2-}$ – including the continental summer maximum over Indiana and Ohio—and annual and winter $NO_3^-$, but underestimated the intensity and extent of the summer continental $NH_4^+$ maximum over Indiana and Ohio. Simulations with CAMx [*Baker*, 2006] and PMCAMx [*Gaydos et al.*, 2007; *Karydis et al.*, 2007] found consistent agreement with daily observations of $PM_{2.5}$ and its constituents. A climate sensitivity study of speciated aerosols in the region [*Dawson et al.*, 2007] found a strong response of $PM_{2.5}$ to changes in temperature, mixing height, wind speed, and humidity in both winter and summer, along with locally varying sensitivity to precipitation. Here, we diagnose CMAQ performance for a range of individual species, consider how these modeled distributions reflect atmospheric processes, and compare our results with earlier studies.

### 3.2. Data and Methods

Model results were compared with 2002 observations from several national monitoring networks. Samples from the EPA Speciation Trends Network (STN) [*US EPA*, 2001] each day and IMPROVE [*Malm et al.,* 2004] every 3 days, along with

weekly observations from the Clean Air Status and Trends Network (CASTNet) [*Sickles and Shadwick*, 2007], provide aerosol concentration and speciation at representative urban, rural, and remote locations, respectively. For each network, all sites in the states of Illinois, Indiana, Minnesota, Michigan, Ohio, and Wisconsin were included in the study (40 STN, 14 CASTNet, 6 IMPROVE). The given citations detail the methods and uncertainty associated with each of the measurement protocols. Simulation of aerosol number concentration was assessed using hourly data from the Bondville, Illinois, NOAA Global Monitoring Division site, co-located with CASTNet observations.

### 3.3. Model Performance Evaluation

Aerosol seasonality is considered monthly and in the four seasons: January – March (JFM); April – June (AMJ); July – September (JAS); October – December (OND). These definitions of the four seasons are delayed one month from the standard seasonal definitions to better capture cycles in lake-land temperature gradient, with land and lake both coldest in JFM; land warmer than lake in AMJ; land and lake both warmest in JAS; and lake warmer than land in OND. These patterns were defined both from the MM5 modeled meteorology and from measured surface temperatures taken at NOAA buoy 45007 in southern Lake Michigan and at the NOAA National Weather Service station at the Dane County Regional Airport in Madison, Wisconsin, at the same latitude approximately 150 km upwind of the lake. This lake-land seasonal cycle is nearly identical to that reported for Lake Erie, except that the shallower Lake Erie is ice-covered more frequently and completely [*Schertzer et al.*, 1987].

Model predictions are compared with surface observations using model bias, error, normalized mean bias, normalized mean error, fractional bias (FB), fractional error (FE), and the coefficient of determination ($r^2$) between predicted-observed pairings as performance metrics:

$$Bias = \frac{1}{N}\sum_{i=1}^{N}(P_i - O_i) \qquad Error = \frac{1}{N}\sum_{i=1}^{N}|P_i - O_i|$$

$$FB = \frac{2}{N}\sum_{i=1}^{N}\left(\frac{P_i - O_i}{P_i + O_i}\right) \qquad FE = \frac{2}{N}\sum_{i=1}^{N}\frac{|P_i - O_i|}{P_i + O_i}$$

where $P_i$ is the predicted value of the concentration at monitor $i$, $O_i$ is the observed concentration at monitor $i$, and $N$ is the total number of prediction-observation pairings used for the comparison. Fractional bias and error are particularly useful model performance indicators because they are unitless, symmetrical (equally weighting positive and negative biases), and bounded: values for FB range between -2.0 (extreme underprediction) to +2.0 (extreme overprediction), while FE ranges between 0.0 and 2.0. Values of the FB that are equal to -0.67 are equivalent to underprediction by a factor of two, while values of the FB that are equal to +0.67 are equivalent to overprediction by a factor of two. For Table 3-1 and all subsequent analogous tables, we present monthly mean observed and modeled concentrations at each observational network, along with FB, FE, and $r^2$ for all predicted-observed pairings in that month.

*3.3.1. Aerosol mass concentrations ($PM_{2.5}$ and $PM_{10}$)*

Performance for all PM species at IMPROVE, STN, and CASTNet sites is summarized in Figure 3-1, a bugle plot [*Boylan and Russell*, 2006] displaying aggregate model fractional bias as a function of increasing concentration level. The plot also includes PM model bias performance goals (±30%) and performance criteria (±60%) suggested by *Boylan and Russell* [2006]. CMAQ captured monthly $PM_{2.5}$ variation well (Table 3-1). CMAQ performance against STN $PM_{2.5}$ observation is much better from April to July, when CMAQ matches monthly mean values for the network observations very well (fractional bias ≤ 0.1, error < 0.6 $\mu g/m^3$). From September to March, CMAQ captures month-to-month variability but consistently overpredicts $PM_{2.5}$ due to biases in $NO_3^-$, $NH_4^+$, OM, and unspeciated fine mass. Modeled $PM_{2.5}$ variability at IMPROVE sites show a substantial underprediction of peak values (Figure 3-2) in June and July, explained by the low bias in summertime OM, and an overestimation of $PM_{2.5}$ in the winter, due mostly to overprediction in $NO_3^-$, OM, and unspeciated mass (not shown).

CMAQ calculates $PM_{10}$ as the sum of $PM_{2.5}$, coarse mode soil and crustal material, and other unspecified coarse mode material; sea salt aerosol is negligible over the region in both CMAQ and source-apportioned observations [*Kim et al.*, 2005]. Regional $PM_{10}$ is consistently underestimated from March through September at the rural IMPROVE sites, with CMAQ's unspeciated coarse mode aerosols, which comprise 30% of simulated $PM_{10}$ mass, contributing a consistent negative bias. *Tesche et al.* [2006]

attribute the negative $PM_{10}$ bias to CMAQ's simulation of all speciated aerosols in Aitken and accumulation modes only. Sectional aerosol modeling, which resolves aerosols in explicit size bins, is required to model coarse particle speciation, improve performance potential for $PM_{10}$, and model the ultra-giant particles that have been documented downwind of the Great Lakes [*Lasher-Trapp and Stachnik*, 2007].

Considering performance independent of concentration, fractional bias and fractional error results are summarized in Table 3-2 according to four levels of performance suggested by *Morris et al*. [2005]. We note that performance is good or excellent for 91 of 168 species-month-network pairs (52%), and only problematic for 23 (14%). When aggregated to seasonal profiles at all observational networks, only the underestimation of low $NO_3^-$ concentrations in spring and summer (Figure 3-3) is problematic with respect to contemporary performance standards. While the performance of our 2002 simulation is encouraging, especially considering that biomass burning emissions were not specific to our study year, we note that no CMAQ modeled species can be classified as good or excellent at all networks throughout the year.

A comparison of simulated seasonal mean $PM_{2.5}$ speciation versus that measured at the STN network monitors in the study domain is presented in Figure 3-3. Despite errors in the total $PM_{2.5}$ mass, modeled seasonal speciation profiles are generally consistent with observations, including the summertime maximum in $SO_4^{2-}$ and wintertime maximum in $NO_3^-$. Despite biases in their concentrations, the relative

abundances of EC and $NH_4^+$ are especially well simulated, with regionally-averaged seasonal predictions of their percentage contribution to total $PM_{2.5}$ mass of 3.5% to 4.2% (EC) and 11.0% to 13.0% ($NH_4^+$). These fractional contributions never differ from observed estimates of $PM_{2.5}$ speciation by more than 1.2%% and 2.8%, respectively, and EC contribution to PM2.5 is within 0.1% in summer and fall. The relative abundance of organic matter is very well simulated at urban sites in winter (observed fraction = 21.4%, modeled fraction = 21.6%), but erroneous throughout the rest of the year, The overprediction of $SO_4^{2-}$ in summer and fall, underprediction of OM from April to December, and overprediction of unspeciated CMAQ fine particle mass in fall and winter contribute most significantly to total $PM_{2.5}$ biases.

To better evaluate the processes controlling CMAQ representation of $PM_{2.5}$ and its component species we examine seasonal spatial patterns for each compound. Seasonality of spatial patterns in simulated $PM_{2.5}$ mass is rather limited, as shown in Figure 3-4. Regional average concentrations of ~15 $\mu g/m^3$ are characteristic over a wide area in all seasons, but the spatial extent of this area is smallest in spring (AMJ), extending from southeastern Wisconsin, southern Michigan, and eastern Illinois into Indiana, Ohio, and neighboring states. In other seasons, the extent of this ~15 $\mu g/m^3$ or greater region is wider, extending furthest west in autumn (OND), and reaching the highest concentrations throughout Indiana (the state with most persistent high regional $PM_{2.5}$) in summer (JAS). Seasonal mean concentrations in excess of 25-30 $\mu g/m^3$ are seen in the Chicago region year-round (lowest in AMJ). Spatial patterns in seasonal averages of $PM_{2.5}$ follow those

of $NH_4^+$ (Suppl. Fig. 3-1), with a correlation coefficient $r > 0.94$ between the regional maps for all four seasons. This reinforces the importance of rural area sources in the regional aerosol burden throughout the year. Seasonal spatial patterns in $PM_{10}$ (not shown) are very similar to $PM_{2.5}$, but with wider regions of Indiana and Illinois exhibiting concentrations of ~25 $\mu g/m^3$ and higher in winter, summer, and fall, and even more intense local urban hot-spots than appear in the $PM_{2.5}$ figures.

### *3.3.2 Sulfate ($SO_4^{2-}$)*

Like total $PM_{2.5}$, $SO_4^{2-}$ (Figure 3-5) shows a regional spatial signal typical with a minimum over the forested, lightly populated areas north of Lake Superior to maxima downwind of Chicago and in the Ohio River Valley (ORV). A regional cloud of $SO_4^{2-}$ is found over the southeastern portions of the region throughout the year, with a minimum in winter and a maximum in summer, with wide areas in southern Illinois, southern Indiana, and southern Ohio with concentrations from 9 – 11 $\mu g/m^3$. These areas of high $SO_4^{2-}$ have been extensively attributed to coal-fired power plants in the ORV [e.g. *Kim et al.*, 2007; *Zhao et al.*, 2007]. Additional major sources include local emissions from metal smelting and refining operations, as well as urban plumes from Chicago, St. Louis, and other major cities.

Monthly variations in $SO_4^{2-}$ performance are shown in Table 3-3. Observations at all sites exhibit peak values in June and July with a secondary peak in September, a

pattern which CMAQ captures at the IMPROVE sites better than at CASTnet or STN. Overall, sulfate is consistently underpredicted in winter and overpredicted in summer (especially at urban sites), as also found by *Tesche et al*. [2006]. Since there is limited seasonality in primary emissions, and trends in model performance are consistent throughout the winter and summer, these seasonal biases are likely due to modeled representation of heterogeneous chemical processes rather than deposition or emissions. On an annual basis, CMAQ tends to overestimate low concentrations (<1 $\mu g/m^3$) and underestimate the occurrence of concentrations in the range of 2-7 $\mu g/m^3$. Simulated daily and weekly variability in $SO_4^{2-}$ concentration is well correlated with observations, with annual time series for all sites yielding $r^2 > 80\%$ for CASTNet and IMPROVE. Urban STN sites had a lower daily $r^2$ value of 68% on an annual basis, as local condensation of urban $SO_2$ emissions is less correlated with meteorological variability than regionally transported background $SO_4^{2-}$.

### *3.3.3. Nitrate ($NO_3^-$)*

Figure 3-6 shows seasonal patterns in surface $NO_3^-$ concentrations, which exhibit a seasonality almost exactly opposite that of $SO_4^{2-}$, with maximum concentrations in fall (OND) and winter (JFM). As simulated in CMAQ, $NO_x$ emissions from urban sources condense as they are transported, leading to $NO_3^-$ maxima downwind of Chicago and Detroit in the winter. In spring and summer, when higher temperatures cause $NO_y$ to partition mostly to the gas phase, local peaks in aerosol $NO_3^-$ are evident over the large

metropolitan areas of the region, with only trace amounts in rural and remote areas. In fall, and to a less pronounced degree in winter, regional background $NO_3^-$ is not consistently advected across the southern lakes (Michigan, Huron, and Erie), so above-lake concentrations are noticeably lower than surrounding regional air. Cyclonic airflow around the southern portions of each lake, rotating around the low-pressure centers above the warm water, suppresses cross-lake transport, thus leading to low above-lake $NO_3^-$ concentrations (Figure 3-6d).

Nitrate's seasonality, with a December peak and August minimum, is adequately simulated. However, CMAQ also includes an anomalous secondary peak in March, with an average overprediction in excess of 0.9 $\mu g/m^3$ across each of the networks. This bias, the largest for any month, is greatest at urban STN sites (1.17 $\mu g/m^3$), but more significant at IMPROVE sites, where the error represents an overprediction in excess of 80%. Table 3-4 highlights an overprediction in winter at all networks, consistent with *Mathur et al.* [2008]. Despite overprediction in winter and underprediction in summer, model bias is only conclusively beyond the range of measurement uncertainty for the high concentrations found in March, November, and December, when such measurement uncertainty would also be at a minimum [*Karlsson et al.*, 2007]. Possible reasons for these discrepancies between CMAQ and observations of aerosol $NO_3^{2-}$ include the use of equilibrium gas-aerosol partitioning, uncertainties in the uptake of nitric acid by aerosols, heterogeneous reactions on the surface of aerosols, and measurement uncertainties for total (gaseous + aerosol) ammonia/ammonium and

sulfate/sulfuric acid *Yu et al*., 2005]. Daily and weekly variability in $NO_3^-$ observations is simulated in CMAQ with less fidelity than $SO_4^{2-}$, with $r^2$ of 58% for STN (daily), 63% for IMPROVE (daily), and 75% for CASTNet(weekly), based on annual time series.

### *3.3.4. Ammonium ($NH_4^+$)*

Ammonium in the Midwest is dominated by dispersed area ammonia ($NH_3$) emissions from agricultural fertilizers, including anhydrous ammonia and manure spreading. These agricultural patterns are most evident in summer (Supp. Fig. 1). Local enhancement by conversion of $NO_x$ and nitric acid leads to urban peaks of comparable magnitude throughout the year, especially in the vicinity of Chicago, and industrial areas of Indiana and Ohio in winter and fall.

While seasonality in $SO_4^{2-}$ and $NO_3^-$ is the result of seasonal climate differences determining the condensation rates of relatively constant precursor emissions, $NH_4^+$ has no simple seasonal cycle, driven instead primarily by the seasonality of agricultural practices. Here, the $NH_3$ emissions inventory and its seasonal variation is a critical factor, and *Gilliland et al*. [2006] demonstrated through inverse modeling with CMAQ that the NEI 2001 inventory used is reasonable, but may be slightly biased high in winter and low in summer. Our CMAQ simulation of $NH_4^+$ is quite skillful throughout the year—more so at the rural CASTNet sites than for urban areas, as shown in Table 3-5. We note that in

our simulation, there is no apparent seasonality to CMAQ bias. The complicated monthly variations in $NH_4^+$ concentrations are captured well by CMAQ, although monthly variability in response to the cycle of agricultural emissions is exaggerated. Ammonium time series correlation with observations was similar to $NO_3^-$, with $r^2$ of 63% (STN) and 70% (CASTNet).

*3.3.5. Carbonaceous Aerosols*

Both elemental carbon (EC) and organic carbon (OC) are simulated in CMAQ. EC is a non-reactive primary pollutant dominated by emissions in urban areas. Organic carbon, calculated as the total mass of organic aerosols (i.e. organic mass, OM), is comprised of directly emitted (primary) OC, as well as secondary organic aerosols (SOA) from both biogenic and anthropogenic precursor emissions.

Elemental carbon concentrations are highest in all seasons near urban areas, with limited transport from these emissions hotspots. As shown in Table 3-6, simulated urban concentrations, captured by the STN network sites, are representative throughout most of the year, although there is a strong positive bias in the winter, peaking in January at 0.52 $\mu g/m^3$. This bias has been suggested as an emissions overestimate by *Lane et al.* [2007] and supported by *Karydis et al.* [2007]. In all seasons, regional background concentrations from area sources and long-range transport are less than half of urban levels. Rural concentrations from the IMPROVE sites are underestimated from May

through October, but winter performance is very good, with monthly average network-wide concentrations simulated to within 0.001 $\mu g/m^3$. The improved correlation between CMAQ and observations at the IMPROVE network (49%) versus STN (27%) indicates that large-scale transport processes affecting rural areas are better simulated than local emissions and dispersion from urban areas.

The regional spatial extent of total modeled OM is very similar to the patterns in EC, but with concentrations 5 to 10 times greater (Table 3-7). In January, when modeled and observed OM is dominated by primary emissions, the spatial correlation (r) between month mean EC and OM concentrations reaches 0.97. Overall, seasonal variation in the regional burden of OM is poorly represented in CMAQ. Modeled OM is positively biased in winter, and negatively biased in summer. The summertime underprediction is likely due to the CMAQ's insufficient SOA formation at high temperatures and relative humidity. Modeled and observed daily time series vary widely in skill from month to month, with monthly $r^2$ ranging from 3% to 36% (STN) and 1% to 72% (IMPROVE). Despite these problems, OM concentrations are simulated in spring and fall with very little bias in both urban and remote areas.

In comparing model and measured organic aerosols, it is necessary to convert total calculated OM with the measured OC. We employ the conventional value of 1.4 to inflate OC measurements to modeled OM, consistent with the IMPROVE methodology and prior observational studies in the region [e.g. *Offenberg and Baker*, 2000]. Since

CMAQ employs an internal conversion factor of 1.2 to convert OC to OM in the model, we inflate CMAQ modeled primary OM output by 1.167 to ensure consistency with the 1.4 factor applied to observations (*i.e.* 1.2 x 1.167 = 1.4), following *US EPA* [2005b, 2005c]. This OM/OC ratio is considerably lower than that estimated by recent studies, including 1.81 ± 0.07 observed by *Bae et al.* [2006a] in St. Louis; 1.5-1.9 found in upstate New York [*Bae et al.*, 2006b]; 1.7±0.2, the annual average at 38 IMPROVE sites [*Malm and Hand*, 2007]; and 1.6 (urban) and 2.1 (non-urban) recommended by *Turpin and Lim* [2001]. It is, however, within the wide 1.1-1.9 range suggested by *Chen et al.* [2006] for August conditions in the Eastern U.S. This variation in OC/OM rations suggests that a more sophisticated algorithm should be deployed for the interpretation of model predictions of OM, and the application of a single conversion factor may contribute to the negative bias in our predicted OM. Still, uncertainty associated with the OM/OC factor does not explain the very poor representation of seasonal and daily variability.

One advantage of model-based aerosols analysis is the ability to estimate primary and secondary contributions to OM, and identify the sources of these aerosols. Consistent with previous studies by *Yu et al.* [2007] and *Karydis et al.* [2007], we find that OM in the Midwest is dominated by the primary component, with the contribution of primary to total OM varying seasonally from 52% in June to 70% in January. Accurate representation of the sources and formation pathways of SOA remains a challenge, and our chemical mechanism in CMAQ, like that of most contemporary global and regional

CTMs, currently underestimates SOA [e.g. *Bhave et al*., 2007; *Zhang et al*., 2006a; *Zhang et al*., 2006b]. Because there are no routine SOA measurements in this region, we compare our SOA performance with that of other published regional studies. *Robinson et al*. [2007] found SOA account for more than 80% of summertime OM in PMCAMx except in urban areas. Other analyses using chemical mass balance [*Sheesley et al., 2004; Subramanian et al*. 2007] suggest that most OM is of secondary origin throughout the year in the Eastern U.S., with primary OC an equal or than SOA only in winter.

In our simulations, biogenic SOA contributes more than 50% of OM in the forested and lightly populated north of the region throughout the year, but usually contributes less than 25% of OM in polluted areas. During the spring and summer growing seasons, OM north of Lake Superior is nearly all biogenic, and biogenic SOA contributes more than 80% of total carbon mass and 40%-55% of seasonal average $PM_{2.5}$. Anthropogenic SOA also exhibits strong seasonality, but with different spatial and temporal patterns, largely driven by photochemical activity. Like $O_3$, anthropogenic SOA is photochemically produced in spring and summer over Lake Erie and Lake Michigan, particularly near urban plumes. Thus, $O_3$ and anthropogenic SOA are highly correlated over the Great Lakes in the summer (Supp. Figs. 2 and 3, Figure 4-7). Although anthropogenic SOA and $O_3$ in the Midwest are produced by similar processes, only a small fraction of simulated summertime above-lake $PM_{2.5}$ (<3%) is due to SOA. Over Lake Michigan, JAS average modeled PM2.5 is comprised mostly of $SO_4^{2-}$ (40-60%), with $NH_4^+$, primary OM, and unspeciated mass each contributing 10-20%.

Summertime OM is strongly underpredicted at sites in western Michigan, however, supporting the finding [*Robinson et al.*, 2007] that traditional SOA modules such as CMAQ's SORGAM underestimate this anthropogenic SOA production over the Great Lakes. Summertime biogenic SOA is also underestimated throughout the region due to the absence of SOA formation from photo-oxidation of isoprene, which recent modeling studies have indicated would represent an increase over our simulated SOA of 50% [*Lane and Pandis*, 2007] to 100% [*Zhang et al.* ,2007; *Liao et al.*, 2007; *van Donkelaar et al.*, 2007] of simulated SOA in this region.

*3.3.6. Aerosol Number Concentration*

Hourly observations of aerosol number concentration at Bondville, Illinois, were compared with CMAQ predictions of the sum of Aitken, accumulation, and coarse lognormal modes. Bondville is a village roughly 5 km west of the Champaign-Urbana metropolitan area, and less than 1 km from an interstate highway. It is impacted by representative levels of regional background pollution, with lesser local influences from copper smelting, metal plating, and limestone [*Buzcu-Guven et al.*, 2007]. In this environment, CMAQ simulates number concentration to the correct order of magnitude, but with a consistent negative bias (Figure 3-2h; Table 3-8). The correct order of magnitude is the only aspect of number concentration at Bondville adequately reproduced in CMAQ. Observed seasonality is not simulated and number concentration is

underpredicted in all months but September. Although our underprediction is obvious, in fact CMAQ performs better here than in other CMAQ studies simulating number concentration in Atlanta, Georgia [*Park et al.*, 2006] and the Pacific Northwest [*Elleman et al.*, 2004], which both found frequent underprediction by factors of 10 to 1000. The observed distribution for number concentration at Bondville is closer to Gaussian than the log-normal found for mass concentrations (Suppl. Fig. 4). CMAQ's trimodal system, lacking an ultrafine mode that would disperse mass across a greater number of particles, thus underpredicts aerosol abundance.

Spatial distribution in simulated aerosol number concentration is consistent with bulk aerosol mass concentrations of $PM_{2.5}$ and $PM_{10}$, but with less pronounced seasonality. Number concentration throughout the region is dominated by secondary $SO_4^{2-}$ and $NO_3^-$, and the dispersion of number concentration is highly correlated with the sum of these species (r=0.80), and more so than for either species alone. Smelting operations, evident in the localized maximum in northeast Minnesota in Figure 3-4 near taconite mining and processing facilities, generate local enhancement due to new $SO_4^{2-}$ particles comparable to the highest urban peaks over Chicago and Toronto.

## 3.4. Modeled and Observed Relationships among Aerosol Species

### *3.4.1. Interspecies Comparisons*

Relationships between time series of speciated aerosols offer unique insight into the composition of multi-species aerosol conglomerations, and highlight where the dynamics of different species are controlled by the same physical processes. For instance, ammonium sulfate and bisulfate are the most prevalent ionic aerosols in the region [*Baker*, 2006], and the relatively high correlation between $NH_4^+$ and $SO_4^{2-}$ in observed daily STN ($r^2$=67%) and CASTNet ($r^2$=62%) time series reflect the shared fate of ammonium sulfate particles. The lower correlation between OC and insoluble EC at STN sites ($r^2$=31%) reflects the different removal processes and characteristic lifetimes. Comparison of correlation relationships between species in model and measurements illustrates the extent to which model processes accurately reflect observed processes. Moreover, chemical mass balance source apportionment in the region [*Lee et al.*, 2003] has identified a chemical signature for interaction between secondary organic and inorganic aerosols, due to as-yet unidentified chemical and/or physical processes, that might be identified in a mechanistic model.

The ionic complex of $SO_4^{2-}$ and $NH_4^+$ shows weaker than expected connections in CMAQ throughout the year. Correlations between mass concentrations in CMAQ (36% CASTNet, 51% STN) are lower than in observations (62%, 67%). Although $SO_4^{2-}$ and $NH_4^+$ concentrations are less correlated than expected, interestingly, the errors in these two species are highly correlated. The normalized biases of cotemporaneous predictions of $SO_4^{2-}$ and $NH_4^+$ at CASTNet sites show an $r^2$=71%. Similarly, the normalized errors between these two species are correlated with $r^2$=74%. These strong links between both

species' error further suggest that incomplete or erroneous processes consistently impact both species at the same times. As model processes are changed or added, we suggest that this pairing may be a particularly useful metric for evaluating incremental improvements in chemical transport model performance. Nitrate and $SO_4^{2-}$ are completely uncorrelated, as would be expected, while nitrate and ammonium are weakly correlated in both model and observations. Daily correlation for $SO_4^{2-}$ with $PM_{2.5}$ is about one-third weaker in CMAQ (57% IMPROVE, 42% STN) than in observations (80%, 64%), but much stronger for $NO_3^-$ and $PM_{2.5}$ (38% IMPROVE, 49% STN, compared to observations of 9%, 23%). The simulated relationship between $NH_4^+$ and $PM_{2.5}$ (86% STN) is consistent with observations (75%). These temporal associations, when viewed in light of model bias, suggest that despite uncertainty in emissions sources [*Simon et al*., 2008], the chemical transport of $NH_4^+$ as part of a multi-species regional aerosol complex is being adequately simulated with confidence. The weaker relationships of $SO_4^{2-}$, which is simulated correctly as an independent pollutant, imply that other chemicals interacting with $SO_4^{2-}$ are not well simulated, and/or that the interactions themselves are not captured.

We find that the relationships between OC, EC, and $PM_{2.5}$ are much stronger in CMAQ than observations. EC and $PM_{2.5}$ are much more strongly correlated in CMAQ (82% IMPROVE, 69% STN) than observations (64%, 22%). The same tendency is found for OC and $PM_{2.5}$ – model comparison yielded 49% IMPROVE, 68% STN, while observed correlations were 7% and 43%, respectively. Moreover, EC and OC are also

more closely linked to each other as modeled (57%, 84%) than observed (45%, 31%), although stronger relationships (91%) have been observed in suburban Maryland in winter [*Chen et al.*, 2001]. Daily correlations with $PM_{2.5}$ in CMAQ are higher for EC and OC than for $SO_4^{2-}$, and close to $NH_4^+$, the species which *Bell et al.* [2007] found to be most closely correlated with total $PM_{2.5}$ mass in detrended daily data across the United States.

These results suggest that CMAQ underestimates—or simply does not simulate—the real-world processes that differentiate the transport and variability of OC, EC, and the secondary inorganics that contribute most to $PM_{2.5}$. The problem is greatest at urban sites near emissions sources, but also evident at remote sites, suggesting that sub-gridscale chemistry and dispersion are not entirely responsible for the missed processes. Rather, the ubiquitous overcorrelation between these species implies that important chemical or physical processes are not captured. *Robinson et al.* [2007] demonstrate that a dynamic aging and partitioning scheme for SOA and its low-volatility gas-phase precursors significantly enhances modeled SOA contribution to total OM in our study region, and produces a more realistic spatial representation of SOA. Our findings that EC and OM are overly correlated in both space and time in a traditional model are consistent with the suggestion by *Robinson et al.* [2007] that partitioning of primary organic aerosols could reduce these errors in the simulation of OM.

*3.4.2. Performance Statistics Comparisons*

Time series correlation applied to bias and error indicates whether simulated time series are damped, exaggerated, or erroneous. At the level of an observational network in aggregate, with hundreds of independent samples, these statistics allow for a preliminary attribution of error among emissions, meteorology, and model processes. In a simulation of chemistry and transport that fully resolves the chemical and physical processes that lead to observed concentrations, temporal variability in bias and error would not consistently be strongly correlated (or anti-correlated) with either observations or model output: differences would approach random and, if they had any structure, would be normally distributed, with $r^2 \approx 0$ with both observations and predictions. At the opposite extreme, a simple system with an invalid model might display an invariant observation but a series of variable model predictions, bias and error would be exactly correlated with the model time series ($r^2 = 1.0$) and completely uncorrelated with observations ($r^2 = 0$).

Contemporary simulations of chemical transport are expected to fall between these extremes: able to simulate some but not all relevant processes, displaying structure in bias and error, and with intermediate degrees of correlation between performance statistics and both predictions and observations. If this is the case, the differences in these correlations can then indicate the relative importance of variability in modeled and observed time series on model bias.

As models of any complex nonlinear system improve over time, they may be expected follow a progression through three performance regimes. First, with gross bias, simply not simulating important aspects of observed variability. Then, with a model that is conceptually and structurally correct, but with slight parametric errors in rates of change that lead to damped or exaggerated oscillation. Then, as bulk parameters are replaced with more mechanistic or detailed probabilistic representations and rate constants are fine-tuned, performance is driven by slightly erroneous nonlinear processes or compensating errors, and might asymptotically approach zero bias and a normal bias distribution with continued model improvement. Each regime is, in general, subtler than those that precede it, so although all three types of error will likely be present in any simulation, the generalized performance regime will indicate which type of model error is most important.

These general characteristics manifest in more concrete ways in chemical transport models. We theorize that contemporary emissions inventories underestimate spatial and temporal variability. Thus, when the correlation between observed time series and bias/error is high and the correlation between the simulated time series and bias/error is low, error is a result of greater fluctuation in observations than in the model, and time-invariant properties such as emissions rates (and any similar missing consistent influences) are likely the primary cause. Meanwhile, a stronger correlation between modeled time series and bias/error indicates a consistently biased variable forcing, whether damped or exaggerated, implicating parametric errors in linear model processes

and rate constants. Finally, similar non-zero correlations between bias/error and both observed and modeled time series implicate erroneous nonlinear model processes, such as the timing of the passage of frontal systems in model meteorology.

Table 9 contains $r^2$ of bias and error with observed and modeled time series, averaged across all monitoring networks. For $NO_3^-$, $SO_4^{2-}$, $NH_4^+$, and $PM_{2.5}$, we find that modeled time series are much more highly correlated with bias and error than observations at all networks. For these species, the model:bias ratio is more than 5 times the observations:bias ratio, and the model:error ratio is consistently double the observations:error ratio, approaching 50%. We conclude that model performance for secondary inorganic aerosols is likely limited by CMAQ's representation of model processes that govern condensation, growth, and chemical yields. $PM_{10}$, as the sum of all modeled species, demonstrates no consistent source of model uncertainty.

In contrast, bias and error for OM is correlated in observations with $r^2$ more than 3 times greater than the model time series. At IMPROVE sites, especially, observations are very strongly correlated with bias (78%) and error (73%) and completely uncorrelated with CMAQ (2% and 3%, respectively). This suggests that either regional biogenic emissions rates are more erroneous than primary OM emissions in urban areas; that important, pervasive processes are not simulated; or potentially both.

At first glance, correlation relationships for EC are nearly equal, suggesting that nonlinear processes are responsible. This is consistent with the model treatment, where meteorology-driven transport, dispersion and removal are the only processes affecting this non-reactive, hydrophobic species. However, attribution of EC bias is highly dependent on site orientation: at remote IMPROVE sites, regional background observations are slightly correlated with bias (30%) and error (33%) and completely uncorrelated with CMAQ (4%, 1%) – indicative of a consistent bias in local emissions or regional background concentrations. At STN sites, this is reversed, and bias and error are correlated with CMAQ results (45%, 48%) but not with observations (8%, 14%). This suggests that the positive bias is due to an underestimation of transport away from urban emissions sources. This may be due to the coarse resolution or a positive bias in deposition rates.

Taken together, these results broadly support our hypotheses from both direct bias and error statistics and correlations between species: emissions biases and missing model processes are responsible for biases in carbonaceous aerosols, while parametric details in model mechanisms are more important than emissions in CMAQ bias for secondary inorganics. However, we note that since chemical transport model performance for speciated aerosols will always be strongly affected by emissions, linear processes, and nonlinear processes, our approach only indicates which aspect of the modeling system is most responsible for variability in model performance.

### 3.5. Conclusions

We applied the CMAQ model to simulate aerosol speciation and dynamics over the Great Lakes region in an annual study for 2002. Our aim in this evaluation was to examine the skill of CMAQ over this complex region, and build understanding of chemical and physical processes controlling aerosol distribution over the Upper Midwestern U.S. and Southern Canada. In this area, $PM_{2.5}$ is a year-round air quality problem, driven by $NO_3^-$ in the winter, $SO_4^{2-}$ in the summer, and $NH_4^+$, OM, EC and other components year-round. Overall, $PM_{2.5}$ concentrations are lowest in the springtime, and lowest in regions away from major cities and the industrial facilities of the ORV. The shallow boundary layer above the Great Lakes in the spring (cool lake, warm land) enhances SOA formation in a manner analogous to near-surface $O_3$. This enhancement persists into the summer (JAS), but the lake effect is less pronounced as the water and land temperature equalize. In the fall (warm lake, cool land), circulations around the lakes lead to above-lake minima, most notable in maps of $NO_3^-$ and total $PM_{2.5}$. Anthropogenic emissions of aerosols and their precursors are shown to have little seasonality, highlighting the importance of seasonal climate variability in aerosol concentrations.

We find that CMAQ performance is good or average for most speciated aerosols at three representative observational networks. The model shows the greatest errors in simulating low spring and summer $NO_3^-$ concentrations, as well as unspeciated fine and coarse aerosol mass. These species-by-species comparisons indicate general overestimates of $PM_{2.5}$ in fall and winter months, and overestimate of $PM_{10}$ in summer

months. Overall performance statistics are generally comparable to prior modeling studies in larger spatial domains covering eastern North America, with some notable exceptions. We find CMAQ 2002 annual performance for $NO_3^-$, $NH_4^+$ and OM much improved over *Tesche et al*. [2006], but differences in emissions, meteorology, and model configuration contribute uncertainty as to the source of this improvement. Our errors in $NO_3^-$ are comparable to errors in $SO_4^{2-}$ for most of the year, consistent with *Karydis et al*. [2007] but differ from other recent modeling studies [e.g. *Tesche et al*., 2006; *Yu et al*., 2005] which find that $SO_4^{2-}$ is simulated much better than $NO_3^-$. Sulfate performance is superior to that found with PMCAMx using the same meteorology [*Karydis et al., 2007*], while July OM [*Gaydos et al.,* 2007; *Karydis et al.,* 2007] is considerably less skillful, likely due to our study's insufficient biomass burning emissions and limited SOA formation pathways. Skill in simulating OM for other seasons, and ratios of primary to secondary OM are highly consistent with the results of *Karydis et al*. [2007], despite different representations of SOA. Bias and daily correlations with observations at IMPROVE sites for $SO_4^{2-}$, OC, $PM_{2.5}$, and $PM_{10}$ are slightly improved over an earlier CMAQ study using the same aerosol mechanism in June [*Mebust et al*., 2003], while summertime $NO_3^-$ remains substantially underpredicted. Seasonal spatial patterns in $PM_{2.5}$ are similar to those simulated in PMCAMx by *Karydis et al*. [2007], *Gaydos et al*. [2007], and *Dawson et al*. [2007], but differ in extent and intensity.

We analyze time series of simulated and observed concentrations to evaluate whether CMAQ is capturing the physical and chemical processes that link and/or

differentiate aerosol species. We find that CMAQ underestimates the correlation between $SO_4^{2-}$ and $PM_{2.5}$, which – combined with an independent evaluation of $SO_4^{2-}$ showing simulation skill – suggest that interactions between $SO_4^{2-}$ and other $PM_{2.5}$, constituents are not adequately captured. In contrast, EC, OC, and $PM_{2.5}$ are overly correlated, indicating that CMAQ is missing important processes that distinguish the emissions, chemistry, and transport of carbonaceous aerosols. To understand why modeled chemical and physical processes diverge from the observed atmospheric system, process analysis, data assimilation, and adjoint studies would be excellent techniques to apply to the relationships among speciated aerosols in this region.

**References**

Bae, M.S., J.J. Schauer, and J.R. Turner (2006a), Estimation of the monthly average ratios of organic mass to organic carbon for fine particulate matter at an urban site, *Aerosol Sci. Tech.*, 40 (12), 1123-1139, doi: 10.1080/02786820601004085.

Bae, M.S., K.L. Demerjian, and J.J. Schwab (2006b), Seasonal estimation of organic mass to organic carbon in PM2.5 at rural and urban locations in New York state, *Atmos. Environ.,* 40(39), 7467-7479, doi:10.1016/j.atmosenv.2006.07.008.

Baker, K. (2006), Photochemical Model Performance for PM2.5 Sulfate, Nitrate, Ammonium, and pre-cursor species SO2, HNO3, and NH3 at Background Monitor Locations in the Central and Eastern United States, Presentation to the 5th annual CMAS Conference, Research Triangle Park, NC, 16 October 2006.

Bell, M.L., F. Dominici, K. Ebisu, S.L. Zeger, and J.M. Samet (2007), Spatial and temporal variation in PM2.5 chemical composition in the United States for health effects studies, *Environ. Health Persp.*, 115(7 ), 989-995, doi:10.1289/ehp.9621.

Bhave, P.V., G.A. Pouliot, and M. Zheng (2007), Diagnostic model evaluation for carbonaceous PM2.5 using organic markers measured in the southeastern U. S., *Environ. Sci. Tech.*, 41(5), 1577–1583, doi: 10.1021/es061785x.

Boylan, J.W., and A.G. Russell (2006), PM and light extinction model performance metrics, goals, and criteria for three-dimensional air quality models. *Atmos. Environ.*, 40, 4946-4959, doi:10.1016/j.atmosenv.2005.09.087.

Buzcu-Guven, B., S.G. Brown, A. Frankel, H.J. Hafner, and P.T. Roberts (2007), Analysis and apportionment of organic carbon and fine particulate matter sources at multiple sites in the Midwestern United States, *J. Air Waste Manag. Assoc.*, 57(5), 606-619.

Byun D. W., and K. L. Schere (2006), Review of the governing equations, computational algorithms, and other components of the Models-3 Community Multiscale Air Quality (CMAQ) modeling system, *Appl. Mech. Rev.*, 59, 51–77, doi:10.1115/1.2128636.

Chang J.S., R.A.Brost, I.S.A.Isaksen, S.Madronich, P.Middleton, W.R.Stockwell, and C.J.Walcek (1987), A three-dimensional eulerian acid deposition model: Physical concepts and formulation, *J. Geophys. Res.,* 92, 14,681-14,700.

Chen, L.W.A., B.G. Doddridge, and R.R. Dickerson (2001), Observation of carbonaceous aerosols and carbon monoxide at a suburban site: Implication for an

emission inventory, *10th International Emissions Inventory Conference*, Denver, CO, 1-3 May, 2001.

Chen, J.J., H.T. Mao, R.W. Talbot, and R.J. Griffin (2006), Application of the CACM and MPMPO modules using the CMAQ model for the eastern United States, *J. Geophys. Res.,* 111 (D23), D23S25, doi:10.1029/2006JD007603.

Dawson, J. P., Adams, P. J., and S. N. Pandis (2007), Sensitivity of PM2.5 to climate in the Eastern U.S.: a modeling case study, *Atmos. Chem. Phys. Discuss.*, 7, 6487-6525, www.atmos-chem-phys.net/7/4295/2007.

Dye, T.S., P.T. Roberts, and M.E. Korc (1995), Observations of Transport Processes for Ozone and Ozone Precursors during the 1991 Lake Michigan Ozone Study, *J. Appl. Met.*, 34(8), 1877–1889, doi: 10.1175/1520-0450(1995)034<1877:OOTPFO>2.0.CO;2.

Elleman, R. A., R.A. Kotchenruther, D.S. Covert, C.F. Mass and J. Chen (2004). CMAQ Aerosol Number and Mass Evaluation for Pacific Northwest, *Models-3 User's Workshop*, Research Triangle Park, NC.

Eshel, G., and J.J. Bernstein (2006), Relationship Between Large-Scale Atmospheric States, Subsidence, Static Stability and Ground-Level Ozone in Illinois, USA, *Water, Air, & Soil Pollution*, 171, 111-133, doi: 10.1007/s11270-005-9021-x.

Gaydos, T., R. Pinder, B. Koo, K. Fahey, G. Yarwood, and S. N. Pandis (2007), Development and application of a three-dimensional Chemical Transport Model, PMCAMx, *Atmos. Environ.*, 41, 2594–2611, doi:10.1016/j.atmosenv.2006.11.034.

Gégo, E., P.S. Porter, C. Hogrefe, and J.S. Irwin (2006), An objective comparison of CMAQ and REMSAD performances, *Atmos. Environ.*, 40(26), 4920-4934, doi:10.1016/j.atmosenv.2005.12.045.

Gery, MW., G.Z. Whitten, J.P. Killus, and M.C. Dodge (1989), A Photochemical Kinetics Mechanism For Urban And Regional Scale Computer Modeling, *J. Geophys. Res.*, 94 (D10), 12925-12956.

Gilliland, A.B., K.W. Appel, R.W. Pinder, and R.L. Dennis (2006), Seasonal NH3 emissions for the continental united states: Inverse model estimation and evaluation, *Atmos. Environ.*, 40(26), 4986-4998, doi:10.1016/j.atmosenv.2005.12.066.

Hanna, S.R., and J.C. Chang (1994), Relations between Meteorology and Ozone in the Lake Michigan Region, *J. Appl. Met.*, 34(3), 670–678, doi: 10.1175/1520-0450(1995)034<0670:RBMAOI>2.0.CO;2.

Hogrefe, C., J. Biswas, B. Lynn, K. Civerolo, J.-Y. Ku, J. Rosenthal, C. Rosenzweig, R. Goldberg, and P.L. Kinney (2004), Simulating regional-scale ozone climatology over the Eastern United States: Model evaluation results, *Atmos. Environ.*, 38 (17), 2627-2638, doi:10.1016/j.atmosenv.2004.02.033.

Hogrefe, C., P.S. Porter, E. Gégo, A. Gilliland, R. Gilliam, J. Swall, J. Irwin, and S.T. Rao (2006), Temporal features in observed and simulated meteorology and air quality over the Eastern United States. *Atmos. Environ.,* 40(26):5041–5055, doi:10.1016/j.atmosenv.2005.12.056.

Karlsson, V., K. Pyy, and H. Saari (2007), Measurement Uncertainty of Sulphur and Nitrogen Containing Inorganic Compounds By 1-Stage and 2-Stage Filter-pack Methods, *Water, Air, and Soil Pollution*, 182, 395-405, doi: 10.1007/s11270-007-9350-z.

Karydis, V. A., A. P. Tsimpidi, and S. N. Pandis (2007), Evaluation of a three-dimensional chemical transport model (PMCAMx) in the eastern United States for all four seasons*, J. Geophys. Res.*, 112, D14211, doi:10.1029/2006JD007890.

Kerr .SC., J.J. Schauer, and B. Rodger (2004), Regional haze in Wisconsin: sources and the spatial distribution, *J. Env. Eng. Sci.,* 3(3), 213-222, doi: 10.1139/S04-003.

Kim, E., P.K. Hopke, D.M Kenski, and M. Koerber (2005), Sources of fine particles in a rural Midwestern area, *Environ. Sci. Tech.*, 39, 4953-4960, doi: 10.1021/es04907749.

Kim, M., S.R. Deshpande, and K.C. Crist (2007), Source apportionment of fine particulate matter (PM2.5) at a rural Ohio River Valley site, *Atmos. Environ.*, 41, 9231–9243, doi:10.1016/j.atmosenv.2007.07.061.

Lane, T.E., and S.N. Pandis (2007), Predicted secondary organic aerosol concentrations from the oxidation of isoprene in the Eastern United States, *Environ. Sci. Tech.*, 41, 3984-3990, doi: 10.1021/es061312q/.

Lane, T. E., R. W. Pinder, M. Shrivastava, A. J. Robinson, and S. N. Pandis (2007), Source contributions to primary organic aerosol; Comparison of the results of a source-resolved model and the Chemical Mass Balance approach, *Atmos. Environ.*, 41, 3758– 3776, doi:10.1016/j.atmosenv.2007.01.006 .

Lasher-Trapp, S., and J.P. Stachnik (2007), Giant and ultragiant aerosol particle variability over the eastern Great Lakes region, *J. Appl. Met. Clim.*, 46(5), 651-659.

Lee, P.K.H., J.R. Brook, E. Dabek-Zlotorzynska, and S.A. Mabury (2003), Identification of the major sources contributing to PM2.5 observed in Toronto, *Environ. Sci. Tech.*, 37(21), 4831-4840, doi: 10.1021/es026473i S0013-936X(02)06473-8.

Liao, H., D. K. Henze, J. H. Seinfeld, S. Wu, and L. J. Mickley (2007), Biogenic secondary organic aerosol over the United States: Comparison of climatological simulations with observations, *J. Geophys. Res.*, 112, D06201, doi:10.1029/2006JD007813.

Lyons, W.A., and H.S. Cole (1976), Photochemical Oxidant Transport: Mesoscale Lake Breeze and Synoptic-Scale Aspects, *J. Appl. Met.*, 15(7),733–743, doi: 10.1175/1520-0450(1976)015<0733:POTMLB>2.0.CO;2.

Malm, W.C., and J.L. Hand (2007) An examination of the physical and optical properties of aerosols collected in the IMPROVE program*, Atmos. Environ.*, 41(16), 3407-3427, doi:10.1016/j.atmosenv.2006.12.012.

Malm, W.C., B.A. Schichtel, M.L. Pitchford, L.L. Ashbaugh, and R.A. Eldred (2004), Spatial and monthly trends in speciated fine particle concentration in the United States, *J. Geophys. Res., 109*(D3), D03306, doi:10.1029/2003JD003739.

Mathur, R., S. Yu, D. Kang, and K.L. Schere (2008), Assessment of the wintertime performance of developmental particulate matter forecasts with the Eta-Community Multiscale Air Quality modeling system, *J. Geophys. Res.*, 113(D2), D02303, doi:10.1029/2007JD008580.

Mebust, M.R., B.K. Eder, F.S. Binkowski, and S.J. Roselle (2003), Models-3 Community Multiscale Air Quality (CMAQ) model aerosol component: 2: Model evaluation, *J. Geophys. Res.,* 108(D6), doi:10.1029/2001JD001410.

Morris, R.E., D.E. McNally, T.W. Tesche, G. Tonnesen, J.W. Boylan, and P. Brewer (2005), Preliminary evaluation of the community multiscale air quality model for 2002 over the southeastern United States, *J. Air Waste Manag. Assoc.*, 55, 1694-1708.

Offenberg, J.H., and J.E. Baker (2000), Aerosol size distributions of elemental and organic carbon in urban and over-water atmospheres, *Atmos. Environ.*, 34(10), 1509-1517, doi:10.1016/S1352-2310(99)00412-4.

Olerud, D., and A. Sims (2004), MM5 2002 modeling in support of VISTAS (Visibility Improvement—State and Tribal Association), Baron Adv. Meteorol. Syst. , LLC, Research Triangle Park, N.C. (Available at http://www.baronams.com/projects/VISTAS)

Park, S.K., A. Marmur, S.B. Kim, D. Tian, Y. Hu, P.H. McMurry, and A.G. Russell (2006), Evaluation of Fine Particle Number Concentrations in CMAQ, *Aerosol Sci. Tech.*, 40:11, 985 – 996, doi: 10.1080/02786820600907353

Phillips, S.B., and P.L. Finkelstein (2006), Comparison of spatial patterns of pollutant distribution with CMAQ predictions, *Atmos. Environ.*, 40(26), 4999-5009, doi:10.1016/j.atmosenv.2005.12.064.

Rao, V., N. Frank, A. Rush, and F. Dimmick (2003), Chemical speciation of PM2.5 in urban and rural areas in national air quality and emissions trends report. /http://www.epa.gov/air/airtrends/aqtrnd03S.

Rizzo, M.J., and P.A, Scheff (2007), Fine particulate source apportionment using data from the USEPA speciation trends network in Chicago, Illinois: Comparison of two source apportionment models, *Atmos. Environ.*, 41(29), 6276-6288, doi:10.1016/j.atmosenv.2007.03.055

Robinson, A.L., N.M. Donahue, M.K. Shrivastava, E.A. Weitkamp, A.M. Sage, A.P. Grieshop, T.E. Lane, J.R. Pierce, and S.N. Pandis (2007), Rethinking Organic Aerosols: Semivolatile Emissions and Photochemical Aging, *Science*, 315, 1259, DOI: 10.1126/science.1133061.

Schell, B., I.J. Ackermann, H. Hass, F.S. Binkowski, and A. Ebel (2001), Modeling the formation of secondary organic aerosol within a comprehensive air quality model system, *J. Geophys. Res.*, 106, 28275-28293, doi:10.1029/2001JD000384.

Schertzer, W. M., J. H. Saylor, F. M. Boyce, D. G. Robertson, and F. Rosa (1987), Seasonal Thermal Cycle Of Lake Erie, *J. Great Lakes Res.*, 13(4):468-486.

Sickles, J.E., and D.S. Shadwick (2007), Seasonal and regional air quality and atmospheric deposition in the eastern United States, *J. Geophys Res.*, 112(D17), D17302, doi: 10.1029/2006JD008356.

Sillman, S., P. J. Samson, and J. M. Masters (1993), Ozone Production in Urban Plumes Transported Over Water: Photochemical Model and Case Studies in the Northeastern and Midwestern United States, *J. Geophys. Res.*, 98:12687-12699.

Sheesley, R. J., J. J. Schauer, E. Bean, and D. Kenski (2004), Trends in Secondary Organic Aerosol at a Remote Site in Michigan's Upper Peninsula, *Env. Sci. Tech.*, 38, 6491-6500, doi: 10.1021/es049104q.

Simon, H., D.T. Allen, and A.E. Wittig (2008), Fine particulate matter emissions inventories: Comparisons of emissions estimates with observations from recent field programs, *J. Air Waste Manag. Assoc.*, 58(2), 320-343.

Subramanian R., N.M. Donahue, A. Bernardo-Bricker, W.F. Rogge, and A.L. Robinson (2007), Insights into the primary-secondary and regional-local contributions to organic aerosol and PM2.5 mass in Pittsburgh, Pennsylvania, *Atmos. Environ.*, 41(35), 7414-7433, doi: 10.1016/j.atmosenv.2007.0.

Tesche, T.W., R. Morris, G. Tonnesen, D. McNally, J. Boylan, and P. Brewer (2006), CMAQ/CAMx annual 2002 performance evaluation over the eastern US, *Atmos. Environ.*, (40)26, 4906-4919, doi:10.1016/j.atmosenv.2005.08.046.

Turpin, B.J., and H.J. Lim (2001), Species Contributions to PM2.5 Mass Concentrations: Revisiting Common Assumptions for Estimating Organic Mass, *Aerosol Sci. Tech.*, 35(1), 602-610.

US EPA (2001), Evaluation of PM2.5 speciation sampler performance and related sample collection and stability issues. *Report* EPA-454/R-01-008, U.S. Environmental Protection Agency, Research Triangle Park, N.C.

US EPA (2005c), CMAQ Model Performance Evaluation for 2001, *Docket* OAR-2003-0053-1716, U.S. Environmental Protection Agency, Research Triangle Park, N.C.

US EPA (2008), Nonattainment Areas Map - Criteria Air Pollutants, effective date of nonattainment designations June 2008, available at http://www.epa.gov/air/data/nonat.html?us~USA~United%20States.

van Donkelaar, A., R.V. Martin, R.J.Park, C.L.Heald, T.M. Fu, H. Liao, and A. Guenther (2007), Model evidence for a significant source of secondary organic aerosol from isoprene, *Atmos. Environ.*, 41(6), 1267-1274, doi:10.1016/j.atmosenv.2006.09.051.

Wolff, G.T., P.J. Lioy; G.D. Wight; R.E. Meyers, and R.T. Cederwall, (1977), An investigation of long-range transport of ozone across the midwestern and eastern United States, *Atmos. Environ.*, 11(9), 797-802.

Yu, S., R. Dennis, S. Roselle, A. Nunes, J. Walker, B. Eder, K. Schere, J. Swall, and W. Robarge (2005), An assessment of the ability of three-dimensional air quality models with current thermodynamic equilibrium models to predict aerosol $NO_3^-$, *J. Geophys. Res.*, 110, D07S13, doi:10.1029/2004JD004718.

Yu, S., P.V. Bhave, R.L. Dennis, and R. Mathur (2007), Seasonal and Regional Variations of Primary and Secondary Organic Aerosols over the Continental United States: Semi-Empirical Estimates and Model Evaluation, *Env. Sci. Tech.*, 41, 4690-4697, doi: 10.1021/es061535g.

Zhang, Y., P. Liu, A. Queen, C. Misenis, B. Pun, C. Seigneur, and S.-Y. Wu (2006a), A comprehensive performance evaluation of MM5-CMAQ for the summer 1999 Southern Oxidants Study episode, Part II. Gas and aerosol predictions, *Atmos. Environ.*, 40, 4839– 4855, doi:10.1016/j.atmosenv.2005.12.048.

Zhang, Y., P. Liu, B. Pun, and C. Seigneur (2006b), A comprehensive performance evaluation of MM5-CMAQ for the Summer 1999 Southern Oxidants Study episode, Part III. Diagnostic and mechanistic evaluations, *Atmos. Environ.*, 40, 4856– 4873, doi:10.1016/j.atmosenv.2005.12.046.

Zhang, Y., J.P. Huang, D.K. Henze, and J.H. Seinfeld (2007), Role of isoprene in secondary organic aerosol formation on a regional scale, *J. Geophys. Res.*, 112(D20), D20207, doi:10.1029/2007JD008675.

Zhao, W.X., and P.K. Hopke (2006), Source investigation for ambient PM2.5 in Indianapolis, IN, *Aerosol Sci. Tech.*, 40(10), 898-909, doi:10.1080/02786820500380297.

Zhao, W.X., P.K. Hopke, and L.M. Zhou (2007), Spatial distribution of source locations for particulate nitrate and sulfate in the upper-midwestern United States, *Atmos. Environ.*, 41(9), 1831-1847, doi: 10.1016/j.atmosenv.2006.10.060.

## Tables

**Table 3-1.** CMAQ monthly performance for $PM_{2.5}$ and $PM_{10}$

For Table 3-1 and all subsequent tables in this chapter, model predictions are compared with surface observations at each observational network: IMPROVE, STN, and CASTNet. Monthly mean observations (Obs) are shown along with monthly mean predicted concentrations (CMAQ) in units of $\mu g/m^3$, along with fractional bias (FB), fractional error (FE), and $r^2$ (%) for all predicted-observed pairings in that month: daily, each day (STN); daily, every 3 days (IMPROVE); and weekly (CASTnet).

| Month | $PM_{2.5}$ | | | | | | | | | | $PM_{10}$ | | | | |
|---|---|---|---|---|---|---|---|---|---|---|---|---|---|---|---|
| | STN | | | | | IMPROVE | | | | | CASTNet | | | | |
| | Obs | CMAQ | FB | FE | $r^2$ | Obs | CMAQ | FB | FE | $r^2$ | Obs | CMAQ | FB | FE | $r^2$ |
| Jan. | 14.71 | 19.56 | 0.42 | 0.44 | 53 | 6.31 | 10.26 | 0.31 | 0.43 | 86 | 8.68 | 12.12 | 0.16 | 0.40 | 85 |
| Feb. | 11.12 | 13.97 | 0.30 | 0.47 | 52 | 4.91 | 6.86 | 0.26 | 0.42 | 71 | 6.68 | 8.08 | 0.06 | 0.36 | 71 |
| Mar. | 11.70 | 13.88 | 0.17 | 0.39 | 63 | 6.24 | 7.57 | -0.12 | 0.56 | 73 | 9.22 | 8.82 | -0.35 | 0.67 | 54 |
| Apr. | 12.31 | 11.27 | -0.10 | 0.43 | 17 | 7.18 | 7.57 | -0.08 | 0.43 | 45 | 10.86 | 8.58 | -0.35 | 0.55 | 33 |
| May | 10.07 | 9.09 | -0.03 | 0.42 | 34 | 6.85 | 6.13 | -0.24 | 0.42 | 61 | 10.78 | 6.99 | -0.55 | 0.64 | 56 |
| June | 17.97 | 15.36 | -0.05 | 0.28 | 64 | 13.49 | 9.45 | -0.42 | 0.51 | 55 | 19.21 | 10.49 | -0.70 | 0.72 | 50 |
| July | 18.56 | 16.18 | -0.05 | 0.31 | 36 | 13.22 | 9.78 | -0.44 | 0.52 | 76 | 19.40 | 11.13 | -0.74 | 0.77 | 58 |
| Aug. | 14.07 | 13.26 | 0.11 | 0.32 | 55 | 9.24 | 9.09 | -0.12 | 0.32 | 80 | 14.56 | 10.32 | -0.49 | 0.54 | 82 |
| Sep. | 14.21 | 16.79 | 0.20 | 0.34 | 66 | 9.33 | 11.34 | 0.14 | 0.39 | 74 | 14.07 | 12.90 | -0.21 | 0.40 | 74 |
| Oct. | 10.20 | 12.84 | 0.29 | 0.42 | 71 | 6.07 | 8.47 | 0.20 | 0.43 | 72 | 9.13 | 10.05 | -0.07 | 0.41 | 72 |
| Nov. | 12.02 | 13.87 | 0.18 | 0.37 | 54 | 6.27 | 9.32 | 0.32 | 0.45 | 68 | 8.37 | 10.90 | 0.16 | 0.38 | 62 |
| Dec. | 17.37 | 21.94 | 0.31 | 0.46 | 59 | 7.02 | 11.22 | 0.44 | 0.55 | 78 | 9.65 | 12.83 | 0.19 | 0.44 | 73 |

**Table 3-2.** Seasonal average CMAQ performance

| | JFM | AMJ | JAS | OND |
|---|---|---|---|---|
| Sulfate | Good | Good | Good | Good |
| Nitrate | Good | Problematic | Problematic | Good |
| Ammonium | Good | Good | Good | Good |
| Elemental Carbon | Average | Average | Good | Average |
| Organic Mass | Average | Average | Average | Average |
| $PM_{2.5}$ | Good | Good | Good | Good |
| $PM_{10}$ | Good | Average | Average | Average |

Excellent, fractional bias ± 15% and fractional error ≤ 35%; good, fractional bias ± 30% and fractional error ≤ 50%; average, fractional bias ± 60% and fractional error ≤ 75%; problematic, fractional bias > ± 60% and fractional error > 75%.

**Table 3-3.** CMAQ monthly performance for sulfate ($SO_4^{2-}$)

Same as Table 3-1, but for $SO_4^{2-}$.

| Month | STN | | | | | IMPROVE | | | | | CASTNet | | | | |
|---|---|---|---|---|---|---|---|---|---|---|---|---|---|---|---|
| | Obs | CMAQ | FB | FE | $r^2$ | Obs | CMAQ | FB | FE | $r^2$ | Obs | CMAQ | FB | FE | $r^2$ |
| Jan. | 2.14 | 2.11 | -0.07 | 0.39 | 38 | 1.93 | 1.50 | -0.37 | 0.47 | 61 | 2.21 | 1.78 | -0.24 | 0.27 | 58 |
| Feb. | 1.89 | 1.71 | -0.25 | 0.41 | 65 | 1.41 | 1.10 | -0.38 | 0.52 | 63 | 1.87 | 1.52 | -0.25 | 0.32 | 52 |
| Mar. | 2.75 | 2.39 | -0.31 | 0.51 | 46 | 2.30 | 1.52 | -0.61 | 0.64 | 79 | 3.17 | 2.37 | -0.35 | 0.36 | 80 |
| Apr. | 3.16 | 2.77 | -0.35 | 0.57 | 37 | 2.72 | 2.20 | -0.43 | 0.51 | 67 | 3.31 | 2.99 | -0.20 | 0.32 | 69 |
| May | 2.66 | 2.80 | -0.14 | 0.47 | 55 | 2.51 | 2.52 | -0.38 | 0.56 | 75 | 3.30 | 3.57 | -0.05 | 0.23 | 92 |
| June | 5.42 | 6.71 | 0.13 | 0.39 | 77 | 4.82 | 5.05 | -0.10 | 0.45 | 84 | 6.57 | 7.78 | 0.16 | 0.24 | 91 |
| July | 5.45 | 7.51 | 0.26 | 0.41 | 62 | 4.82 | 5.12 | -0.02 | 0.34 | 86 | 6.79 | 7.72 | 0.11 | 0.21 | 87 |
| Aug. | 4.10 | 6.17 | 0.34 | 0.49 | 59 | 3.91 | 4.65 | 0.08 | 0.41 | 79 | 5.55 | 7.41 | 0.29 | 0.33 | 80 |
| Sep. | 5.06 | 5.94 | 0.12 | 0.42 | 73 | 4.34 | 5.4 | 0.11 | 0.43 | 83 | 6.10 | 6.61 | 0.06 | 0.18 | 76 |
| Oct. | 2.47 | 2.82 | -0.03 | 0.41 | 82 | 2.00 | 2.19 | -0.16 | 0.43 | 72 | 2.86 | 3.01 | -0.06 | 0.26 | 79 |
| Nov. | 2.47 | 2.11 | -0.22 | 0.40 | 37 | 1.76 | 1.57 | -0.24 | 0.43 | 60 | 2.22 | 1.84 | -0.20 | 0.24 | 80 |
| Dec. | 2.87 | 2.94 | -0.11 | 0.44 | 24 | 1.84 | 1.64 | -0.14 | 0.51 | 64 | 2.94 | 2.47 | -0.18 | 0.26 | 71 |

**Table 3-4.** CMAQ monthly performance for nitrate ($NO_3^-$)

Same as Table 3-1, but for $NO_3^-$.

| Month | STN | | | | | IMPROVE | | | | | CASTNet | | | | |
|---|---|---|---|---|---|---|---|---|---|---|---|---|---|---|---|
| | Obs | CMAQ | FB | FE | $r^2$ | Obs | CMAQ | FB | FE | $r^2$ | Obs | CMAQ | FB | FE | $r^2$ |
| Jan. | 3.96 | 4.00 | -0.01 | 0.35 | 61 | 1.85 | 2.41 | 0.13 | 0.58 | 64 | 3.77 | 3.75 | 0.02 | 0.21 | 74 |
| Feb. | 2.73 | 2.67 | -0.07 | 0.50 | 58 | 1.16 | 1.37 | 0.16 | 0.64 | 70 | 2.88 | 2.60 | 0.04 | 0.32 | 80 |
| Mar. | 2.58 | 3.75 | 0.25 | 0.57 | 50 | 1.11 | 1.99 | 0.20 | 0.81 | 52 | 2.86 | 3.83 | 0.35 | 0.45 | 49 |
| Apr. | 2.56 | 2.15 | -0.40 | 0.73 | 35 | 1.09 | 1.26 | -0.23 | 0.89 | 43 | 1.65 | 1.69 | -0.02 | 0.47 | 43 |
| May | 1.83 | 1.08 | -0.66 | 0.89 | 14 | 0.69 | 0.38 | -1.05 | 1.19 | 10 | 1.09 | 0.62 | -0.67 | 0.82 | 16 |
| June | 1.65 | 1.01 | -0.80 | 1.03 | 8 | 0.51 | 0.15 | -1.34 | 1.40 | 12 | 0.67 | 0.39 | -0.68 | 0.93 | 4 |
| July | 1.01 | 0.80 | -0.80 | 1.09 | 5 | 0.30 | 0.15 | -1.38 | 1.53 | 6 | 0.74 | 0.25 | -0.98 | 1.11 | 6 |
| Aug. | 0.97 | 0.5 | -0.89 | 1.12 | 29 | 0.32 | 0.14 | -1.25 | 1.39 | 4 | 0.56 | 0.27 | -0.73 | 0.95 | 19 |
| Sep. | 1.21 | 1.49 | -0.29 | 0.79 | 58 | 0.32 | 0.43 | -0.61 | 1.11 | 46 | 0.76 | 0.82 | -0.04 | 0.75 | 2 |
| Oct. | 1.90 | 2.46 | 0.01 | 0.62 | 64 | 1.06 | 1.57 | 0.08 | 0.87 | 76 | 2.16 | 3.07 | 0.23 | 0.42 | 76 |
| Nov. | 3.42 | 3.71 | -0.05 | 0.46 | 58 | 1.94 | 2.65 | 0.23 | 0.59 | 55 | 2.95 | 3.27 | 0.14 | 0.27 | 59 |
| Dec. | 4.91 | 5.51 | 0.01 | 0.43 | 67 | 2.31 | 3.05 | 0.25 | 0.55 | 77 | 4.75 | 5.21 | 0.10 | 0.26 | 68 |

**Table 3-5.** CMAQ monthly performance for ammonium ($NH_4^+$)

Same as Table 3-1, but for $NH_4^+$.

| Month | STN | | | | | CASTNet | | | | |
|---|---|---|---|---|---|---|---|---|---|---|
| | Obs | CMAQ | FB | FE | $r^2$ | Obs | CMAQ | FB | FE | $r^2$ |
| Jan. | 1.66 | 1.95 | 0.28 | 0.41 | 63 | 1.61 | 1.71 | 0.05 | 0.15 | 77 |
| Feb. | 1.21 | 1.40 | 0.15 | 0.44 | 63 | 1.31 | 1.30 | 0.05 | 0.22 | 74 |
| Mar. | 1.52 | 1.95 | 0.14 | 0.41 | 66 | 1.71 | 1.95 | 0.11 | 0.23 | 68 |
| Apr. | 1.69 | 1.58 | -0.18 | 0.45 | 38 | 1.42 | 1.49 | 0.00 | 0.24 | 57 |
| May | 1.29 | 1.27 | -0.07 | 0.50 | 40 | 1.30 | 1.25 | -0.10 | 0.26 | 74 |
| June | 2.22 | 2.45 | 0.08 | 0.36 | 77 | 2.15 | 2.24 | 0.04 | 0.29 | 68 |
| July | 1.85 | 2.36 | 0.30 | 0.48 | 43 | 2.06 | 1.99 | 0.02 | 0.26 | 63 |
| Aug. | 1.43 | 1.85 | 0.40 | 0.57 | 57 | 1.74 | 1.81 | 0.05 | 0.23 | 68 |
| Sep. | 1.90 | 2.22 | 0.32 | 0.47 | 77 | 1.92 | 2.01 | 0.04 | 0.20 | 72 |
| Oct. | 1.21 | 1.65 | 0.35 | 0.53 | 70 | 1.40 | 1.74 | 0.20 | 0.32 | 62 |
| Nov. | 1.68 | 1.85 | 0.11 | 0.38 | 61 | 1.42 | 1.62 | 0.13 | 0.17 | 74 |
| Dec. | 2.28 | 2.66 | 0.14 | 0.38 | 69 | 2.12 | 2.38 | 0.10 | 0.19 | 85 |

**Table 3-6.** CMAQ monthly performance for elemental carbon (EC)

Same as Table 3-1, but for EC.

| Month | STN | | | | | IMPROVE | | | | |
|---|---|---|---|---|---|---|---|---|---|---|
| | Obs | CMAQ | FB | FE | $r^2$ | Obs | CMAQ | FB | FE | $r^2$ |
| Jan. | 0.47 | 0.99 | 0.55 | 0.64 | 26 | 0.25 | 0.31 | 0.25 | 0.33 | 87 |
| Feb. | 0.45 | 0.71 | 0.26 | 0.54 | 16 | 0.20 | 0.22 | 0.20 | 0.39 | 65 |
| Mar. | 0.45 | 0.61 | 0.03 | 0.52 | 29 | 0.24 | 0.22 | -0.16 | 0.39 | 67 |
| Apr. | 0.54 | 0.49 | -0.24 | 0.55 | 13 | 0.25 | 0.24 | -0.10 | 0.45 | 12 |
| May | 0.47 | 0.38 | -0.34 | 0.57 | 21 | 0.26 | 0.15 | -0.42 | 0.51 | 66 |
| June | 0.66 | 0.63 | -0.17 | 0.50 | 26 | 0.45 | 0.21 | -0.75 | 0.76 | 20 |
| July | 0.55 | 0.65 | 0.13 | 0.48 | 33 | 0.36 | 0.24 | -0.52 | 0.64 | 43 |
| Aug. | 0.47 | 0.56 | 0.17 | 0.49 | 33 | 0.34 | 0.24 | -0.36 | 0.45 | 67 |
| Sep. | 0.64 | 0.67 | 0.03 | 0.45 | 40 | 0.33 | 0.25 | -0.24 | 0.39 | 80 |
| Oct. | 0.58 | 0.60 | -0.08 | 0.54 | 34 | 0.32 | 0.24 | -0.22 | 0.40 | 55 |
| Nov. | 0.44 | 0.60 | 0.16 | 0.54 | 31 | 0.25 | 0.25 | 0.06 | 0.32 | 71 |
| Dec. | 0.65 | 0.90 | 0.25 | 0.55 | 36 | 0.31 | 0.30 | 16.00 | 0.39 | 66 |

**Table 3-7.** CMAQ monthly performance for organic mass (OM)

Same as Table 3-1, but for OM

| Month | STN | | | | | IMPROVE | | | | |
|---|---|---|---|---|---|---|---|---|---|---|
| | Obs | CMAQ | FB | FE | $r^2$ | Obs | CMAQ | FB | FE | $r^2$ |
| Jan. | 3.21 | 4.58 | 0.45 | 0.61 | 27 | 1.27 | 1.86 | 0.41 | 0.46 | 72 |
| Feb. | 2.76 | 3.39 | 0.38 | 0.68 | 14 | 1.13 | 1.51 | 0.41 | 0.50 | 47 |
| Mar. | 2.07 | 2.29 | 0.27 | 0.70 | 15 | 1.13 | 1.20 | 0.02 | 0.45 | 44 |
| Apr. | 2.40 | 2.03 | 0.02 | 0.71 | 3 | 1.24 | 1.58 | 0.15 | 0.50 | 1 |
| May | 2.11 | 1.68 | -0.07 | 0.61 | 21 | 1.51 | 1.15 | -0.13 | 0.51 | 33 |
| June | 5.01 | 2.09 | -0.74 | 0.78 | 23 | 3.70 | 1.45 | -0.71 | 0.73 | 13 |
| July | 5.92 | 2.16 | -0.90 | 0.93 | 17 | 3.31 | 1.44 | -0.68 | 0.72 | 13 |
| Aug. | 4.12 | 1.98 | -0.62 | 0.69 | 23 | 2.10 | 1.52 | -0.29 | 0.45 | 21 |
| Sep. | 4.06 | 2.92 | -0.23 | 0.48 | 17 | 1.97 | 1.85 | -0.01 | 0.37 | 43 |
| Oct. | 2.59 | 2.36 | 0.07 | 0.57 | 36 | 1.49 | 1.56 | 0.08 | 0.40 | 29 |
| Nov. | 2.58 | 2.20 | -0.01 | 0.50 | 32 | 1.32 | 1.36 | 0.16 | 0.42 | 43 |
| Dec. | 4.66 | 4.14 | 0.17 | 0.61 | 27 | 1.29 | 1.88 | 0.46 | 0.57 | 48 |

**Table 3-8.** CMAQ monthly performance for aerosol number concentration at Bondville, Illinois. Same as Table 3-1, but for number concentration. Observed and modeled number concentrations in $10^9$ particles/$m^3$. FB and FE calculated from hourly values. $r^2$ (%) shown for hourly and daily time series.

| Month | IMPROVE | | | | | |
|---|---|---|---|---|---|---|
| | Obs | CMAQ | FB | FE | $r^2$ (daily) | $r^2$ (hourly) |
| Jan. | 5.41 | 2.34 | -0.73 | 0.76 | 14 | 4 |
| Feb. | 5.60 | 1.71 | -0.95 | 0.96 | 23 | 10 |
| Mar. | 6.42 | 2.26 | -0.91 | 0.96 | 4 | 2 |
| Apr. | 6.59 | 1.36 | -1.17 | 1.18 | 36 | 6 |
| May | 7.51 | 1.47 | -1.24 | 1.25 | 38 | 7 |
| June | 7.21 | 1.57 | -1.16 | 1.16 | 7 | 0 |
| July | 7.12 | 1.54 | -1.13 | 1.14 | 12 | 3 |
| Aug. | 3.53 | 1.71 | -0.51 | 0.60 | 4 | 5 |
| Sep. | 2.38 | 2.58 | 0.21 | 0.61 | 2 | 1 |
| Oct. | 5.27 | 1.97 | -0.79 | 0.85 | 28 | 1 |
| Nov. | 3.86 | 1.98 | -0.57 | 0.68 | 16 | 2 |
| Dec. | 4.44 | 1.89 | -0.78 | 0.79 | 0 | 5 |

**Table 3-9.** Annual average CMAQ bias and error correlation with observed and modeled time series ($r^2$)

| | Bias | | Error | |
|---|---|---|---|---|
| | Observed | Modeled | Observed | Modeled |
| Sulfate | 7% | 43% | 25% | 47% |
| Nitrate | 1% | 34% | 20% | 40% |
| Ammonium | 3% | 18% | 14% | 28% |
| Elemental Carbon | 19% | 25% | 23% | 24% |
| Organic Mass | 56% | 15% | 51% | 17% |
| $PM_{2.5}$ | 2% | 34% | 21% | 41% |
| $PM_{10}$ | 10% | 21% | 33% | 13% |

## Figures

**Figure 3-1.** 2002 CMAQ performance for all aerosol species across the IMPROVE, STN, and CASTNet networks, comparing monthly average concentrations ($\mu g/m^3$) with mean fractional bias (% of average concentration). Graph includes sulfate, nitrate, ammonium, organic mass, elemental carbon, soil matter, and coarse matter, as well as aggregate $PM_{2.5}$ and $PM_{10}$. Lines reflect the +/- 30% "goal" (green) and +/- 60% "criteria" (red) levels for acceptable regional model performance in simulating aerosols, as defined by *Boylan and Russell* [2006].

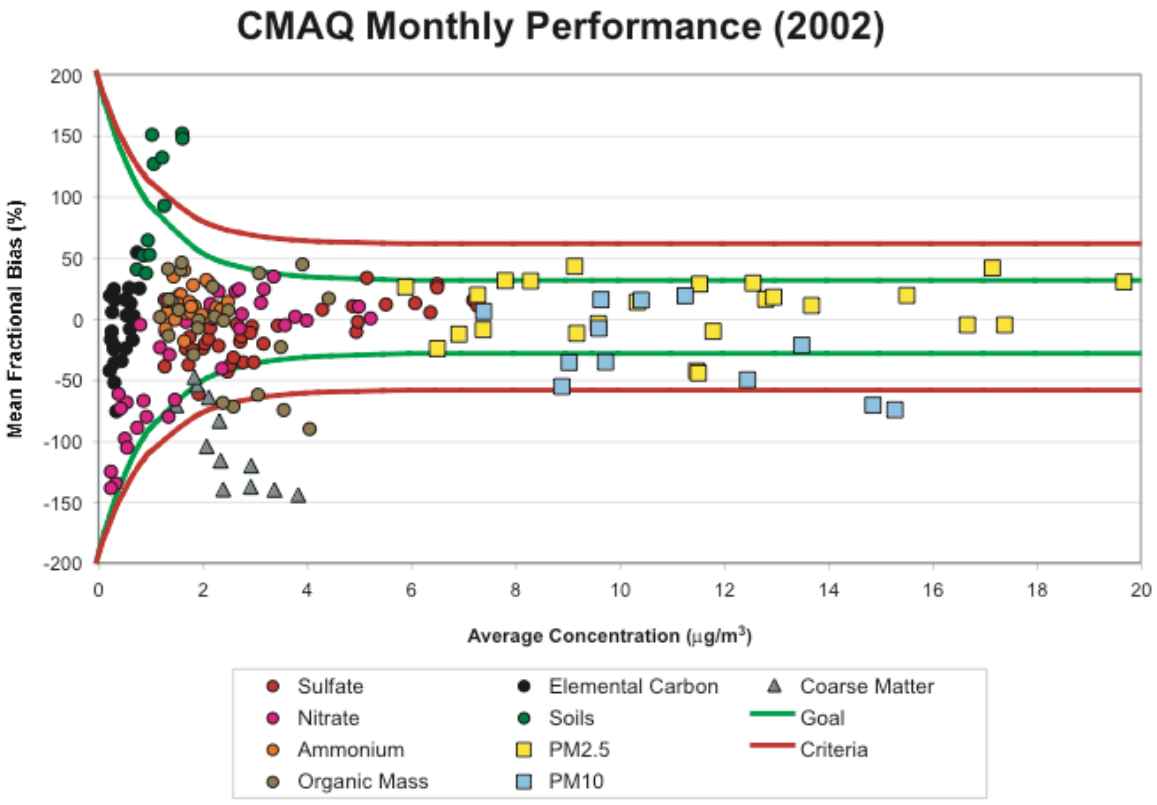

**Figure 3-2.** Scatter plots show monthly mean CMAQ model predictions vs. aerosol mass concentrations ($\mu g/m^3$) at STN and IMPROVE sites for (a) PM2.5; (b) PM10; (c) sulfate; (d) nitrate; (e) ammonium; (f) elemental carbon; (g) organic matter, and (h) CMAQ model predictions vs. aerosol number concentrations at the Bondville, IL CASTNet site.

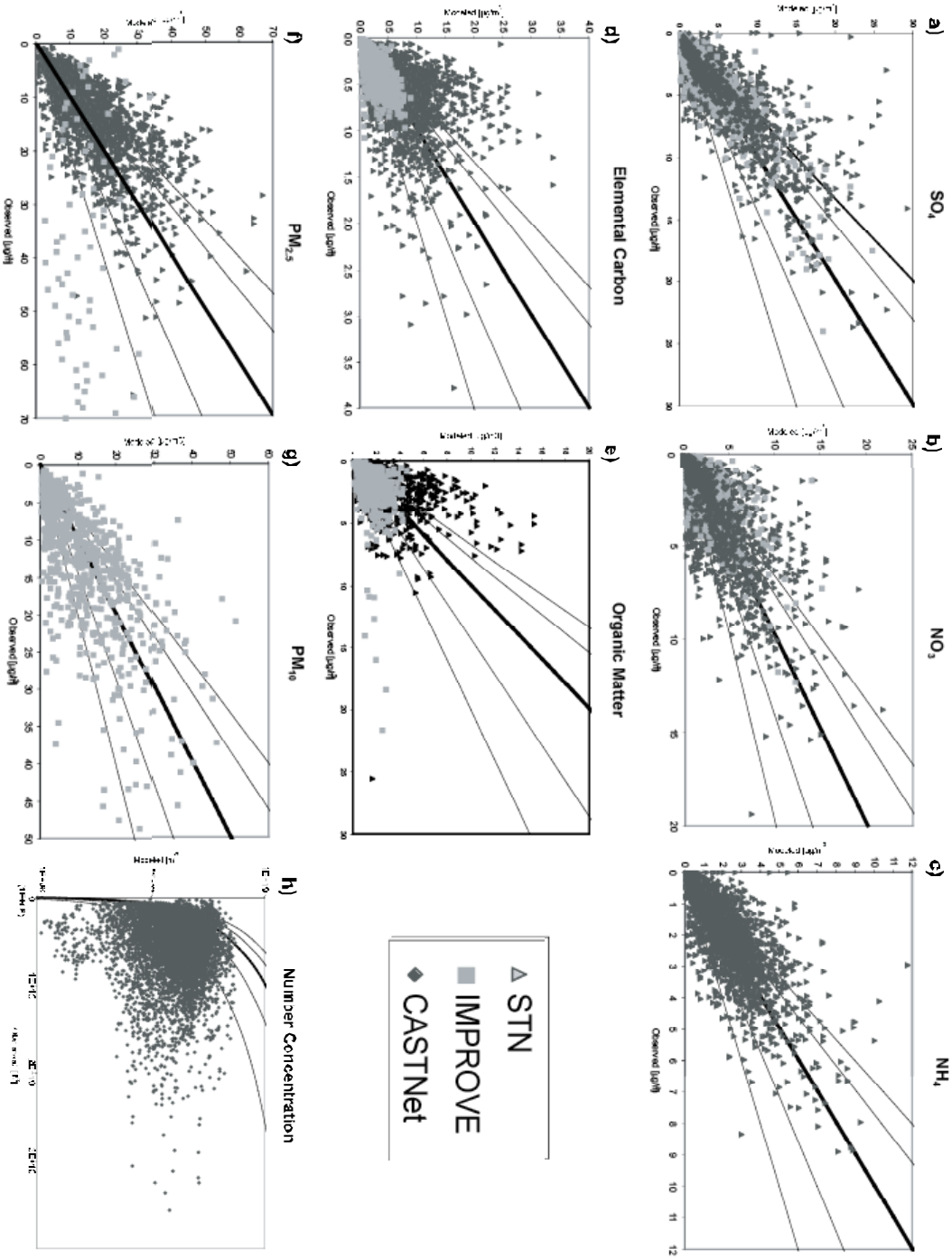

**Figure 3-3.** Seasonal average concentrations of $PM_{2.5}$ and components in $\mu g/m^3$, as measured at the STN measurement sites in the study region. CMAQ performance is shown as bias relative to these observed values on a seasonal basis.

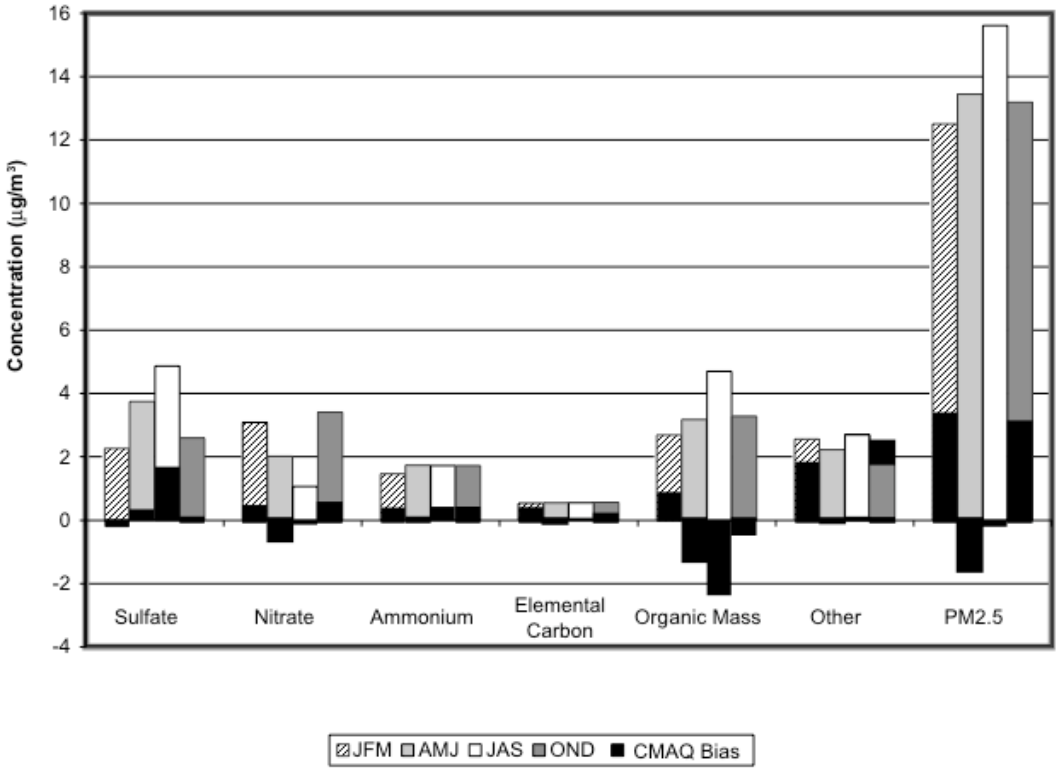

**Figure 3-4.** CMAQ simulated $PM_{2.5}$ ($\mu g/m^3$) in the lowest model layer, shown for each season: a) JFM; b) AMJ; c) JAS; d) OND.

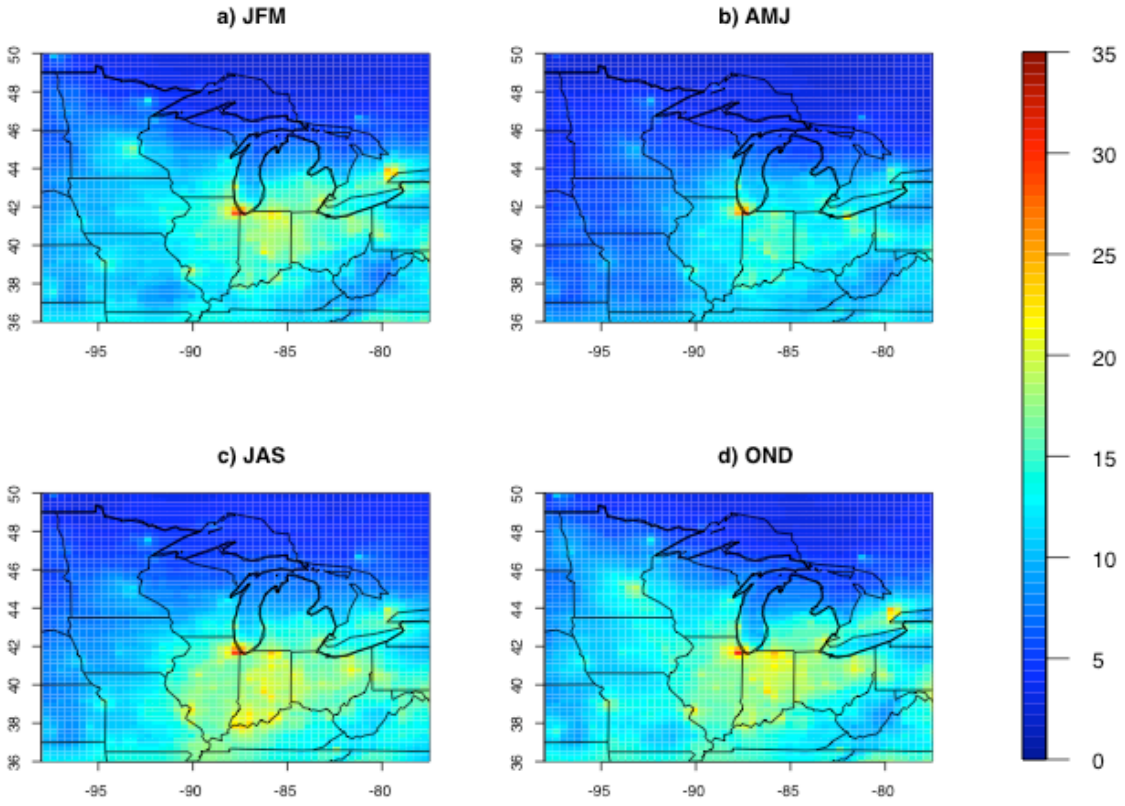

**Figure 3-5.** CMAQ simulated $SO_4^{2-}$ ($\mu g/m^3$) in the lowest model layer, shown for each season: a) JFM; b) AMJ; c) JAS; d) OND.

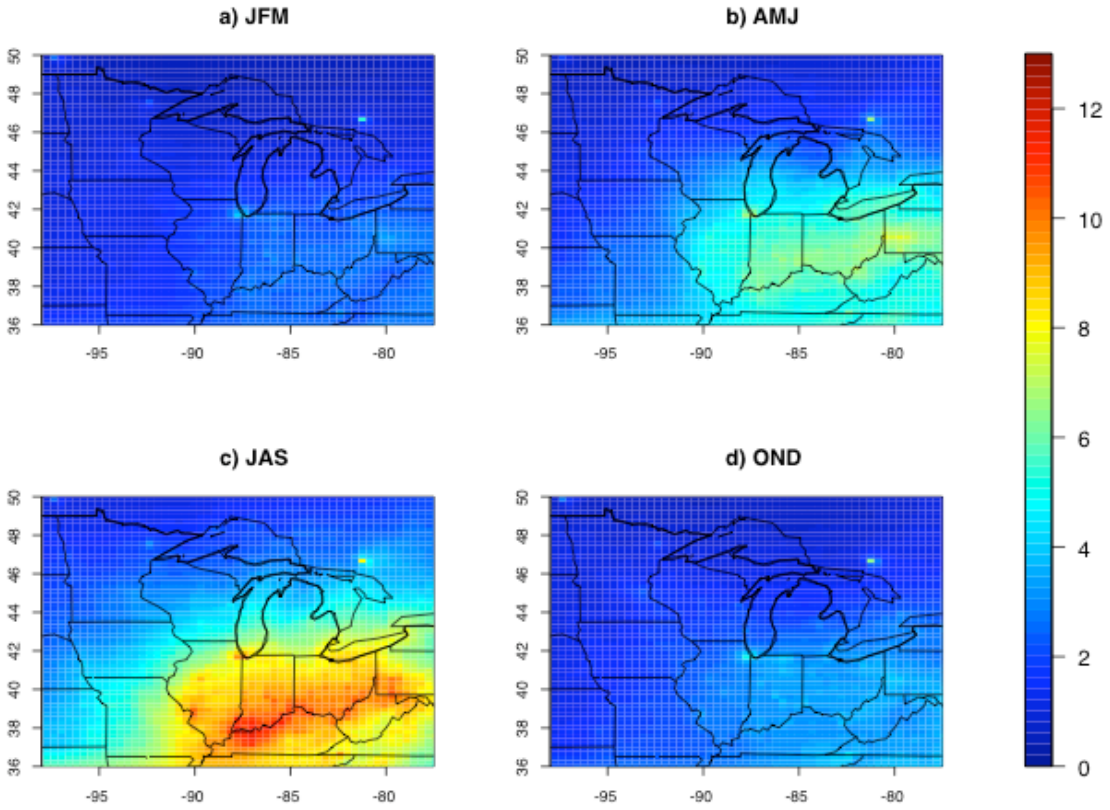

**Figure 3-6.** CMAQ simulated $NO_3^-$ ($\mu g/m^3$) in the lowest model layer, shown for each season: a) JFM; b) AMJ; c) JAS; d) OND.

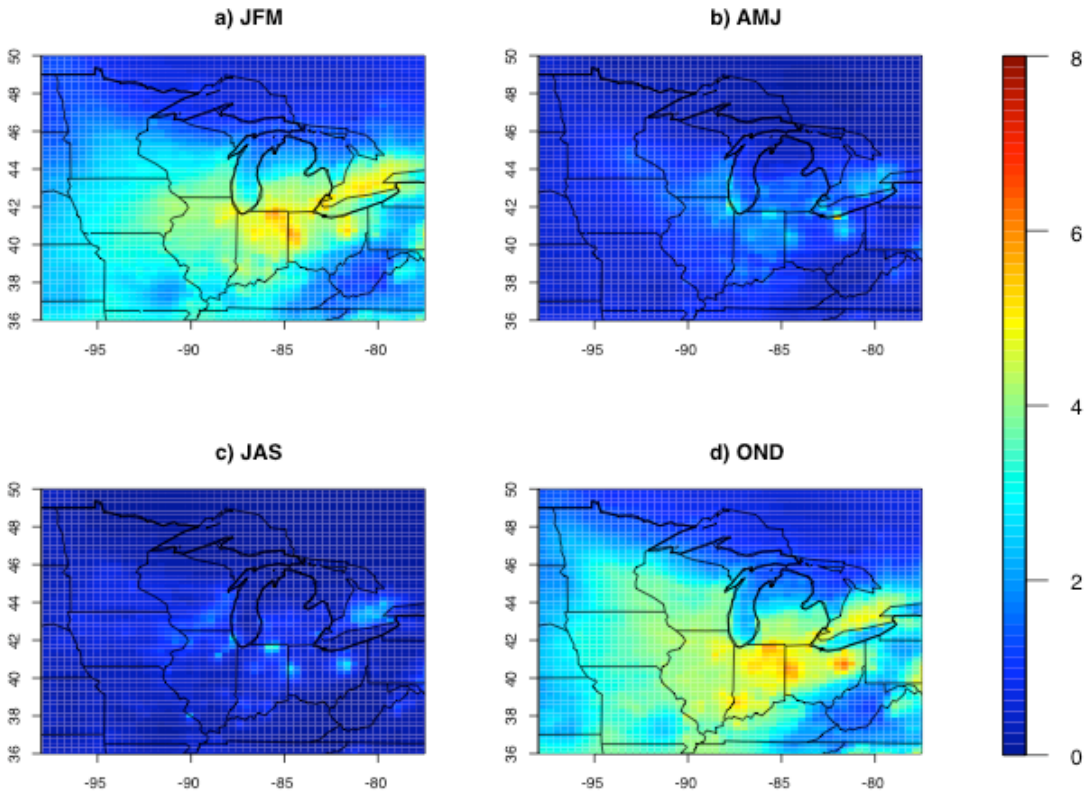

**Supplemental Figures**

**Suppl. Figure 1.** CMAQ simulated $NH_4^+$ ($\mu g/m^3$) in the lowest model layer, shown for each season: a) JFM; b) AMJ; c) JAS; d) OND. Scale chosen for comparability with nitrate plots, shown in Figure 6.

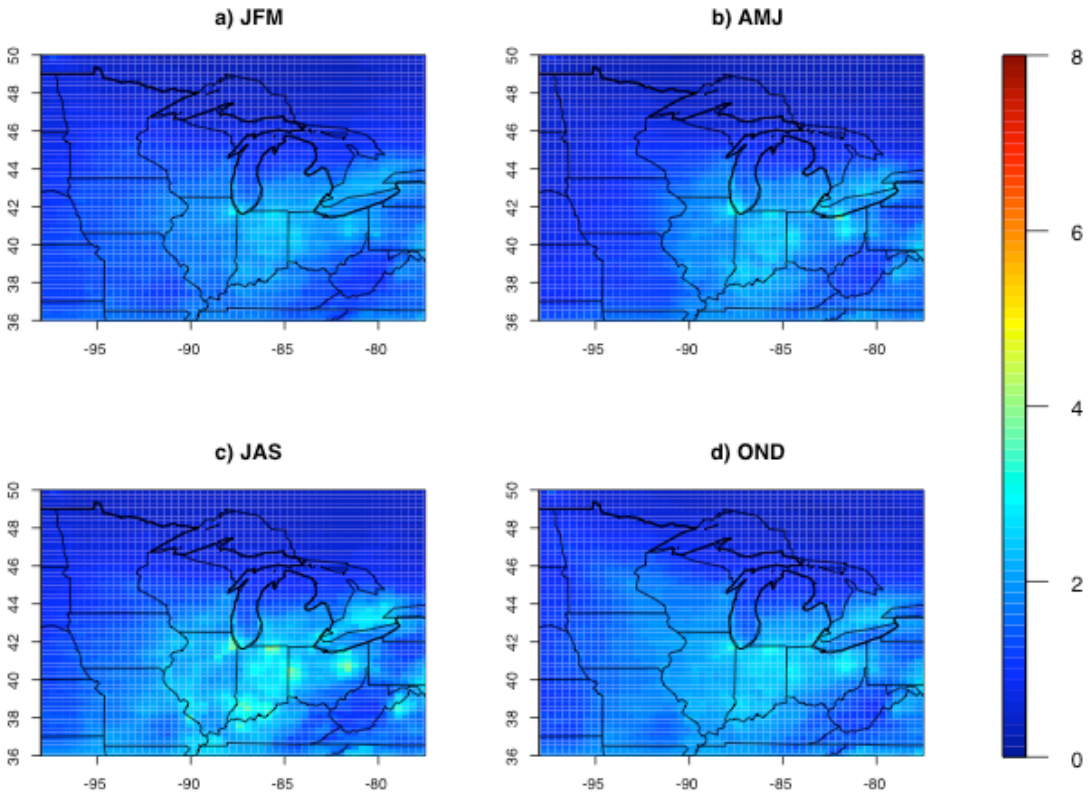

**Suppl. Figure 2.** CMAQ simulated anthropogenic SOA ($\mu g/m^3$) in the lowest model layer, shown for each season: a) JFM; b) AMJ; c) JAS; d) OND.

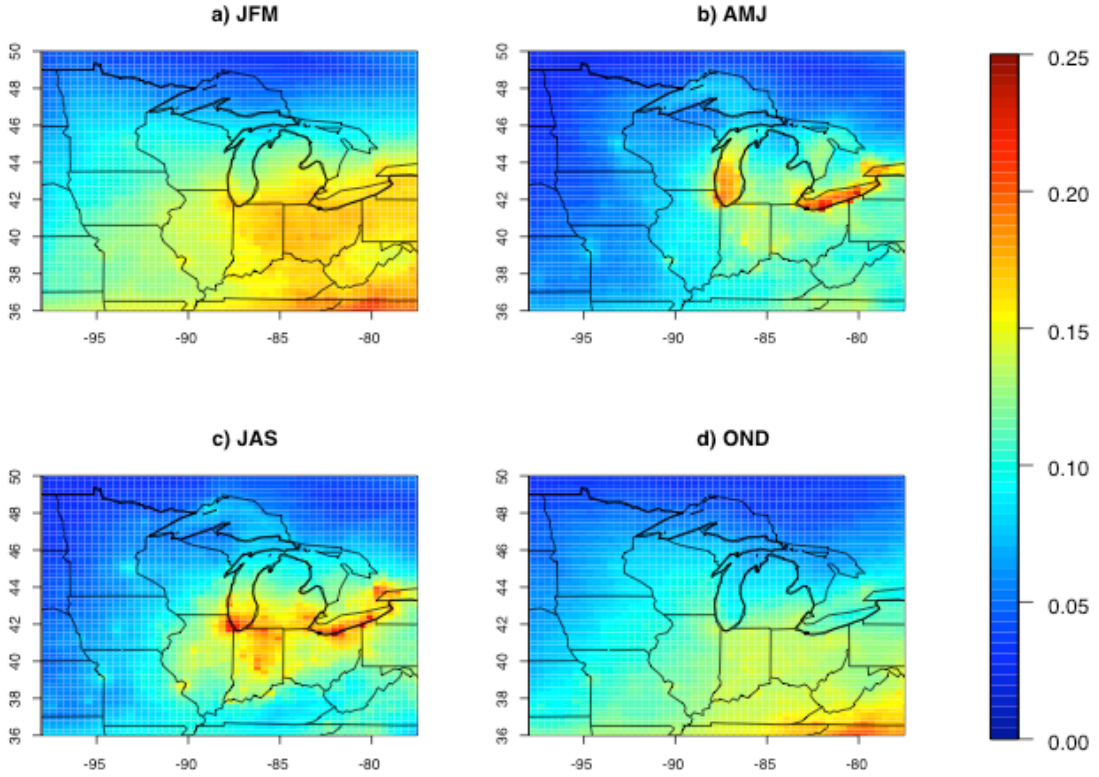

**Suppl. Figure 3.** Correlation ($r^2$) between surface $O_3$ and anthropogenic SOA, as simulated by CMAQ, shown for each month of the $O_3$ season: a) April; b) May; c) June; d) July; e) August; f) September.

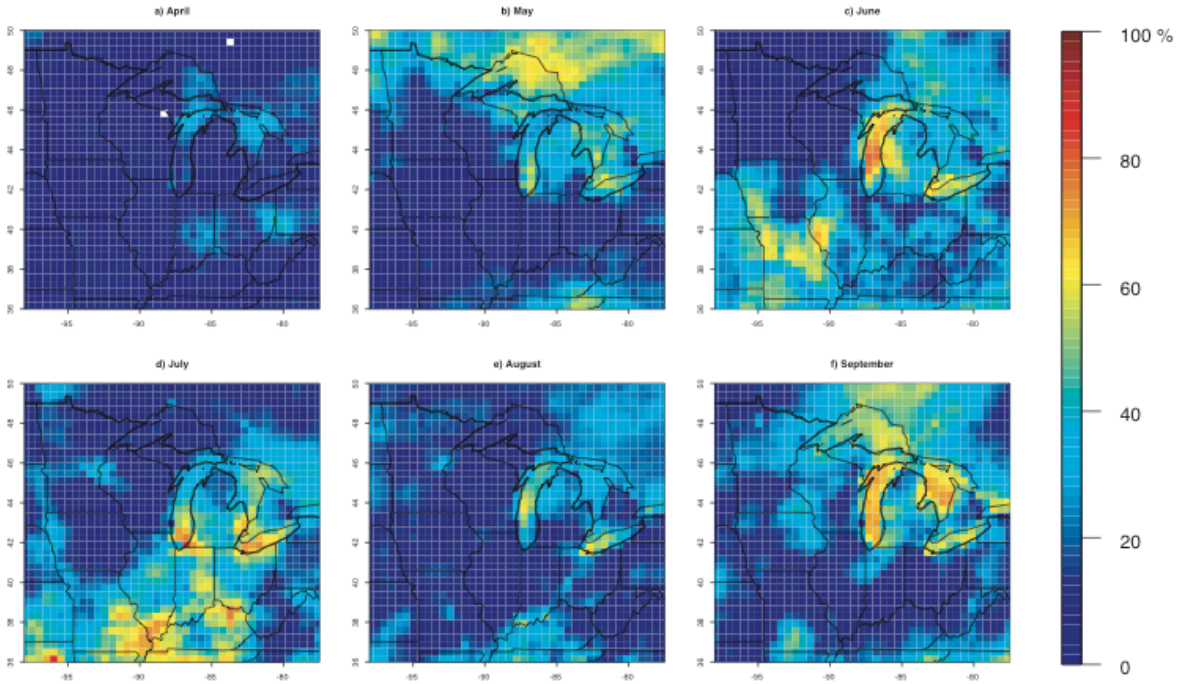

**Suppl. Figure 4.** Histograms of observed (white bars) and simulated (black lines) speciated aerosol mass (a-g) and number concentration (h). Observations of aerosol mass take as the aggregate of observed concentrations from the IMPROVE, CASTNet, and STN sites in our study domain, with CMAQ evaluated at those same locations. Number concentration taken from the NOAA observing station at Bondville, IL.

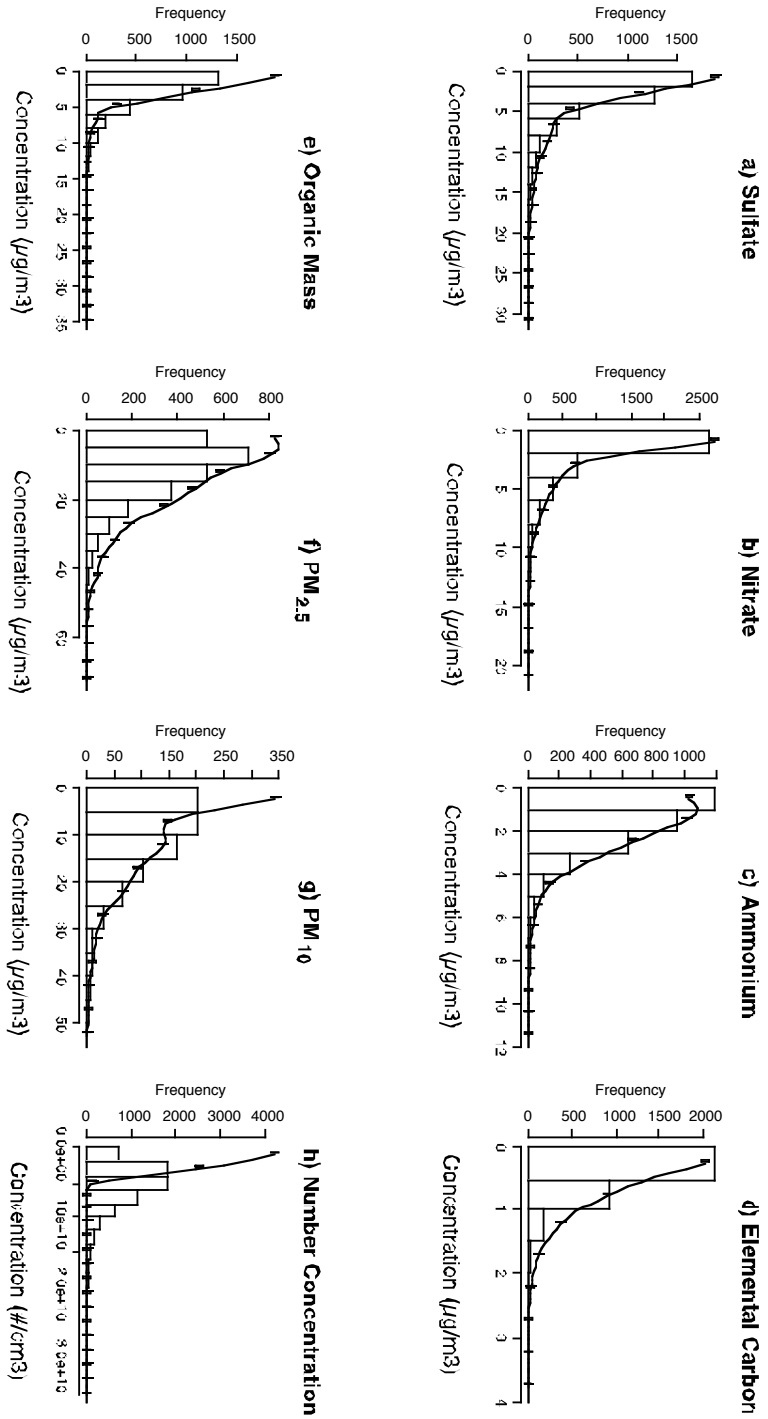

# Chapter 4. Influences of the Great Lakes on Chemical Transport in the Upper Midwestern United States

From: S.N. Spak, T. Holloway, B. Stone, A. Mednick, Influences of the Great Lakes on Chemical Transport in the Midwestern United States (*Journal of Geophysical Research – Atmospheres*, in preparation).

## 4.1. Introduction

Measurements [e.g. *Hastie et al.*, 1999] and modeling studies [e.g. *Sillman et al.*, 1993] have shown that the lakes strongly enhance the formation and transport of ozone ($O_3$) in the summer, as cool lake temperatures lead to a shallow convective layer, capping the rise of emitted precursors and enhancing the photochemical reactions that lead to the production of $O_3$. Due to this photochemical enhancement, the majority of counties bordering Lake Michigan are in non-attainment of the 8-hour National Ambient Air Quality Standard for $O_3$ [*US EPA* Green Book Nonattainment Areas for Criteria Pollutants, http://www.epa.gov/oar/oaqps/greenbk/map8hrnm.html]. Although not often discussed in the context of air quality, wintertime convection and precipitation over the lakes holds the potential to mix pollutants away from emissions sources and affect deposition patterns.

Although the meteorology of the Great Lakes has been extensively studied [e.g. *Scott and Huff*, 1996], and lake-effect summertime $O_3$ formation and transport is well

characterized [e.g. *Sillman et al.,* 1993; *Lennartson and Schwartz*, 2002], the role of the Great Lakes in the seasonality of $O_3$ and aerosol chemical transport has not been carefully examined. Observational studies over the past 30 years [*Berg et al.*, 1977] have established the composition, seasonality, sources, and spatial distribution of aerosols at monitors in urban [*Lee et al.*, 2003; *Rizzo and Scheff*, 2007; *Subramanian et al.*, 2007, *Zhao and Hopke*, 2006; *Zhao et al.*, 2007], rural [*Kerr et al.*, 2004; *Kim et al.*, 2005, 2007], and remote [*Malm et al.*, 2004] sites in the region, including sites near the shores of the lakes [*Sheesley et al.*, 2004] and even over water [*Offenberg and Baker*, 2000]. *Lasher-Trapp and Stachnik* [2007] observed that the boundary layer of the Great Lakes and neighboring areas gives rise to giant (2 $\mu$m < aerodynamic diameter $D$ < 20 $\mu$m) and ultra-giant ($D$ > 20 $\mu$m) particles during the winter, with higher concentrations on trajectories downwind of major urban areas, although the factors contributing to their production and presence remain unclear.

A few studies have attempted to understand observed composition and source contributions through back-trajectories (e.g. *Sheesley et al.*, [2004]; *Kim et al.*, [2005, 2007]; *Zhao et al.* [2007]), but only one dynamical modeling study to date has focused on the influence of lake effect meteorology on aerosol transport in the region. In an analysis focused on the impacts of the lake breeze on the transport of a particle tracer in summertime episodes, *Harris and Kotamarthi* [2005] found that the lake breeze near Chicago impacts the direction of aerosol transport away from the city, but only influenced 34% of released particles.

This study focuses on the role of the Great Lakes in the seasonal dynamics of aerosols and $O_3$ in an annual simulation for 2002 using CMAQ. We identify where lake effect meteorology plays a key role in the seasonality and regional-scale transport dynamics of pollution, and examine the sensitivity of lake effect pollution transport to emissions from the region's largest cities.

## 4.2. Data and Methods

We employed CMAQ (v4.6) as configured in Chapter 2, in the same simulations evaluated in Chapter 3. The study domain covers a 2.23 x $10^6$ $km^2$ region at 36 x 36 km grid resolution (Figure 4-1), with 14 vertical layers to the lower stratosphere (approximately 15 km).

## 4.3. Results and Discussion

### *4.3.1. Lake Effect Meteorology*

The Great Lakes, with their large volume and high heat capacity, have a dramatic influence on regional climate, with acute local effects as well as longer-range impacts on atmospheric circulation. Immediate climatic effects over the lakes are evident in observed and modeled monthly time series of surface temperature, planetary boundary layer (PBL) height, surface pressure, and wind speed (Figure 4-2) at NOAA buoy 45007 in southern

Lake Michigan and at the NOAA National Weather Service station at the Dane County Regional Airport in Madison, Wisconsin, at the same latitude approximately 150 km west of the lake. Madison experiences the same synoptic systems as the lake, but is not subject to lake effect meteorology. The thermal momentum of lake temperature leads to a persistent lag of approximately two months compared to inland Madison. Not only is the seasonal progression delayed, it is profoundly damped, with wintertime temperatures over the lake 10 K warmer and the summer maximum 10 K cooler than at the inland station. These observed characteristics are accurately represented in MM5, with MM5 modeled skin temperature more representative of the observed lake temperature 0.5 m below the surface than the observed surface air temperature, as heat exchange at the surface of lake is the point of radiative equilibrium. We also note that the seasonal cycle observed for Lake Erie is nearly identical to Lake Michigan, except that the shallower Lake Erie is ice-covered more frequently and completely [*Schertzer et al.*, 1987].

As previously mentioned in Chapter 3, the land-lake thermal gradient is responsible for a number of secondary effects on climate strong enough to impact aerosol chemistry and transport. Winds over the lakes are higher due to the shorter roughness length over water than land and combine with secondary circulations and the lake breeze to generate consistently higher wind speeds over the lakes than over land, which reach a maximum in the winter over the warmer lakes (Figure 4-2). From October to February, heat rising off the lake leads to a deeper PBL than over land, with the mixed layer

reaching in excess of 800 m. The cooler lake restricts the height of the marine boundary layer to less than 30 m from May through July.

In order to more clearly identify impacts of the lake effect on the seasonality of chemical transport, we choose to represent the seasons throughout this study according to the temperature cycle of the southern Great Lakes, the location with the highest aerosol and ozone burdens in the region. This seasonal progression begins from a nearly frozen lake in the lake winter season from January through March, when the lake temperature is nearly constant. As the land and the regional airmass warm faster than the lake, the cool lake creates a stable atmosphere from April through June, with a temperature inversion throughout the marine boundary layer evident in Figure 4-3b. From July through September, the lake summer season, the strength of the lake effect reaches a minimum, and the temperature profile over Lake Michigan, including the surface temperature, is nearly identical to Madison. From October to December, the temperature difference between the lake and the ambient air increases, and the increased moisture over the lake leads to lake effect rain and then snow along the leeward (eastern) shores.

Although we used Lake Michigan as an example above, Figure 4-4 shows that Lake Michigan's seasonality of PBL height and wind speed is shared by all of the Great Lakes. The latitudinal temperature gradient in the region is evident in that the strongest difference between lake and land PBL height among the six lakes moves from lake to lake in a seasonal cycle. The stable, low PBL first appears in southern Lake Michigan

and Lake Erie in the spring; during the progression to summer, the most extreme difference is found at Lake Superior, where the surface temperature of the deepest of the lakes rarely exceeds 10 ºC, while the deepest mixed layer in the region can be found over the adjacent shores. In fall, the PBL first rises over the southern lakes. Then, as fall turns to winter, the location of the deepest PBL shifts northward, again reaching an extreme over Lake Superior.

Wind speed and direction also cycle seasonally, with strong northerly winds over much of the region in the winter and westerlies in the spring and fall. The summer is marked by weak winds from the south/southwest across the entire domain. Convergence over southern Michigan, Lake Erie and southern Lake Huron is evident in all seasons, and strongest in the winter.

*4.3.2. The Role of the Great Lakes in the Chemistry and Transport of Fine Aerosols*

Model performance for fine aerosols in this simulation was evaluated in Chapter 3, finding prediction of $PM_{2.5}$ and its speciated components skillful throughout the year relative to contemporary ad-hoc standards and prior modeling regional-scale model studies in eastern North America. CMAQ demonstrates a tendency toward overprediction of $PM_{2.5}$ mass concentrations in winter and fall (due to biases in $NO_3^-$, organic mass, and unspeciated fine mass) and underprediction in spring and summer (attributable in part to insufficient formation of secondary organic aerosols). Despite strong seasonality in

individual species, simulated regional spatial patterns in total $PM_{2.5}$ exhibited little seasonality.

Results of our CMAQ simulation show that the combination of wind and PBL represents a strong local lake effect control on the seasonality of aerosol chemical transport in the immediate vicinity of the Great Lakes. In the fall and winter, a deep PBL and high winds contribute to lower surface aerosol concentrations, enhancing the ventilation and advection of emissions near the surface, limiting the build-up of aerosol concentrations. Figure 3 shows that despite higher local emissions from the Gary-Chicago-Milwaukee area, simulated surface concentrations of $PM_{2.5}$ over southern Lake Michigan are comparable to those in Madison during the winter, and 25% (3 $\mu g/m^3$) lower during the fall, when the atmosphere over the lake reaches its maximum instability. Wintertime episodes of high $PM_{2.5}$ have been attributed directly to region-wide stagnation from stationary synoptic systems [*Chu*, 2004; *Woods*, 2007]. In the spring stable lake season, the very shallow marine boundary conduction layer and light southerly winds trap emissions and regional background pollutant burdens [*Lyons and Cole*, 1976; *Wolff et al.*, 1977] close to the lake surface, enhancing photochemistry and directing them back onshore [*Dye et al.*, 1995]. Evidence is found in Figure 4-3b, with $PM_{2.5}$ concentrations much higher throughout the shallow boundary layer over Lake Michigan than over land, despite the absence of fresh emissions over the lake, indicating that polluted air from terrestrial sources has been transported and aged over the lake without substantial deposition to the lake surface. This phenomenon is less pronounced during the summer

season (Figure 4-3c), when the land and lake lapse rates are nearly identical and the marine boundary layer is no longer so shallow. In the lake summer season, synoptic-scale conditions are again responsible for regional-scale episodes of elevated ground-level pollution [*Hanna and Chang*, 1994], most notably static high pressure systems leading to subsidence-induced boundary layer suppression [*Eshel and Bernstein*, 2006] over land as well as the lakes.

Hourly time series from October through December indicate that the lower seasonal average concentrations in fall and winter over the lakes are, in fact, composites of two distinct transport regimes. Under most circumstances, polluted air masses are advected around the deep boundary layer over the lakes, with minimal dispersion into the clean marine airmass. From October through December, prevailing surface level $PM_{2.5}$ concentrations over the southern lakes are less than 10 $\mu g/m^3$ than 60% of the time, and less than 5 $\mu g/m^3$ 35% of the time. The hourly evolution of $PM_{2.5}$ on a west-east transect across southern Lake Michigan and Lake Erie from October 1 (day 274) through December 31 (day 365) is illustrated in a Hovmöller diagram (Figure 4-5. The locations of Lake Michigan (820-1000 km easting along transect) and Lake Erie (~1300 km easting) are clearly visible in Figure 4-5 as areas where concentrations are consistently lower than elsewhere along the transect. Analysis of four dimensional concentration fields and vertical profiles confirmed that this abrupt change in concentrations over the lakes is consistent throughout the troposphere, and that the phenomenon shown is not merely the result of vertical advection over the warmer lake surface. Episodic regional

high PM episodes (e.g. from day 345-350) typically pass from west to east across the lakes, as synoptic systems under prevailing zonal and northwesterly winds (Figure 4-4) overcome the distinct lake airmasses and advect polluted air over the lakes, with $PM_{2.5}$ concentration peaks over the lake coincident with peaks over land, often reaching similar levels in excess of 35 $\mu g/m^3$. This regional signal in aerosol variability due to synoptic weather systems [*Woods*, 2007] in $PM_{2.5}$ extends to all fine particle species and reaches hundreds of kilometers. The average difference between land and lake $PM_{2.5}$ is greater than the sensitivity of $PM_{2.5}$ in the region to changes in temperature and humidity [*Dawson et al.*, 2007], suggesting that aerosol thermodynamics are a minor factor in the reduction in $PM_{2.5}$ over the southern Great Lakes, relative to the seasonal effects of transport processes. This is certainly the case in spring and fall, when the differences in $PM_{2.5}$ concentrations over lake and land are greatest (Figure 4-2), yet the differences in temperature and humidity are lowest. The pattern of long periods with low concentrations interspersed with episodic peaks further rules out deposition from intermittent lake effect rainfall as the cause of the low concentrations over the lakes.

In a molar balance of gaseous reactive nitrogenous species over Lake Michigan from October to March (not shown), mixing ratios of reactive gaseous nitrogen and its individual components rise and fall episodically in concert with $NO_3^-$ aerosols, without any lag. Thus, partitioning to gaseous nitrogen species over the lakes is not evident to explain the lowered $NO_3^-$ concentrations evident in Figure 4-3. Instead, gaseous species corroborate transport rather than chemistry as the cause of lower concentrations over the

lakes. This persistent lake effect represents a strong limitation on regional-scale west-to-east $NO_3^-$ transport in the region, precisely during the seasons when $NO_3^-$ is present at it highest concentrations. Modeled $NH_3$ concentrations are not enhanced over the lakes, either, so volatilization from $NH_4^+$ aerosol to $NH_3$ cannot explain this phenomenon, providing further evidence that lake effect mediation of aerosol transport rather than a lake effect on aerosol thermodynamics or heterogeneous chemistry is responsible.

We note that in winter and fall, when $PM_{2.5}$ across the sparsely populated northwest of the region is more than 50% OM and mostly biogenic, surface OM levels over Lake Superior are sharply lower than over its southern and northwestern shores, indicating limited transport over the lake. Part of this reduction is due to the lifting and mixing of aerosols in the deep boundary layer over the warm lake, with OM concentrations reaching a maximum at approximately 300-400 m, where OM is 7% higher than at the surface. However, OM throughout the boundary layer remains higher over the shores than over the lake, double at the surface, and over 2 $\mu g/m^3$ more in the lowest 1 km. As this is a time period and place where dispersed natural emissions are responsible for most aerosol mass [*Sheesley et al.*, 2004], and where concentrations are skillfully simulated, the low concentrations over the lake provides confirmation that the majority of the regional aerosol burden in surface air is simply advected around the deep marine boundary layers of the Great Lakes.

Deposition of ionic aerosols, mercury, and aqueous chemicals—and resultant aquatic acidification and contamination of the Great Lakes—has long been studied with regard to their emissions sources and ecological impacts. However, our results indicate that the Great Lakes also impact spatial patterns of aerosol deposition. Most directly, in winter and fall, freshly emitted $SO_2$ and aerosol $SO_4^{2-}$ dry deposit out over the lakes, particularly over the southern Lake Michigan, such that the majority of annual sulfur deposition to the lakes occurs in this period, when ambient aerosol $SO_4^{2-}$ concentrations are at a minimum. Deposition of $NH_4^+$ is also impacted, with the lake surfaces receiving the highest levels of wet and dry deposition in the region November-January and the lowest levels of dry deposition April-September. Nitrate dry deposition is enhanced over the lakes in winter, when ambient concentrations are highest (Table 3-4), and again the lowest in the region from April through September, when only trace nitrate aerosol levels ($< 1\ \mu g/m^3$) are present.

*4.3.3. The Role of the Great Lakes in the Formation and Transport of Ozone*

Prior studies [e.g. *Nolte et al.*, 2008] have found that CMAQ tends to overestimate ambient $O_3$ concentrations while nonetheless reproducing the seasonality, diurnal cycle, an d spatial distribution of $O_3$. This simulation finds a bias of approximately 11 ppb, which is consistent throughout the $O_3$ season and across the study domain. On average, 7 ppb of this overestimate is due to high biases in the continental boundary conditions for $O_3$ and its precursors from MOZART, as determined from a

simulation using climatological clean hemispheric boundary conditions. This bias in MOZART boundary conditions as input to CMAQ was also found by *Lin et al.* [2008] for East Asia. Much of the remaining 3-5 ppb bias is likely due to inventory overestimates of U.S. $NO_x$ emissions from power plants [*Frost et al.*, 2006], along with a 60% overestimate in anthropogenic carbon monoxide [*Hudman et al.*, 2008]. Additional high bias is likely due to the offline calculation of photolysis rate constants, and an overestimate of tropospheric UV radiation available for photochemistry due to severe summertime underprediction of organic aerosol concentrations (Chapter 3), as CMAQ concentrations are less than half of observed values in June and July, limiting associated scattering and reflection. Incoming radiation may also be too high if modeled and assumed climatological abundances in JPROC's standard profiles of ozone and volcanic aerosol in the stratosphere are incorrect, lowering stratospheric absorption.

The lake effect influences on wind and PBL height that modulate the distribution of aerosols combine to impact the seasonality of $O_3$ formation and transport near the Great Lakes. However, while the lakes exert regional influences on climate and aerosol transport, persistent seasonal effects on $O_3$ are limited to the immediate vicinity of the lakes. Ozone concentrations over the lakes are enhanced by lake effect processes throughout the year (Figure 4-7), with lake gridcells an average of 5.3 ppb higher than the adjacent shores, and 3.2 ppb higher than the domain average over land on an annual basis. This excess is due to increased temperature over the lake surfaces in winter and fall, and enhanced photochemistry and transport in the shallow conductance layer in the

spring and summer. Lake enhancement of $O_3$ is highest in summer, averaging 7.1 ppb. Concentrations are elevated over the surface of all the lakes throughout the year, and the reaction-rate influence is relatively uniform in winter (Figure 4-7a) and fall (Figure 4-7d), but the transport-based increase is non-uniform and greatest over the southern lakes in spring (Figure 4-7b) and especially summer (Figure 4-7c). This non-uniformity occurs as generally weak southerly synoptic winds bring emissions from lakeshore cities (Chicago, Cleveland, Gary, Milwaukee) over the lake surface, at which point the lake breeze dominates local wind direction and speed and becomes the dominant factor in the dispersion of $O_3$.

The shallow marine conductance layer in the spring and summer also impacts the diurnal cycle of surface level $O_3$ over the Great Lakes. Over land in the region, both $NO_x$-limited rural areas and VOC-limited urban areas display a secondary night-time recovery [*Bremaund et al.*, 1998] in $O_3$ (Figure 4-8) as the boundary layer subsides (Figure 4-9a) and $O_3$-rich air from aloft subsides and is then depleted. This nighttime recovery is calculated as the maximum increase in $O_3$ concentration after it reaches an evening minimum (before 3.a.m. local time) and before photochemical $O_3$ formation begins at local sunrise. We note that this recovery is short-lived, as after the high daytime boundary layer subsides, a low and stable nocturnal boundary layer forms, limiting the temporal window in which upper tropospheric $O_3$ can descend to the surface. This vertical influx is a particularly important transport-based source of $O_3$ in remote areas in the north of the region, where the diurnal range is less than 10 ppb (Figure 4-10), and

where night-time recovery represents a substantial fraction of diurnal variability. This phenomenon is more direct at the 36 km model scale than in urban observations (Figure 4-9b), where fresh $NO_x$ emissions and local mixing diminish the signal. Modeled night-time recovery over cities (Figure 4-9b) may also be higher than in observations due to the high minimum value set for $Kz_{min}$ in predominantly urban gridcells (Chapter 2.2.2). However, since the height of the marine conductance layer is invariant (Figure 9-a), the marine atmosphere is stable and vertical mixing is greatly diminished, the lake surface does not receive this nocturnal vertical flux. As a result, the marine diurnal cycle over the Great Lakes is typified by a simple sinusodial curve (Figure 4-9b), while Chicago, on the shore of Lake Michigan, is not. This simplified marine diurnal $O_3$ cycle at the surface due to the absence of vertical mixing has been documented over open ocean [e.g. *Chand et al.,* 2003; *Bremaud et al*., 1988], and in the Aegean sea [*Kouvarakis et al*., 2002]. By comparison, the diurnal cycle simulated by CMAQ in East Asia [*Lin et al*., 2008] is damped in remote coastal areas and has a wider range in polluted urban environments, illustrating that the diurnal patterns in $O_3$ over the Great Lakes region are the result of their peculiar boundary layer dynamics, rather than an inherent model artifact. Thus, while the marine conductance layer leads to higher $O_3$ production and greater peak $O_3$ values at the surface, this transport feature also serves to limit nighttime $O_3$ recovery over the Great Lakes, reducing the initial "base" concentration at sun-up, and is therefore an important limitation on the daily maximum $O_3$ value over the lakes as well.

*4.3.4. The Role of the Great Lakes in Pollutant Export Processes*

The Great Lakes exert a strong and consistent impact on regional export within the boundary layer, including transport to the Northeast U.S. and trans-boundary movement across the Canada/U.S. border. For most of the year, northwesterly flow around southern Lake Michigan channels $O_3$ and aerosols originating from this major emissions area southeast over Ohio and on to the Atlantic seaboard, while limiting northward transport. Convergence over Lake Huron and western Lake Erie in winter and spring then further limits northward transport, but carries aerosols from throughout the region to the Northeast U.S. and over the Canadian populations centers of Toronto, Ottawa, and Montreal.

While lake effect transport plays a key role in the seasonality of aerosol concentrations at the surface and throughout the mixed layer, this influence is present but less pronounced in the free troposphere. The spatial patterns shown for the surface layer are consistent throughout the first 3 km of the atmosphere, gradually lofting eastward under prevailing westerly wind shear as simulated concentrations decline linearly with height. Local vertical profiles (Figure 4-3) demonstrate that during the cool seasons, $PM_{2.5}$ export leads to consistent concentrations in the lower free troposphere of 6 – 10 $\mu g/m^3$, more than half of surface concentrations, and lower over the lake. Then, during the spring and summer, export is higher over lake than land, reaching 80% of surface concentrations, and enhanced to a height in excess of 1 km. Thus, along with their large

footprint at the surface, the Great Lakes influence the export of aerosols to the free troposphere, and appear to play a role in the distribution of aerosols at the regional to hemispheric scales by enhancing regional export above the boundary layer in the summer and reducing it in the winter.

It is important to note that while the Great Lakes set up a consistent lake breeze system [*Lyons*, 1972, *Patrinos and Kistler,* 1977] which is present in the 36 km MM5 simulation and important in the local mixing of lake-enhanced summertime $O_3$ [*Lennartson and Schwartz*, 2002], the lake breeze does not appear to play an important role in the regional-scale seasonal dynamics of aerosol formation, chemical transformation, or transport. This is in contrast to the primacy of the land-sea breeze in defining pollution transport that has been found in observations and model studies in many coastal areas (see *Miller et al*. [2003] for a comprehensive review).

**4.4. Summary and Conclusion**

We employed the Community Multiscale Air Quality model to identify the contributions of lake effect meteorology to the seasonality of ozone and aerosol chemical transport in the Great Lakes region. We find that lake effect meteorology—particularly modulation of marine boundary layer height—has a seasonal impact on regional aerosol transport, greatly reducing advection of polluted air over the southern Great Lakes in the fall and winter and enhancing northward transport over the lakes and export to the free troposphere in the spring stable lake season. Climatic conditions lead to typical aerosol

concentrations over the southern lakes 50% lower than over land during the cool seasons. Ozone over the Great Lakes is enhanced throughout the year, by an average of 7.1 ppb higher than the adjacent shores in the summer, as a result of increased temperature over the lake surfaces in winter and fall, and enhanced photochemistry and transport in the shallow conductance layer in the spring and summer. Effects of lake effect meteorology on both aerosols and ozone are most acute over the surface of the lakes themselves, but extend to impact both long-range transport and vertical export.

By identifying how the seasonal cycles of the Great Lakes affect present-day aerosol transport from emissions sources, this study provides a means for gaining deeper understanding of the ways that changes in climate and emissions are mediated by persistent land surface effects in their impacts on air quality. Our results also provide a new context for viewing studies on the sensitivity of aerosols in eastern North America to arbitrary changes in climatic parameters [e.g. *Dawson et al.*, 2007], as well as scenario-based studies [e.g. *Hogrefe et al.*, 2004b, *Tagaris et al.*, 2007], and particularly for understanding spatial patterns in simulated changes in aerosols and ozone in this region. A more thorough understanding of how lake effect transport persistently impacts secondary aerosol concentrations in populous areas, counties in violation of National Ambient Air Quality Standards for fine particles, and Class I visibility areas will also lend further guidance for the siting of new emissions sources in the region.

**References**

Bae, M.S., J.J. Schauer, and J.R. Turner (2006a), Estimation of the monthly average ratios of organic mass to organic carbon for fine particulate matter at an urban site, *Aerosol Sci. Tech.*, 40 (12), 1123-1139, doi: 10.1080/02786820601004085.

Bae, M.S., K.L. Demerjian, and J.J. Schwab (2006b), Seasonal estimation of organic mass to organic carbon in PM2.5 at rural and urban locations in New York state, *Atmos. Environ.,* 40(39), 7467-7479, doi:10.1016/j.atmosenv.2006.07.008.

Berg, W.W., R. Vié le Sage, K. Sato, J.O. Pilotte, S. L. Cohn, J. W. Winchester, and J. W. Nelson (1977), Hourly Variation Of Aerosol Composition In The Great Lakes Basin, *J. Great Lakes Res.*, 3(3-4):278-290.

Bremaud, P. J., F. Taupin, A. M. Thompson, and N. Chaumerliac (1998), Ozone nighttime recovery in the marine boundary layer: Measurement and simulation of the ozone diurnal cycle at Reunion Island, *J. Geophys. Res.*, 103(D3), 3463–3473, doi: 10.1029/97JD01972.

Buzcu-Guven, B., S.G. Brown, A. Frankel, H.J. Hafner, and P.T. Roberts (2007), Analysis and apportionment of organic carbon and fine particulate matter sources at multiple sites in the Midwestern United States, *Journal Of The Air & Waste Management Association*, 57(5), 606-619.

Chand, D., S. Lal, and M. Naja (2003), Variations of ozone in the marine boundary layer over the Arabian Sea and the Indian Ocean during the 1998 and 1999 INDOEX campaigns, *J. Geophys. Res.*, 108(D6), 4190, doi:10.1029/2001JD001589.

Chu, S.H. (2004), PM2.5 episodes as observed in the speciation trends network, *Atmos. Environ.*, 38(31), 5237-5246, doi:10.1016/j.atmosenv.2004.01.055.

Dawson, J. P., Adams, P. J., and S. N. Pandis (2007), Sensitivity of PM2.5 to climate in the Eastern U.S.: a modeling case study, *Atmos. Chem. Phys. Discuss.*, 7, 6487-6525, www.atmos-chem-phys.net/7/4295/2007.

Dye, T.S., P.T. Roberts, and M.E. Korc (1995), Observations of Transport Processes for Ozone and Ozone Precursors during the 1991 Lake Michigan Ozone Study, *J. Appl. Met.*, 34(8), 1877–1889, doi: 10.1175/1520-0450(1995)034<1877:OOTPFO>2.0.CO;2.

Elleman, R. A., R.A. Kotchenruther, D.S. Covert, C.F. Mass and J. Chen (2004). CMAQ Aerosol Number and Mass Evaluation for Pacific Northwest, *Models-3 User's Workshop*, Research Triangle Park, NC.

Eshel, G., and J.J. Bernstein (2006), Relationship Between Large-Scale Atmospheric States, Subsidence, Static Stability and Ground-Level Ozone in Illinois, USA, *Water, Air, & Soil Pollution*, 171, 111-133, doi: 10.1007/s11270-005-9021-x.

Fast, J.D., and W.E. Heilman (2003), The Effect of Lake Temperatures and Emissions on Ozone Exposure in the Western Great Lakes Region, *J. Appl. Meteor.*, 42, 1197–1217, doi: 10.1175/1520-0450(2003)042<1197:TEOLTA>2.0.CO;2.

Fast, J.D., and W.E. Heilman (2005), Simulated sensitivity of seasonal ozone exposure in the Great Lakes region to changes in anthropogenic emissions in the presence of interannual variability, *Atmos. Environ.*, 39, 5291-5306, doi:10.1016/j.atmosenv.2005.05.032.

Frost, G.J., S. A. McKeen, M. Trainer, T.B. Ryerson, J.A. Neuman, J.M. Roberts, A. Swanson, J.S. Holloway, D.T. Sueper, T. Fortin, D.D. Parrish, F.C. Fehsenfeld, F. Flocke, S.E. Peckham, G.A. Grell, D. Kowal, J. Cartwright, N. Auerbach, and T. Habermann (2006), Effects of changing power plant NOx emissions on ozone in the eastern United States: Proof of concept, *J. Geophys. Res.*, 111, D12306, doi:10.1029/2005JD006354.

Hanna, S.R., and J.C. Chang (1994), Relations between Meteorology and Ozone in the Lake Michigan Region, *J. Appl. Met.*, 34(3), 670–678, doi: 10.1175/1520-0450(1995)034<0670:RBMAOI>2.0.CO;2.

Harris, L., and V.R. Kotamarthi (2005), The Characteristics of the Chicago Lake Breeze and Its Effects on Trace Particle Transport: Results from an Episodic Event Simulation, J. *Appl. Met.*, 44(11), 1637–1654, doi: 10.1175/JAM2301.1.

Hastie D.R., J. Narayan, C. Schiller, H. Niki, P.B. Shepson, D.M.L. Sills, P.A. Taylor, W.J. Moroz, J.W. Drummond, N. Reid, R. Taylor; P.B. Roussel, and O.T. Melo (1999), Observational Evidence for the Impact of the Lake Breeze Circulation on Ozone Concentrations in Southern Ontario, *Atmos. Environ.*, 33, 323-335.

Hogrefe, C., J. Biswas, B. Lynn, K. Civerolo, J.-Y. Ku, J. Rosenthal, C. Rosenzweig, R. Goldberg, and P.L. Kinney (2004a), Simulating regional-scale ozone climatology over the Eastern United States: Model evaluation results, *Atmos. Environ.*, 38 (17), 2627-2638, doi:10.1016/j.atmosenv.2004.02.033.

Hogrefe, C., B. Lynn, K. Civerolo, J.Y. Ku, J. Rosenthal, C. Rosenzweig, R. Goldberg, S. Gaffin, K. Knowlton, and P.L. Kinney (2004), Simulating changes in regional air pollution over the eastern United States due to changes in global and regional climate and emissions, *J. Geophys. Res.*, 109(D22), D22301, doi: 10.1029/2004JD004690.

Huang, H.C., X.Z. Liang, K.E. Kunkel, M. Caughey, and A. Williams, 2007: Seasonal Simulation of Tropospheric Ozone over the Midwestern and Northeastern United States: An Application of a Coupled Regional Climate and Air Quality Modeling System. *J. Appl. Meteor. Climatol.*, 46, 945–960, doi: 0.1175/JAM2521.1.

Hudman, R.C., L. T. Murray, D. J. Jacob, D. B. Millet, S. Turquety, S. Wu, D. R. Blake, A. H. Goldstein, J. Holloway, and G. W. Sachse (2008), Biogenic versus anthropogenic sources of CO in the United States, *Geophys. Res. Lett.*, 35, L04801, doi:10.1029/2007GL032393.

Kerr .SC., J.J. Schauer, and B. Rodger (2004), Regional haze in Wisconsin: sources and the spatial distribution, *J. Env. Eng. Sci.,* 3(3), 213-222, doi: 10.1139/S04-003.

Kim, E., P.K. Hopke, D.M Kenski, and M. Koerber (2005), Sources of fine particles in a rural Midwestern area, *Environ. Sci. Tech.*, 39, 4953-4960, doi: 10.1021/es04907749.

Kim, M., S.R. Deshpande, and K.C. Crist (2007), Source apportionment of fine particulate matter (PM2.5) at a rural Ohio River Valley site, *Atmos. Environ.*, 41, 9231–9243, doi:10.1016/j.atmosenv.2007.07.061.

Kouvarakis, G., M. Vrekoussis, N. Mihalopoulos, K. Kourtidis, B. Rappenglueck, E. Gerasopoulos, and C. Zerefos (2002), Spatial and temporal variability of tropospheric ozone (O3) in the boundary layer above the Aegean Sea (eastern Mediterranean), *J. Geophys. Res.*, 107(D18), 8137, doi:10.1029/2000JD000081.

Lasher-Trapp, S., and J.P. Stachnik (2007), Giant and ultragiant aerosol particle variability over the eastern Great Lakes region, *J. Appl. Met. Clim.*, 46(5), 651-659.

Lawrence, M.G., T.M. Butler, J. Steinkamp, B.R. Gurjar, and J. Leliveld (2007), Regional pollution potentials of megacities and other major population centers, *Atmos. Chem. Phys.*, 7, 3969-3987.

Lee, P.K.H., J.R. Brook, E. Dabek-Zlotorzynska, and S.A. Mabury (2003), Identification of the major sources contributing to PM2.5 observed in Toronto, *Environ. Sci. Tech.*, 37(21), 4831-4840, doi: 10.1021/es026473i S0013-936X(02)06473-8.

Lennartson, G.J., and M.D. Schwartz (2002), The lake breeze-ground-level ozone connection in eastern Wisconsin: a climatological perspective, *Int. J. Climatol.*, 22(11), 1347-1364, doi: 10.1002/joc.802.

Lin, M., T. Oki, M. Bentsson, T. Holloway, D.G. Streets, and S. Kanae (2008), Long-range transport of acidifying substance in East Asia-Part I: Model evaluation, *Atmos. Environ.*, in review.

Lyons, W.A. (1972), The Climatology and Prediction of the Chicago Lake Breeze, *J. Appl. Met.*, 11(8), 1259–1270, DOI: 10.1175/1520-0450(1972)011<1259:TCAPOT>2.0.CO;2.

Lyons, W.A., and H.S. Cole (1976), Photochemical Oxidant Transport: Mesoscale Lake Breeze and Synoptic-Scale Aspects, *J. Appl. Met.*, 15(7),733–743, doi: 10.1175/1520-0450(1976)015<0733:POTMLB>2.0.CO;2.

Malm, W.C., and J.L. Hand (2007) An examination of the physical and optical properties of aerosols collected in the IMPROVE program, *Atmos. Environ.*, 41(16), 3407-3427, doi:10.1016/j.atmosenv.2006.12.012.

Malm, W.C., B.A. Schichtel, M.L. Pitchford, L.L. Ashbaugh, and R.A. Eldred (2004), Spatial and monthly trends in speciated fine particle concentration in the United States, *J. Geophys. Res., 109*(D3), D03306, doi:10.1029/2003JD003739.

Miller, S.T.K., B.D. Keim, R.W. Talbot, and H. Mao (2003), Sea breeze: Structure, forecasting, and impacts, *Rev. Geophys.*, 41(3), 1011, doi:10.1029/2003RG000124.

Nolte, C.G., A.B. Gilliland, C. Hogrefe, and L.J. Mickely (2008), Linking global to regional models to assess future climate impacts on surface ozone, *J. Geophys. Res.* (in press), doi:10.1029/2007JD008497.

Offenberg, J.H., and J.E. Baker (2000), Aerosol size distributions of elemental and organic carbon in urban and over-water atmospheres, *Atmos. Environ.*, 34(10), 1509-1517, doi:10.1016/S1352-2310(99)00412-4.

Patrinos, A.A.N., and A.L. Kistler (1977), A numerical study of the Chicago lake breeze, *Boundary-Layer Meteorology*, 12(1), 93-123, DOI: 10.1007/BF00116400.

Phillips, S.B., and P.L. Finkelstein (2006), Comparison of spatial patterns of pollutant distribution with CMAQ predictions, *Atmos. Environ.*, 40(26), 4999-5009, doi:10.1016/j.atmosenv.2005.12.064.

Rao, V., N. Frank, A. Rush, and F. Dimmick (2003), Chemical speciation of PM2.5 in urban and rural areas in national air quality and emissions trends report. /http://www.epa.gov/air/airtrends/aqtrnd03S.

Rizzo, M.J., and P.A, Scheff (2007), Fine particulate source apportionment using data from the USEPA speciation trends network in Chicago, Illinois: Comparison of two

source apportionment models, *Atmos. Environ.*, 41(29), 6276-6288, doi:10.1016/j.atmosenv.2007.03.055

Schertzer, W. M. , J. H. Saylor, F. M. Boyce, D. G. Robertson, and F. Rosa (1987), Seasonal Thermal Cycle Of Lake Erie, *J. Great Lakes Res.*, 13(4):468-486.

Scott, R.W., and F.A. Huff (1996), Impacts of the Great Lakes on Regional Climate Conditions, *J. Great Lakes Res.*, 22(4):845-863.

Sickles, J.E., and D.S. Shadwick (2007), Seasonal and regional air quality and atmospheric deposition in the eastern United States, *J. Geophys Res.*, 112(D17), D17302, doi: 10.1029/2006JD008356.

Sheesley, R. J., J. J. Schauer, E. Bean, and D. Kenski (2004), Trends in Secondary Organic Aerosol at a Remote Site in Michigan's Upper Peninsula, *Env. Sci. Tech.*, 38, 6491-6500, doi: 10.1021/es049104q.

Sillman, S., P. J. Samson, and J. M. Masters (1993), Ozone Production in Urban Plumes Transported Over Water: Photochemical Model and Case Studies in the Northeastern and Midwestern United States, *J. Geophys. Res.*, 98:12687-12699.

Stone, B., A. Mednick, T. Holloway, and S.N. Spak (2007), Is Compact Growth Good For Air Quality? Journal of the American Planning Association, 73:4, 404-418. doi: 10.1080/01944360708978521.

Subramanian R., N.M. Donahue, A. Bernardo-Bricker, W.F. Rogge, and A.L. Robinson (2007), Insights into the primary-secondary and regional-local contributions to organic aerosol and PM2.5 mass in Pittsburgh, Pennsylvania, *Atmos. Environ.*, 41(35), 7414-7433, doi: 10.1016/j.atmosenv.2007.0.

Tagaris, E., K. Manomaiphiboon, K.-J. Liao, L. R. Leung, J.-H. Woo, S. He, P. Amar, and A. G. Russell (2007), Impacts of global climate change and emissions on regional ozone and fine particulate matter concentrations over the United States, *J. Geophys. Res.*, 112, D14312, doi:10.1029/2006JD008262.

US EPA (2001), Evaluation of PM2.5 speciation sampler performance and related sample collection and stability issues. *Report* EPA-454/R-01-008, U.S. Environmental Protection Agency, Research Triangle Park, N.C.

Woods, H.L., T. Holloway (2007), Meteorological Processes Affecting Aerosols in the Great Lakes Region. Unpublished master's thesis, University of Wisconsin-Madison.

Wolff, G.T., P.J. Lioy; G.D. Wight; R.E. Meyers, and R.T. Cederwall, (1977), An investigation of long-range transport of ozone across the midwestern and eastern United States, *Atmos. Environ.*, 11(9), 797-802.

Yu, S., R. Dennis, S. Roselle, A. Nunes, J. Walker, B. Eder, K. Schere, J. Swall, and W. Robarge (2005), An assessment of the ability of three-dimensional air quality models with current thermodynamic equilibrium models to predict aerosol $NO_3^-$, *J. Geophys. Res.*, 110, D07S13, doi:10.1029/2004JD004718.

Zhao, W.X., P.K. Hopke, and L.M. Zhou (2007), Spatial distribution of source locations for particulate nitrate and sulfate in the upper-midwestern United States, *Atmos. Environ.*, 41(9), 1831-1847, doi: 10.1016/j.atmosenv.2006.10.060.

Zhao, W.X., and P.K. Hopke (2006), Source investigation for ambient PM2.5 in Indianapolis, IN, *Aerosol Sci. Tech.*, 40(10), 898-909, doi:10.1080/02786820500380297.

## Figures

**Figure 4-1.** Study region for chemical transport modeling. The transect across the region shown in Figure 6 is outlined in bold. The locations of the points analyzed in Figures 2, 3, and 5 are shown in red, blue, and black.

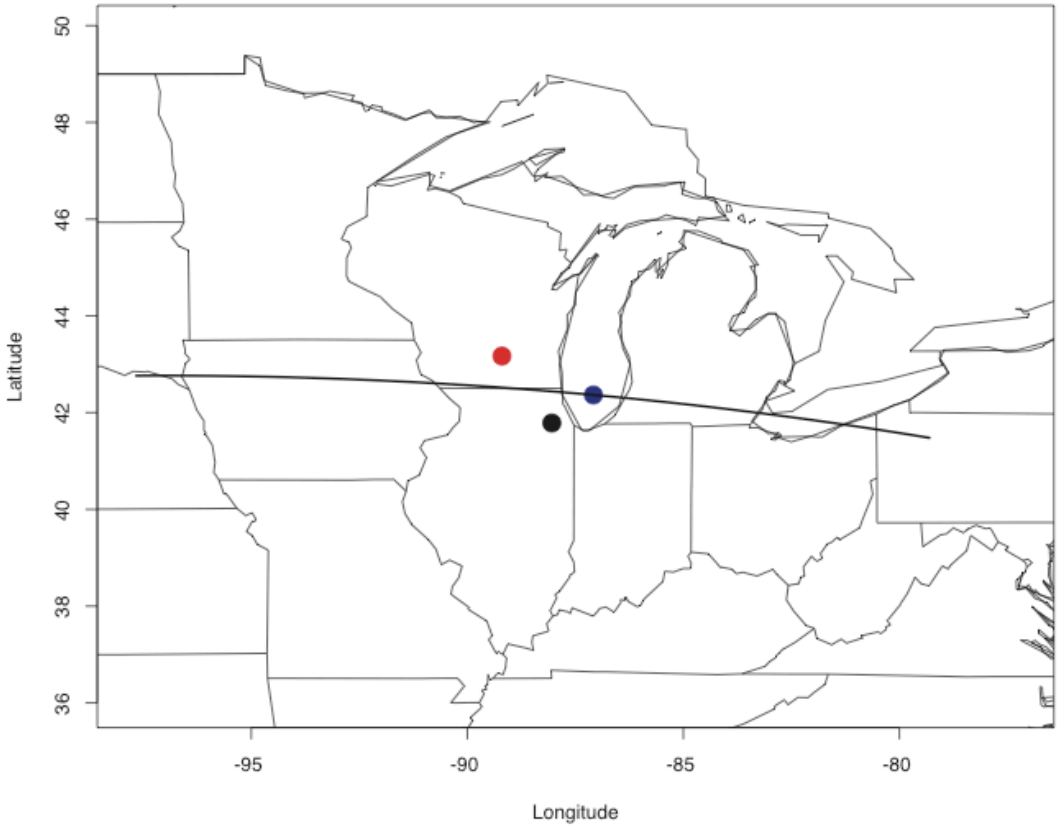

**Figure 4-2.** Observed and simulated lake effect influences on monthly mean climate in the southern Great Lakes. At left, monthly mean surface skin temperature (K), planetary boundary layer height (m), surface pressure (Pa), and wind speed (m/s) at NOAA buoy 45007 in southern Lake Michigan at 87.1° W 42.4° N (blue) and upwind at Madison, Wisconsin at 89.2° W 43.2° N (red). At right, the monthly difference in each quantity (lake – land). MM5 model predictions are shown in solid lines, atmospheric observations in dashes, and subsurface water observations in dots.

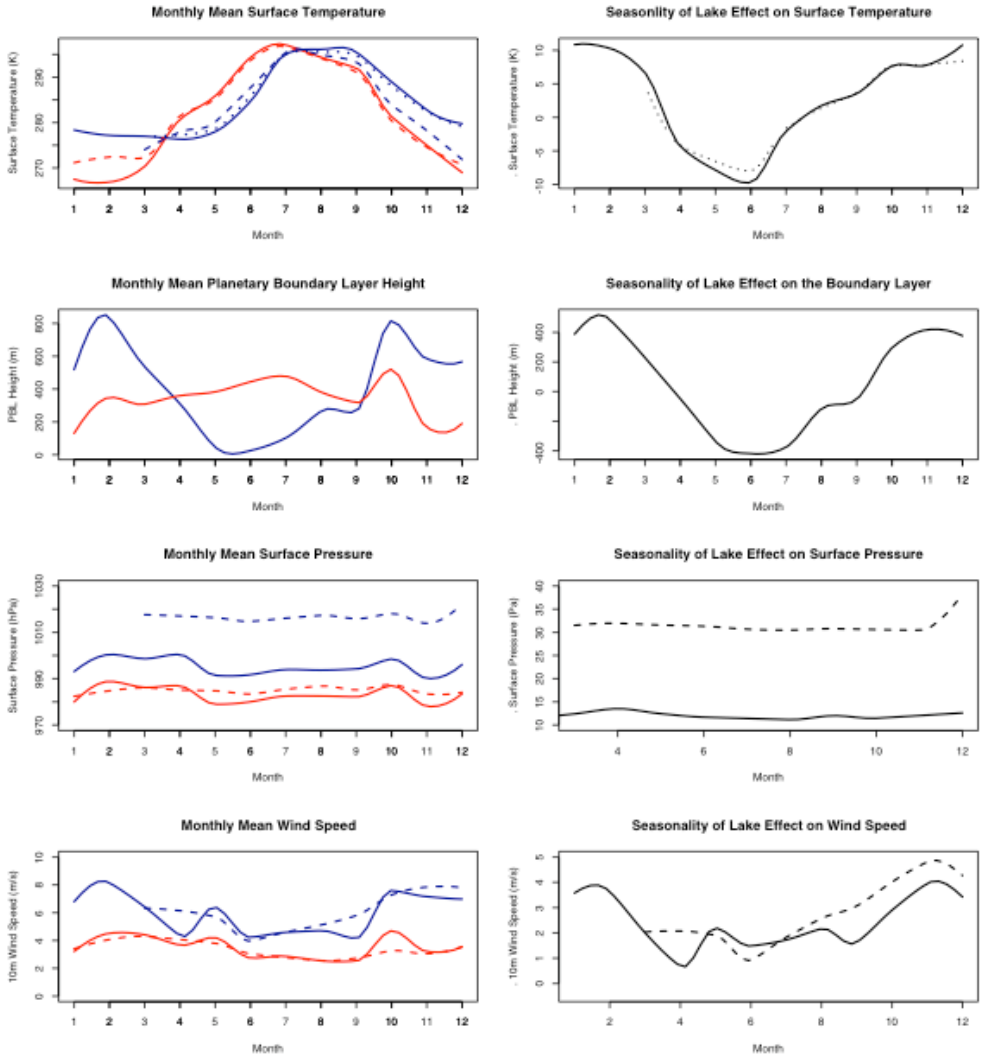

**Figure 4-3.** Seasonality in simulated vertical profiles of temperature (K) and $PM_{2.5}$ concentration ($\mu g/m^3$) over southern Lake Michigan (blue) and Madison, Wisconsin (red). Dotted horizontal lines indicate the seasonal average planetary boundary layer height (m).

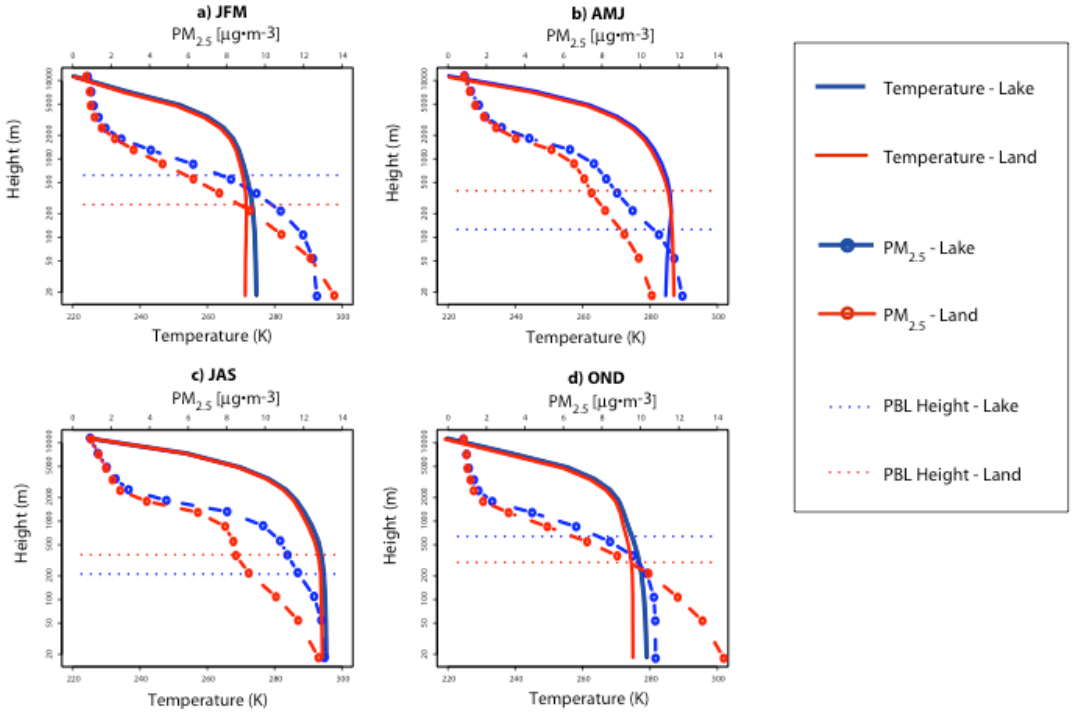

**Figure 4-4.** MM5 simulated planetary boundary layer height (m) and wind vectors at 10 m, shown for each season: a) JFM; b) AMJ; c) JAS; d) OND.

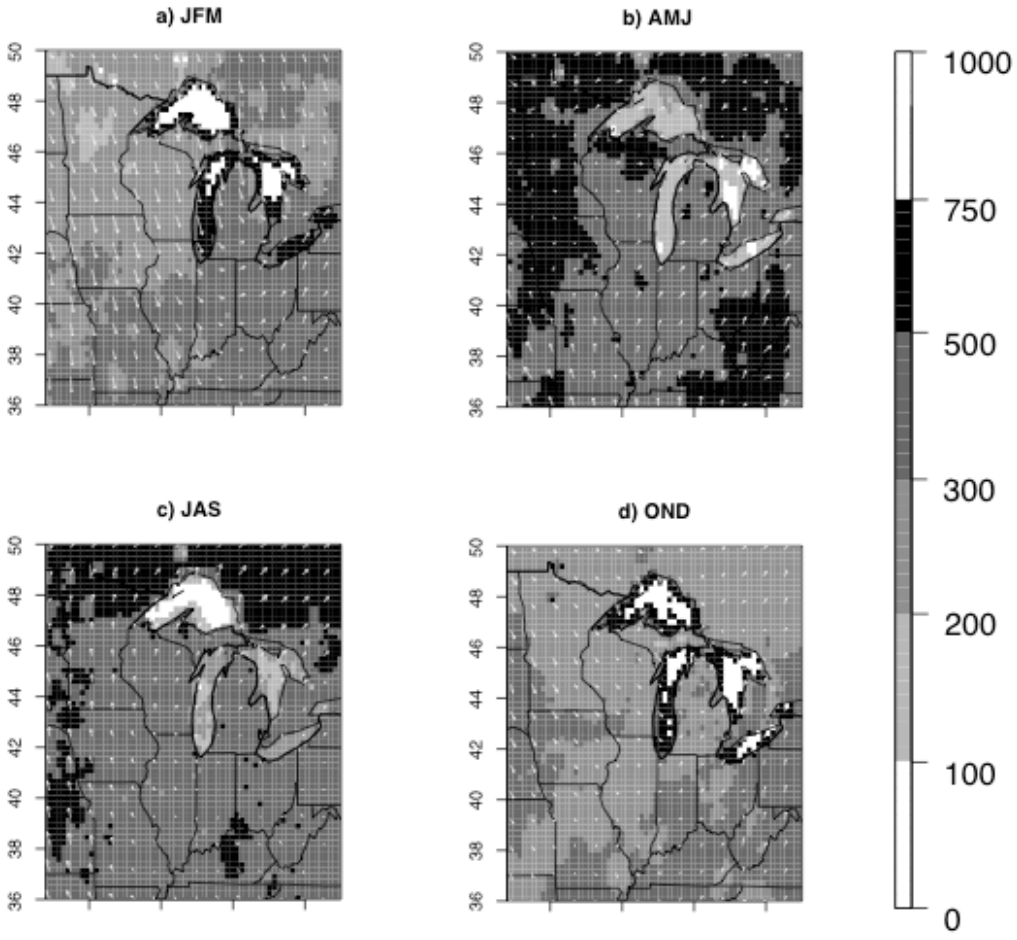

**Figure 4-5.** Hovmöller plot of October 1 (day 274) -December 31 (day 365) hourly time series of simulated $PM_{2.5}$ concentrations ($\mu g/m^3$) on a transect over the southern Great Lakes (outlined in bold in Figure 1) near 42° N. Regional high $PM_{2.5}$ episode circled.

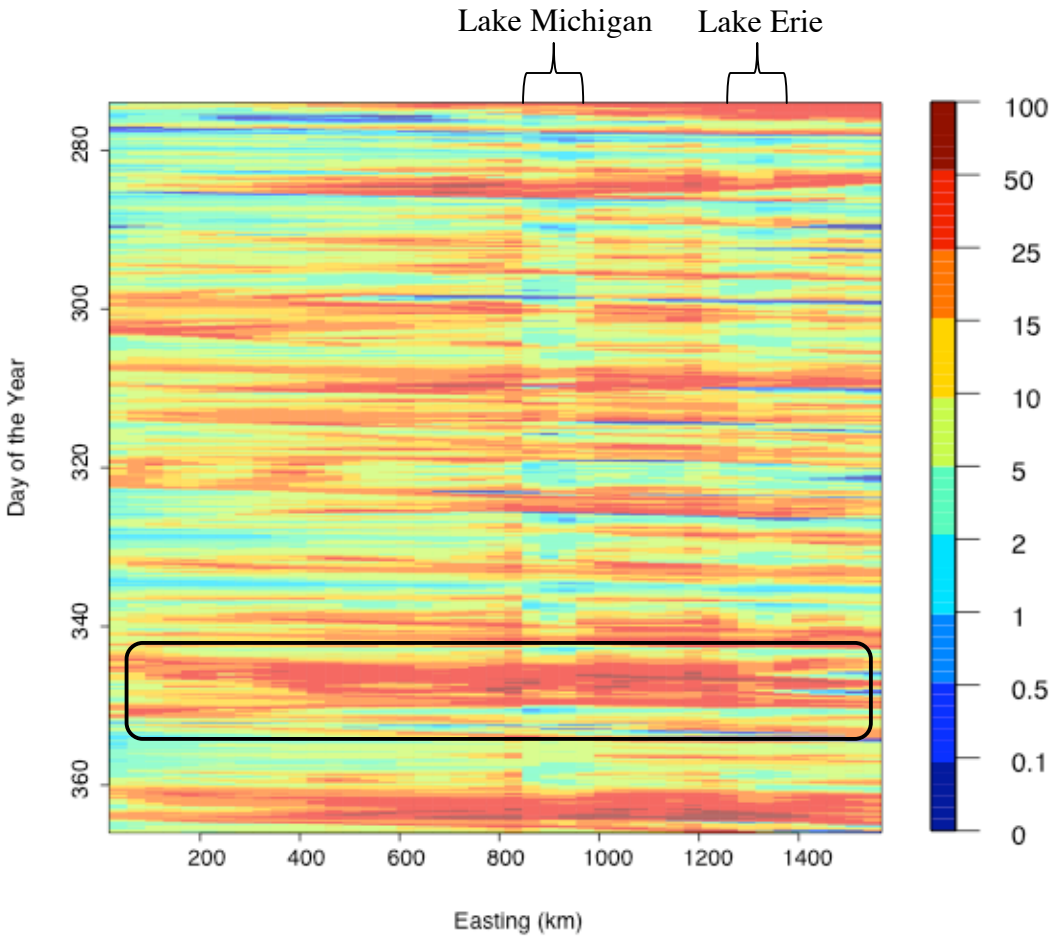

**Figure 4-6.** CMAQ simulated $PM_{2.5}$ concentrations ($\mu g/m^3$) in the lowest model layer, shown for each season: a) JFM; b) AMJ; c) JAS; d) OND.

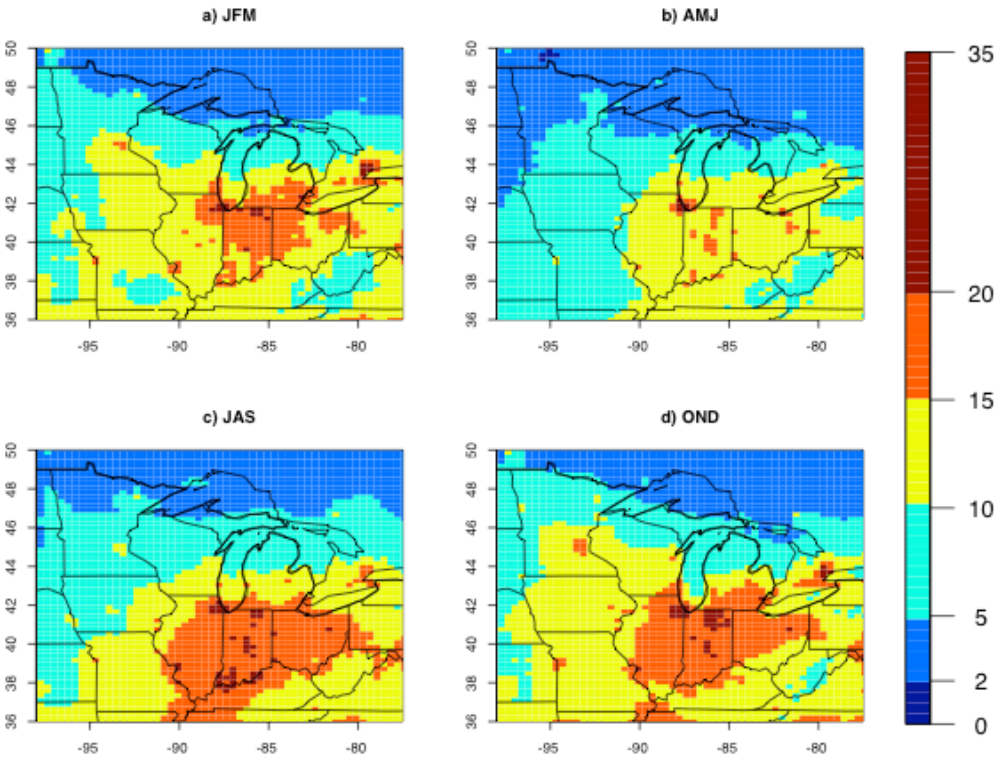

**Figure 4-7.** CMAQ simulated $O_3$ (ppb) in the lowest model layer, shown for each season: a) JFM; b) AMJ; c) JAS; d) OND.

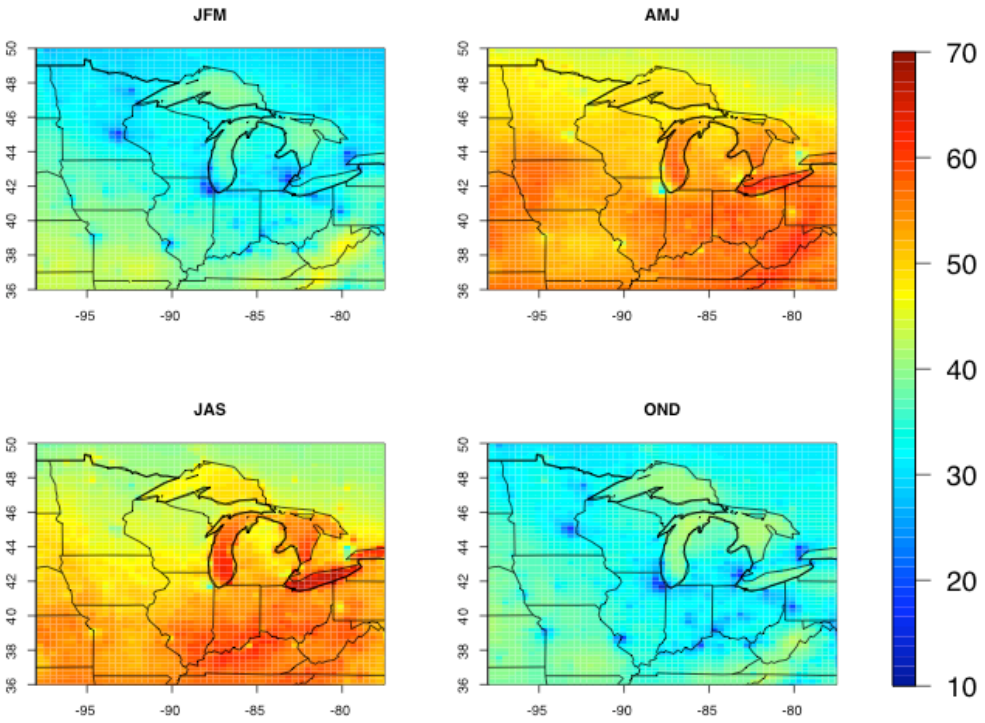

**Figure 4-8.** Simulated June 2002 average nighttime $O_3$ recovery (ppb).

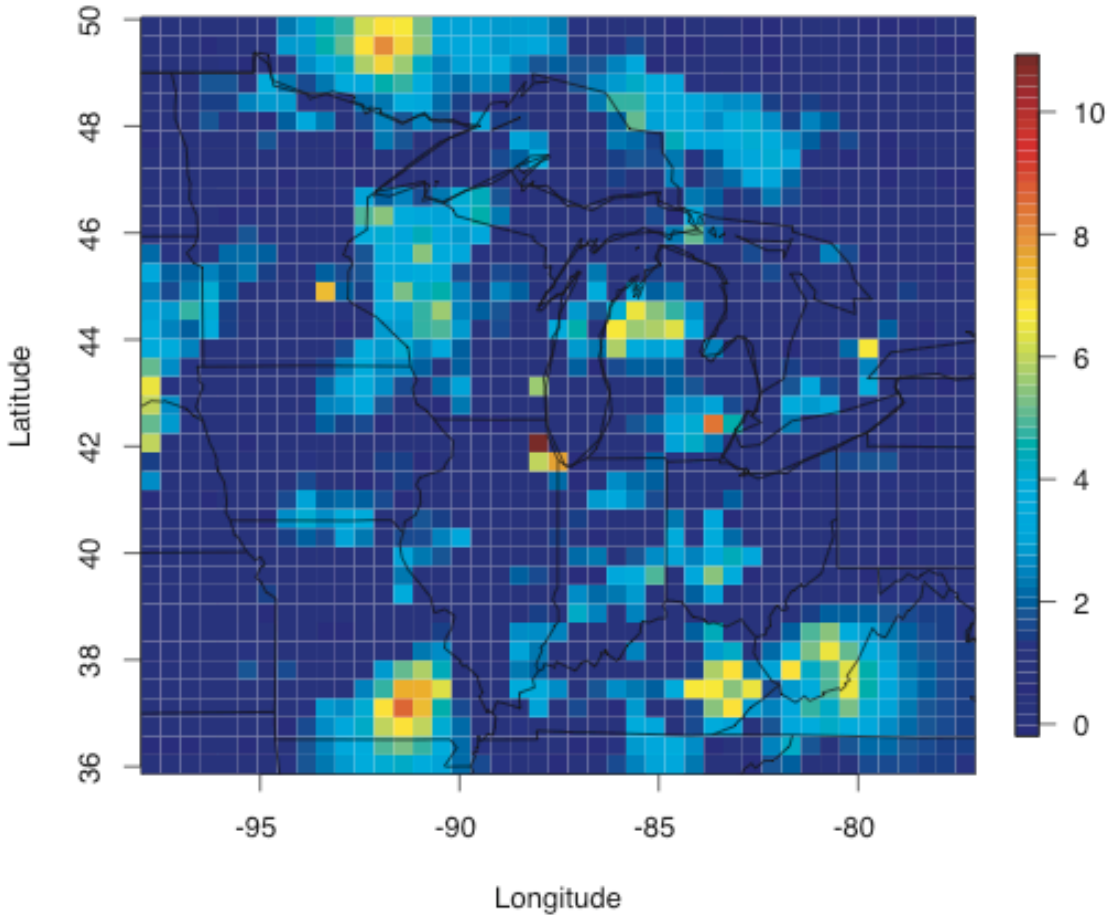

**Figure 4-9.** a) Simulated monthly mean diurnal cycle in PBL height (m) and b) observed and simulated monthly mean diurnal cycle in $O_3$ (ppb) over southern Lake Michigan (blue), Madison, Wisconsin (red), and Chicago, Illinois (black) for June 2002. Model results shown in lines with solid points, EPA AQS $O_3$ observations in lines with open points. Observed values are adjusted by +11 ppb to compensate for model bias.

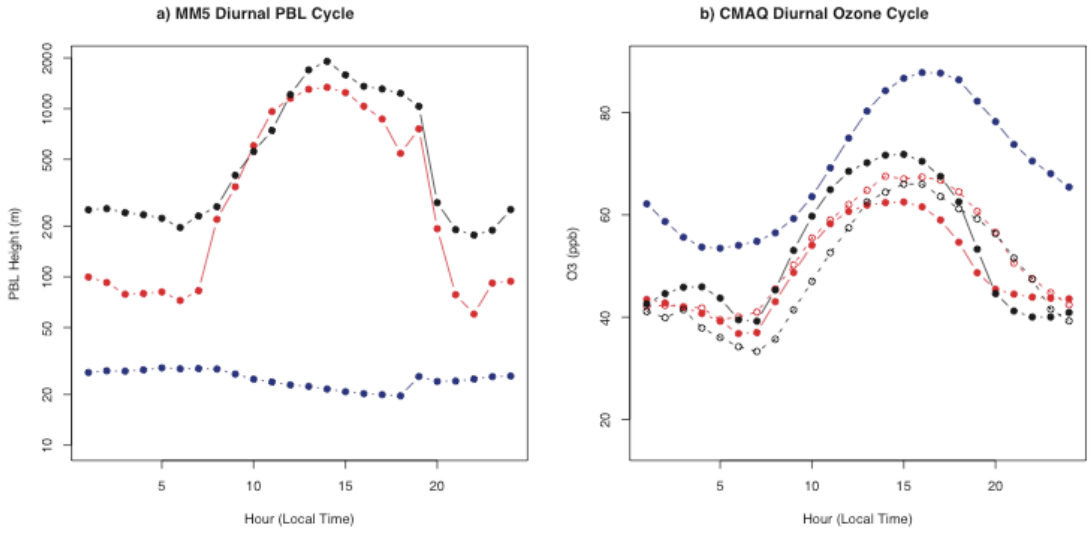

**Figure 4-10.** Simulated June 2002 average diurnal $O_3$ concentration range (ppb), calculated as the differences between the daily maximum and minimum 1-hour average concentrations.

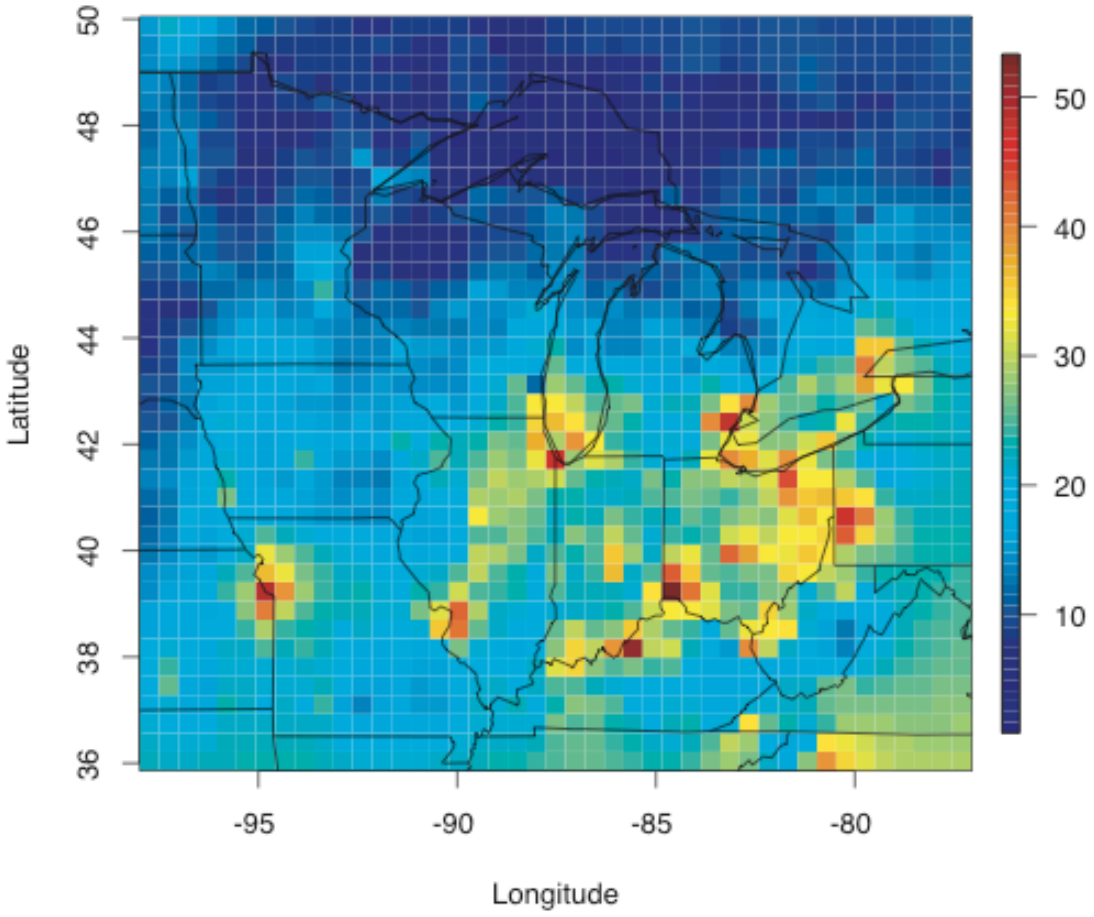

# Chapter 5. Sensitivity of Ozone and Fine Particles to Changes in Anthropogenic Emissions

## 5.1 Introduction

With the notable exceptions of crustal dust, volcanoes, and smoke from forest fires, air quality problems throughout the world are dominated by anthropogenic emissions. In the developed world, most of these emissions are related to energy use; in particular, burning fossil fuels for electricity, transportation, industry, and domestic climate control. In the Upper Midwestern United States, impacts of anthropogenic emissions lead to many counties violating federal health-based ambient air quality standards for both $O_3$ and $PM_{2.5}$ [*USEPA*, 2007]. As a result, the sensitivity of air quality to changes in anthropogenic emissions, particularly to source-specific emissions control technologies, is routinely tested by states, regional planning offices, and federal agencies in order to demonstrate that states, by implementing particular controls, will maintain compliance with the Clean Air Act. However, these controls represent near-term solutions to immediate air pollution problems, such that future air quality is rarely modeled more than 10 years into the future, a point at which potential solutions would be fully implemented and linear assumptions of observed historical changes in emitting activities become highly uncertain.

To date, only a handful of studies have attempted to identify the long-term regional air quality response to changes in anthropogenic emissions [e.g. *Hogrefe et al.*,

2004; *Tao et al*., 2007]. Moreover, most of these studies have applied top-down linear changes based on national-level IPCC emissions scenarios, "dialing up" emissions rates but maintaining the same spatial distribution of emissions sources and emitting activities. In one of the first such studies, *Hogrefe et al*. [2004] found that climate change was responsible for greater increases in air pollution over the eastern United States than local anthropogenic emissions under the A2 scenario. On the other hand, *Tao et al*. [2007] highlighted the important contrasts between A1FI and B1 scenarios to $O_3$ projections (2050 vs. 1998). Under B1, local reductions of $O_3$-precursor emissions offset the climate-induced increases, resulting in an overall decrease across the Midwest, although with localized increases of more than 5 ppb over the Chicago area. In contrast, under A1FI, the climate effect dominates (96% in the Midwest) and produces $O_3$ changes of up to 10 ppb across the eastern U.S.

However, no study to date has studied the potential changes in air quality possible with localized, spatially specific shifts in human behavior and choices in economic activities. In particular, the potential air quality management for land use policy and attendant changes in vehicle travel, the spatial extent and population densities of urban areas. and resultant mobile emissions has yet to be evaluated. As mobile emissions account for 30% to 60% of $NO_x$ and CO emissions in urban areas in the Upper Midwest in the National Emissions Inventory [*USEPA*, 2004], and are a sector in which emission have increased despite major improvements in emissions control technologies [*USEPA*,

2003a], land use policies that reduce automobile travel could represent an important and to date unexamined tool for urban and regional air quality management.

*Stone et al*. [2007] indicated that "smart growth" land use policies based on an urban growth boundary, modeled after the boundary implemented in 1979 in Portland, Oregon, led to densification in urban areas in the Upper Midwest. After 50 years, this enforced densification reduced the frequency and length of automobile trips, with corresponding average reductions in vehicle travel of 10% in the 11 largest Metropolitan Statistical Areas (MSAs), as compared to ongoing urban sprawl without growth boundaries. However, *Stone et al*. found that despite emissions reductions due to smart growth strategies relative to unmitigated urban sprawl, total emissions rates increased due to increases in urban populations.

Here we conduct chemical transport modeling to identify the impacts of changes in urban emissions on $O_3$ and $PM_{2.5}$ in the Great Lakes region. We first run CMAQ at 36 km with fixed urban and rural emissions increases and reductions to understand the potential air quality changes that could potentially be effected through policies of any kind. We then leverage the on-road vehicle travel and emissions inventories developed by *Stone et al*. [2007, 2008] for Projecting the Impact of Land Use and Transportation on Future Air Quality in the Upper Midwestern United States (PLUTO) to estimate the potential air quality benefits specific to land use policies enacted over the 50 years from

2000 to 2050. We then compare these air quality changes to those possible with aggressive adoption of hybrid motor vehicle technologies throughout the region.

## 5.2 Data and Methods

We employed CMAQ, configured as described in Chapter 2. At 36 km, CMAQ was driven by MM5 meteorology as in Chapters 3 and 4. In addition to the base case National Emissions Inventory, we employed five emissions scenarios to evaluate the relative importance of the 11 MSAs in the region with populations greater than 500,000 [*Stone et al.*, 2007]. Following the experimental design of the Task Force on Hemispheric Transport of Air Pollution studies [*LRTAP*, 2007], we tested perturbations of +20% (MSA+) and –20% (MSA-) for all anthropogenic emissions in model gridcells containing the 11 MSAs. In order to understand the relative importance of mobile sources in these urban areas, and to further evaluate the photochemical nonlinearities due to the reduction in aerosol optical depth resulting from reduced primary aerosol emissions, we also used two emissions scenarios (O3+ and O3-) in which the ±20% perturbations were only applied to NOx, anthropogenic VOCs, and CO, the emitted species responsible for photochemical production of $O_3$. A "cities only" scenario (MSA_ONLY) set all anthropogenic emissions in the study domain outside of the 11 MSAs to zero, in order to highlight the importance of interactions between rural and urban emissions on observed regional pollutant burdens. In the MSA_ONLY scenario, agricultural emissions from dust and livestock were considered anthropogenic. We also employed the PLUTO BAU 2050 and SG2 2050 emissions scenarios at 36 km.

At 12 km resolution, we employed the same CMAQ configuration, but driven by WRF meteorology. In addition to the NEI, we ran the PLUTO 2050 mobile scenarios described in Chapter 2. PLUTO scenarios were simulated using emissions factors from the regional year 2000 vehicle fleet. Here we present CMAQ results for the month of July from the business-as-usual (BAU) and incremental smart growth (SG2) scenarios, which provide the most extreme differences in the magnitude and spatial distribution in emissions among the 2050 PLUTO scenarios. The aggressive hybrid-plus scenario was also simulated for BAU in order to compare the relative potential of hybrid technologies and smart growth policies as air pollution control strategies, given sufficient implementation time for both approaches.

Emissions scenarios, resolution, and notation are summarized in Table 5-1.

## 5.3. Results and Discussion

### *5.3.1. Sensitivity of Regional Air Pollution to Changes in Urban and Rural Emissions*

Emissions sensitivity studies highlight that atmospheric chemical transport of $PM_{2.5}$ and $O_3$ in the Great Lakes region—and especially over the surface of the lakes—is strongly dependent on both urban and rural emissions. The response of annual average $PM_{2.5}$ to ±20% changes in anthropogenic emissions from the 11 largest MSAs is highly linear: increases in emissions lead to increases in concentrations, which are greatest near

the urban areas and of equal magnitude with positive and negative perturbations. The MSA+ (Figure 5-1b) and MSA- (Figure 5-1c) scenarios lead to annual average changes of 0.5-1.0 $\mu g/m^3$ across the region, with local changes of 2 $\mu g/m^3$ near most MSAs and the greatest response near Chicago. The O3+ and O3- scenarios, despite changing the emissions precursors for $NO_3^-$ and organic aerosols, two of the dominant species in the region, had minimal impact on annual average $PM_{2.5}$, less than 0.1 $\mu g/m^3$ (Figure 1e and 9f) and not appreciably higher near the MSAs. Chicago, the largest urban area and the only true "megacity" in the region, was the MSA for which annual average $PM_{2.5}$ was the most responsive to the MSA+ and MSA- scenarios and the least responsive to the O3+ and O3- scenarios. Aerosol concentration changes over the Great Lakes are no different than over nearby land.

These results indicate that urban and regional $PM_{2.5}$ concentrations, while highly responsive to changes in urban emissions in general, are relatively unresponsive to changes in pollutant emitted by motor vehicles in urban areas. As a result, local policy initiatives aimed at reducing auto emissions are unlikely to have a large impact on aerosol concentrations and compliance with NAAQS aerosol standards in the cities, at the regional scale, or in long-range transport. However, mobile source controls may be useful for cities on the brink of non-attainment for $PM_{2.5}$ NAAQS.

In contrast to $PM_{2.5}$, summertime $O_3$ responses to changes in emissions, examined through July mean $O_3$ concentrations, were highly nonlinear. With the exception of

Grand Rapids, $O_3$ concentrations near the MSAs decrease in the MSA+ and O3+ scenario (Figure 5-2b) and increase in the MSA- scenario (Figure 5-2c), as changes to VOC emissions in these VOC-limited areas are overwhelmed by additional $NO_x$, so emissions changes mostly affect the magnitude of $NO_X$ titration at night. Chicago responds especially strongly to these changes. Regionally dispersed $O_3$ downwind of the urban areas increases in the MSA+ scenario and decreases with MSA- by 1-3 ppb. We note that Lake Michigan and Lake Erie are particularly responsive to changes in $O_3$ precursor emissions. These results are qualitatively similar with those of *Fast and Heilman* [2005], which found that increases in anthropogenic emissions $NO_x$ and VOC based on the IPCC B2 scenarios for the year 2020 and 2040 increased regional $O_3$ while reducing $O_3$ exposure near the largest MSAs. Results of the O3+ (Figure 5-2e) and O3- (Figure 5-2f) scenarios are nearly identical to MSA+ and MSA-, so changes to the pollutant burdens of other species do not lead to appreciable nonlinear differences in $O_3$ photochemistry. Ozone concentrations are more responsive to decreases in emissions than to increases (Figure 5-3).

Suprisingly, the most extreme changes in both local and regional pollution were found for the MSA_ONLY emissions scenario (Figures 5-9d and 5-10d) for both $O_3$ and $PM_{2.5}$. While urban areas have very high emission densities, and air pollution—particularly ozone—is typically considered a regional problem with urban causes, eliminating anthropogenic emissions outside of the 11 largest MSAs leads to a reduction in annual $PM_{2.5}$ concentrations of more than 10 $\mu g/m^3$ across the region (Figure 5-1d) and

reductions in July $O_3$ of more than 10 ppb (Figure 5-2d). As in the MSA- and O3- cases, some of the greatest reductions in $O_3$ in the MSA_ONLY scenario, in excess of 15 ppb, are found over Lake Michigan, Lake Erie, and southern Lake Huron. Observations [e.g. *Rao et al*., 2003] have indicated that regional $PM_{2.5}$ is characterized by a rural background concentration with an urban excess of mostly carbonaceous aerosols, and these modeling results confirm that rural areas and smaller cities are responsible for a majority of that regional background. Likewise, with a background $O_3$ concentration estimated from sparsely populated areas to the north of the region at 30-35 ppb, dispersed regional anthropogenic $NO_x$ and CO emissions are responsible for 20% to 50% of $O_3$ concentrations in the region, with corresponding impacts on the large cities. Overall, our results suggest that enhanced $O_3$ concentrations over the Great Lakes, long attributed to nearby large urban areas, are due roughly equally to both urban and regional rural anthropogenic emissions. However, this finding must be considered preliminary due to the coarse nature of a "zero out" step function change over wide areas for multiple species in a highly nonlinear chemical system.

### *5.3.2. Sensitivity of Modeled Chemical Transport to Spatial Resolution*

#### 5.3.2.1. Meteorology

The only way to ensure that changes in chemical transport are due exclusively to model resolution is to use the same set of models and run from the prior simulation with a direct one-way nest, thereby changing only resolution. However, we chose to generate 12

km meteorology separately using the currently supported mesoscale meteorological forecasting and research model, WRF, rather than downscale from the same MM5 simulation used in the 36 km studies in Chapters 3 and 4. Numerous changes in meteorology between the 36 km and 12 km simulations limit ability to definitively attribute changes in chemical transport to any particular feature, including resolution. First, the models used differ. Although WRF is the direct successor to MM5, and is built from MM5 physics and model structure, many schemes and parameters differ, including updates of those present in MM5. In this case, the land surface model and planetary boundary layer closure scheme changed between the MM5 and WRF simulations, to reflect improvements and more closely match the schemes with which CMAQ interprets the resultant meteorology fields to compute transport. Second, the MM5 run was patched together from separate weekly simulations that were each initialized from global model analysis and run unconstrained within the domain, with only global boundary conditions affecting the internal MM5 simulation. In contrast, the WRF runs were conducted using analysis nudging within the study domain, constraining the model spatial and temporal progression closer to the input reanalyses, based on observations, at every reanalysis step. These changes would be expected to lead to an improved simulation, but results indicate that is not necessarily the case.

Model meteorology in WRF at 12 km was highly sensitive to the source of input meteorology for boundary conditions and analysis nudging. A simulation was conducted in a two-way nest at 36 km (continental) and 12 km (regional) grids using the same

physics configuration as the LADCO MM5 simulation, and constrained by the 1° x 1° global forecast system FNL final reanalysis every 6 hours, a standard source of input meteorology for both forecast and retrospective studies and using the same GFS forecast model that drove the MM5 simulation. This would expected to result in a similar result, but comparison with the 40 km resolution North American Regional Reanalysis (NARR) [*Mesinger et al.*, 2006] for the month of July 2002 indicated that the standard WRF configuration employed yielded a much lower 2 m temperature than NARR throughout the 12 km domain, with a consistent monthly mean domain-wide bias of –7.300 K. As NARR is informed by surface observations and is among the best consistent representations of the state of the atmosphere over continental North America, this bias was problematic, as underestimates of near-surface temperature would reduce production of O3 and $SO_4^{2-}$ near the surface, possibly leading to low biases in resultant concentrations, and indicative of systematic problems in the simulation. A second WRF simulation was run using the Pleim-Xu land surface model and the accompanying ACM2 boundary layer scheme, constrained by NARR surface pressure every 3 hours.

Both WRF simulations demonstrate important departures from the NARR July 2002 monthly mean 2 m temperature (Figure 5-5). In the first WRF_FNL run, temperatures over the surfaces of the Great Lakes are less than 280 K, and less than 290 K north of the laes (Figure 5-5a). This leads to a difference of 15-20 K in lake surface temperature over both the Great Lakes and the smaller lakes of Minnesota relative to NARR (Figure 5-5d), with underprediction everywhere but the extreme south of the

domain. Temperatures in the WRF_NARR simulation (Figure 5-5b) are higher throughout the region and more closely match NARR, with a slight high bias over land (monthly mean regional bias = 0.928 K) but still 5-10 K cooler than NARR over water (Figure 5–5e). The greatest differences (-11.630 K) are over Lake Superior, with greatest differences on land (~5K) along the coasts Lake Superior and Lake Michigan in gridcells that are classified as mostly land on the 12 km WRF grid but mostly water on the 40 km NARR grid. This second run is generally consistent with NARR across other fields as well, with regional spatial patterns very consistent for water vapor mixing ratio *QV* (Figure 5-6). Monthly mean regional bias is $5.564 \times 10^{-4}$, or 4.25%, and again the greatest difference is over water, with WRF drier over Lake Superior and more moist over the southern Great Lakes and the inland lakes of Minnesota and Manitoba. To reconcile these identified differences and develop confidence, NARR and WRF_NARR output will be compared with surface observations and satellite retrievals of temperature, moisture, and winds over the region, with particular focus over lake surfaces.

The preliminary CMAQ chemical transport results that follow are based on the WRF_FNL simulations with its strong cold bias, and revisions using the WRF_NARR meteorology to better reflect observed weather and climate conditions are ongoing. Although exact values will change with different meteorology driving atmospheric chemical transport, broad results regarding differences in resolution are not expected to differ qualitatively.

5.3.2.2. Ozone

Prior research and regulatory studies with a variety of CTMs, most notably *Tesche et al.* [2006], have stated that CTM performance is equivalent at 36 km and 12 km horizontal resolution. In fact, *Tesche et al.* even used CMAQ and CAMx in a region inclusive of the study domain for 2002 with a similar emissions inventory, and declined to show model aerosol evaluation results at 12 km because of their substantial similarity. However, *Tesche et al.* did not evaluate $O_3$, and did not show any maps, focusing exclusively on model comparison with routine observational networks. It was suggested [*Sillman*, personal communication] that meteorological model resolution could impact $O_3$ photochemistry over the Great Lakes, with a resolved lake breeze potentially contributing to faster mixing over the lake basins through horizontal advection and diffusion.

Examining CMAQ simulations for the month of July 2002, identical except for grid scale and meteorology, we find substantial differences in simulated $O_3$ and $PM_{2.5}$ concentrations at 36 km and 12 km resolutions. First, July mean $O_3$ concentrations tend to be higher throughout the region at 36 km (Figure 5-7a), with average differences of 5-10 ppb, corresponding to nearly all of the bias attributed to bias in global boundary conditions for $O_3$ and its precursors in the 36 km simulations in Chapter 4. Although part of this reduction may be due to the low temperature bias in the 12 km meteorology, much of this difference can be attributed to resolution in that the assumption of complete instantaneous mixing within each grid cell leads to greater and faster mingling between rural and suburban biogenic VOC emissions and anthropogenic $NO_x$ emissions and

freshly formed $O_3$ at 36 km, such that the polluted VOC-limited air has not aged before encountering fresh VOCs. Thus, a larger gridcell would tend to stimulate greater daytime $O_3$ production and reduce $NO_x$ titration near cities. This is confirmed in that at 12 km, where the presence of urban areas other than the large conflagrations of Chicago and the Twin Cities is resolved, $O_3$ concentrations are distinct local minima (Figure 5-7b). Further confirming the explanation that the mixing of $NO_x$ and VOCs to form $O_3$ occurs after transport at higher resolution is the eastward shift of the local $O_3$ maxima from the ORV at 12 km, in line with simulations by *Godowitch et al.* [2008]. There is also a pronounced increase in $O_3$ over central and southern Illinois at 12 km, which suggests that the weak northerly winds over that area in the summer (Figure 4-4) are more important to transport from the ORV in the 12 km simulation, in addition to the higher biogenic VOC emissions in 12 km gridcells that are better resolved as heavily managed corn and soybean, with resultant biogenic VOC emissions.

Simulated $O_3$ concentrations are also substantially lower over the lakes at 12 km, and the enhancement is distributed more evenly over the surfaces of the lakes (Figure 5-7b). In addition, although both simulations yield higher $O_3$ concentrations over the southern Great Lakes than over nearby shores—among the highest in the region—this is more pronounced at 36 km.

5.3.2.2. Aerosols

Simulated aerosol concentrations also display resolution-dependent differences. Unlike $O_3$, the majority of aerosol mass is either emitted as primary pollutant, or rapidly condensed from gaseous precursors (e.g., in the summer, $SO_4^{2-}$ and SOA, the dominant aerosol species in the region). Primary aerosols also tend to deposit relatively close to their emissions sources in models. Therefore, unlike $O_3$, higher resolution would be expected to increase $PM_{2.5}$ concentrations near urban areas, and we see just that in our simulations (Figure 5-7d). However, $PM_{2.5}$ concentrations are also higher region-wide at 12 km, particularly over lower Michigan and southeastern Wisconsin. We also note that the lower surface concentrations over Lake Michigan than over nearby land are more pronounced at 12 km. Overall, this change leads to a shift from a pronounced low bias in July $PM_{2.5}$ mass concentrations at 36 km (Table 3-1) to a slight positive bias at 12 km. However, the change comes without a marked increase in SOA contribution to aerosol mass, suggesting that the some of the improvement over the results shown in Chapter 3 may be for the wrong reasons. One of these compensating factors is the increase in urban concentrations of primary elemental and organic carbonaceous aerosols, improving their underprediction. The model distinction between primary and secondary organic aerosols is particularly important for determining whether organic mass deposits near emissions sources, enhancing local concentrations, or are transported in semi-volatile gas form before becoming aerosols, increasing concentrations further downwind after regional dispersion.

### *5.3.3. Sensitivity of Regional Air Pollution to Mobile Emissions Inventories*

#### 5.3.3.1. Differences in Travel and Emissions

The PLUTO bottom-up and NEI top-down estimation methodologies yield substantially similar total VMT estimates at the state and regional levels and in most counties (Table 5-2). The regional aggregate difference is just 0.39% of the NEI, with an average county-level difference is 1.72%. We note that despite general similarities, there are striking differences between the spatial distribution of VMT in the two inventories (Figure 5-8). Estimates differ least in rural areas, where census tracts are large and population density is low and relatively homogenous. At the county level, VMT estimates differ most in urban areas. The NEI, incorporating urban traffic counts and allocating emissions by the number of roadway miles, assigns the urban cores of cities greater emissions densities, and may in the process underestimate the suburban component. In contrast, the ORNL transferability method employed by PLUTO, and allocated by census tract area, has no direct basis for estimating the travel patterns associated with each tract, and so assumes that people travel exclusively within the census tracts where people live. This leads to higher PLUTO VMT and emissions in the collar counties around Chicago (Figure 5-8) and lower densities in the downtown urban core. Also as a result of fundamental differences in allocation, PLUTO does not capture long-haul travel on Interstate highways that NEI includes, as seen in southwestern Wisconsin along I-90/94.

Despite general agreement in VMT, emissions resulting from these inventories diverge greatly. PLUTO's cluster-specific cold start fractions from NPTS trip frequency and duration consistently suggest a lower NOx/VOC emissions ratio, as cold starts increase VOC emissions by 30-230% and lower NOx by 70-75% in the MOBILE6 model [*USEPA*, 2002]. The NPTS cold start fraction, and to a lesser extent differences in assumed average speeds, led to substantially higher emissions of VOCs and CO in PLUTO than in the NEI (Table 5-3). $NO_x$ and $PM_{2.5}$ emissions were little changed at the regional aggregate, but considerably lower in PLUTO in the average (rural) county. This emissions comparison alone suggests that typical model biases in $O_3$ (high) and SOA (low), while certainly attributable to structural deficiencies in model mechanisms, may also be due in part to mobile emissions biases related to broad application of the low default national cold start fraction of 20.6% of all starts [*USEPA*, 2003].

5.3.3.2. Differences in Ozone Concentrations

As a result of differences in emissions factors and in the spatial allocation of emissions in urban areas, urban surface-level $O_3$ concentrations were highly sensitive to the change from the 2001 NEI mobile emissions to the PLUTO 2000 inventory. Figure 5-9a shows that July mean $O_3$ from the NEI emissions exceeds PLUTO by 6 ppb in Chicago and Minneapolis, and are locally higher over each of the 11 largest MSAs. This model sensitivity to emissions factors is substantial, particularly for cities (like Madison) within 6 ppb of exceeding the NAAQS for $O_3$. However, despite differences in spatial patterns in emissions, the regional distribution of $O_3$ was only slightly higher for the NEI,

with a regional mean difference of 1 ppb. PLUTO $O_3$ was only higher immediately downwind of Chicago, near Gary, Indiana, and over Detroit, Michigan. The significant differences in VMT and emissions along interstate highways did not lead to changes in resultant $O_3$ concentrations.

*5.3.3.3. Differences in Fine Particle Concentrations*

Fine particle concentrations were generally slightly higher for the 2001 NEI than PLUTO (Figure 5-9b), over urban areas and throughout the region. Differences in most of the 11 PLUTO MSAs exceeded 1 $\mu g/m^3$. However, PLUTO concentrations were higher in the suburbs of Chicago, Minneapolis, and Detroit, coincident with PLUTO's higher suburban VMT rates.

*5.3.4. Sensitivity of Regional Air Pollution to Changes in Mobile Emissions Associated with Future Land Use Changes*

5.3.4.1. Changes from 2000 to 2050

We employed the 2050 BAU simulation as the "base case" 2050 emissions scenario for comparison of air quality impacts relative to present-day emissions. Changes in July monthly mean air quality between simulations with the PLUTO 2000 and 2050 BAU mobile emissions scenarios were pronounced, as the 2050 scenarios represent increases in MSA mobile emissions in excess of 60% [*Stone et al.*, 2008]. These changes

are qualitatively similar to those found in the MSA+ scenario for both $PM_{2.5}$ (Figure 5-1b) and $O_3$ (Figure 5-2b), but were also highly sensitive to model horizontal resolution.

At the 36 km grid, localized $O_3$ differences in excess of 5 ppb were found over each of the MSAs (Figure 5-10a) due to $NO_x$ titration, reaching in excess of 10 ppb over the urban center of the Chicago MSA, and regional $O_3$ was generally unchanged or lower. At 12 km, these changes were considerably more modest, with MSAs lower by 2-6 ppb (Figure 5-10b), consistent with the resolution dependence found in the base case 2002 simulation. Regional changes due to increased urban and rural mobile emissions remained under 1 ppb. Fine particle concentrations also increased with additional emissions (Figure 5-11), again with a modest change of 1 – 1.5 $\mu g/m^3$ over the 11 largest MSAs and a regionally-dispersed change of roughly 0.5 $\mu g/m^3$.

5.3.4.2. Impacts of Smart Growth Policies

After 50 years of implementation, the SG2 aggressive smart growth scenario led to small changes in air quality relative to BAU, without new land use policies. Smart growth reduced $O_3$ concentrations only slightly (Figure 5-12a), and only locally in the 11 largest MSAs to which the urban growth boundaries were applied. Ozone concentrations actually increased under SG2 in the city centers of Chicago and the Twin Cities as they densified. Aerosol concentrations were little changed, with minimum and maximum changes adjacent to each other in the large MSAs (Figure 5-12b). Overall, SG2 land use policies alone further reduced urban $O_3$ over BAU by an additional 20% - 30%, and

mitigated roughly 30% of the slight increase in $PM_{2.5}$ from 2000 in the region's most populated urban centers.

5.3.4.3. Relative Impacts of Smart Growth Policies and Hybrid Vehicle Technologies

An aggressive switch to hybrid vehicles actually increased urban $O_3$ levels from 2000, as reduced $NO_x$ emissions result in a less VOC-limited environment and reduced $NO_x$ titration. In comparison with the SG2 incremental growth policy, hybrids represent a trade-off between urban and regional $O_3$ pollution (Figure 5-13a): substantially higher urban concentrations (>4 ppb in each of the MSAs) and slightly lower regional concentrations (1 – 2 ppb), with downwind impacts as far away as upstate New York.

This trade-off is further complicated in that lower levels of primary emissions in the hybrid scenario resulted in lower urban and regional $PM_{2.5}$ than the SG2 scenario, which concentrates emissions in urban areas (Figure 5-13b). Reductions in July mean $PM_{2.5}$ concentrations due to hybrids even outweigh the increase in $PM_{2.5}$ from 2000 to 2050. Thus, hybrid vehicles represent a challenging trade-off in air quality management: they reduce urban and regional aerosol pollution, and compensate for increases in the number of vehicles and travel rates that accompany population growth, but these benefits are accompanied by a nearly 10% increase in urban $O_3$ levels.

## 5.4. Conclusions

The Community Multiscale Air Quality Model is used to simulate the impacts of changes in anthropogenic emissions on ozone and aerosol chemistry in the Great Lakes region of North America. Regional aerosol concentrations respond in a linear manner to ±20% changes in emissions from the 11 largest metropolitan areas in the region, where emission densities are highest. Ozone response to changes in urban emissions is nonlinear, with local and regional changes in ozone of opposite sign, and regional ozone pollution more sensitive to decreases in urban emissions than to increases. Simulation with rural and small-city emissions "zeroed out" confirm observational evidence that the majority of regional fine particle pollution is due to rural sources with a localized urban excess. Surprisingly, rural and small-city anthropogenic emissions are responsible for roughly half of regional $O_3$ concentrations, although this finding is inconclusive due to the coarse nature of the experiment in such a nonlinear chemical system.

Urban $O_3$ and $PM_{2.5}$ concentrations are highly sensitive to the influence of cold start fractions on the NOx/VOC ratio of mobile emissions, with July average $O_3$ changing by up to 10% in urban areas between otherwise identical simulations. Changes in urban air quality accompanying changes in mobile emissions from 2000 to 2050 are resolution-dependent, with less change on a 12 km grid than at 36 km. "Smart growth" land use policies, even in an extreme form, can compensate for only 30% of the increase in $O_3$ and $PM_{2.5}$.

Compared to land use policies, hybrid vehicles, a technology-based approach to pollution control, increase urban $O_3$ concentrations while reducing $PM_{2.5}$ and regional $O_3$. Thus, air quality managers must consider changes on a population-weighted basis, taking into account the relative health impacts of changes in $O_3$ and $PM_{2.5}$ on specific populations. Fortunately, since the greatest effects of changes in vehicle emissions are highly localized in urban areas, land use and transportation policies can be set locally by municipal, county, and state planners for each MSA, taking into account local sensitivity in travel rates and local population health concerns, rather than requiring a consistent regional policy that would require interstate cooperation or federal oversight. In this regard, land use and vehicle technology policies fall into the same localized transportation management scheme for air quality that urban areas in the region already use for summertime reformulated gasoline and vehicle inspection and maintenance programs.

Finally, results indicate the strengths and weaknesses of CTM simulation for evaluating the impacts of changes in mobile area source emissions due to long-range policy efforts. On one hand, CTMs clearly capture the effects of emissions on the nonlinear chemistry, and represent the only means of doing so. In this regard, CTMs represent a sound *structural* approach to policy analysis for air quality. However, the many data sources, estimates, and arbitrary modeling choices required to run a CTM for policy analysis lead to substantial *parametric uncertainty*. Results are resolution-dependent, and the magnitude of the signal of 50-year land use policy changes is less than

the parametric noise in the fraction of trips that begin with a cold start, a highly uncertain estimate. Moreover, given the many compensating errors in model chemistry, meteorology, emissions, and boundary conditions, it is often difficult to determine conclusively which set of inputs is "right," even with the time and budget for a thorough sensitivity analysis. Thus, while CTMs are certainly highly useful in long-term air quality policy analysis, they also present challenges in experimental design for which neither expert knowledge nor painstaking systematic evaluation will necessarily suffice.

**References**

Fast, J.D., and W.E. Heilman (2005), Simulated sensitivity of seasonal ozone exposure in the Great Lakes region to changes in anthropogenic emissions in the presence of interannual variability, *Atmos. Environ.*, 39, 5291-5306, doi:10.1016/j.atmosenv.2005.05.032.

Godowitch, J. M., C. Hogrefe, and S. T. Rao (2008), Diagnostic analyses of a regional air quality model: Changes in modeled processes affecting ozone and chemical-transport indicators from NOx point source emission reductions, *J. Geophys. Res.*, 113, D19303, doi:10.1029/2007JD009537.

Hogrefe, C., B. Lynn, K. Civerolo, J.-Y. Ku, J. Rosenthal, C. Rosenzweig, R. Goldberg, S. Gaffin, K. Knowlton, and P. L. Kinney (2004), Simulating changes in regional air pollution over the eastern United States due to changes in global and regional climate and emissions, *J. Geophys. Res.*, 109, D22301, doi:10.1029/2004JD004690, 2004.

LRTAP (2007), Hemispheric Transport Of Air Pollution 2007. United Nations *Report*: Air Pollution Studies No. 16. ISSN 1014-4625, ISBN 978-92-1-116984-3.

Mesinger, F., G. DiMego, E. Kalnay, K. Mitchell, P.C. Shafran, W. Ebisuzaki, D. Jovic, J. Woollen, E. Rogers, E.H. Berbery, M.B. Ek, Y. Fan, R. Grumbine, W. Higgins, H. Li, Y. Lin, G. Manikin, D. Parrish, and W. Shi (2006), North American Regional Reanalysis. *Bull. Amer. Meteor. Soc.*, 87, 343–360.

Rao, V., N. Frank, A. Rush, and F. Dimmick (2003), Chemical speciation of PM2.5 in urban and rural areas in national air quality and emissions trends report. /http://www.epa.gov/air/airtrends/aqtrnd03S.

Sillman, S., personal communication, 12/13/2007.

Stone, B., A. Mednick, T. Holloway, and S.N. Spak (2007), Is Compact Growth Good For Air Quality? Journal of the American Planning Association, 73:4, 404-418. doi: 10.1080/01944360708978521.

Stone, B., A. Mednick, T. Holloway, and S.N. Spak (2008), Climate Change Mitigation through Smart Growth Development and Vehicle Fleet Hybridization (*Environmental Science & Technology*, in review).

Tao, Z., A. Williams, H.-C. Huang, M. Caughey, and X.-Z. Liang (2007), Sensitivity of U.S. surface ozone to future emissions and climate changes, *Geophys. Res. Lett.*, 34, L08811, doi:10.1029/2007GL029455, 2007.

Tesche, T.W., R. Morris, G. Tonnesen, D. McNally, J. Boylan, and P. Brewer (2006), CMAQ/CAMx annual 2002 performance evaluation over the eastern US, *Atmos. Environ.*, (40)26, 4906-4919, doi:10.1016/j.atmosenv.2005.08.046.

USEPA (2002), Sensitivity Analysis of MOBILE6.0, EPA420-R-02-035.

USEPA (2003), User's Guide to MOBILE6.1 and MOBILE6.2 Mobile Source Emission Factor Model, EPA420-R-03-010.

USEPA (2004), Documentation For The Onroad National Emissions Inventory (NEI) For Base Years 1970-2002, ftp://ftp.epa.gov/EmisInventory/2002finalnei/documentation/mobile/onroad_nei_base1970_2002.pdf, accessed 9/28/07.

USEPA (2007), Region 5: State Designations, as of August 15, 2007, http://www.epa.gov/ozonedesignations/regions/region5desig.htm, accessed 10/2/07

**Tables**

**Table 5-1.** Emissions scenarios, notation and CMAQ resolutions employed

| | | | Resolution | |
|---|---|---|---|---|
| Scenario Name | Inventory Year | Description | 36 km | 12 km |
| NEI | 2001 | US EPA NEI | √ | √ |
| MSA+ | 2001 | Anthropogenic emissions in 11 largest MSAs increased 20% | √ | |
| MSA- | 2001 | Anthropogenic emissions in 11 largest MSAs decreased 20% | √ | |
| O3+ | 2001 | Anthropogenic NOx/CO/VOC emissions in 11 largest MSAs increased 20% | √ | |
| O3- | 2001 | Anthropogenic NOx/CO/VOC emissions in 11 largest MSAs decreased 20% | √ | |
| PLUTO 2000 | 2000 (mobile) | 2000 census tract-level emissions from *Stone et al.*, | | √ |
| PLUTO BAU | 2050 (mobile) | Business-as-usual (no land use restrictions) | √ | √ |
| BAU Hybrid Plus | 2050 (mobile) | BAU with aggressive adoption of hybrid electric vehicles | | √ |
| PLUTO SG2 | 2050 (mobile) | Urban growth boundary with aggressive urban growth share | | √ |

**Table 5-2.** State and county level differences in estimated vehicle travel (millions of VMT per year) and normalized differences (%) as a regional aggregate and county-level average, PLUTO 2000 – NEI 2001. Normalized difference calculated with respect to NEI 2001.

| | | | State | | County | |
|---|---|---|---|---|---|---|
| State | PLUTO 2000 | NEI 2001 | Difference | Normalized Difference | Mean Difference | Normalized Difference |
| Illinois | 118,872 | 106,270 | 12,601 | 11.86% | 124 | 10.94% |
| Indiana | 64,226 | 72,786 | -8,560 | -11.76% | -93 | -15.24% |
| Michigan | 93,712 | 98,781 | -5,069 | -5.13% | -61 | 7.59% |
| Minnesota | 53,571 | 53,235 | 337 | 0.63% | 4 | -4.56% |
| Ohio | 109,952 | 109,193 | 759 | 0.69% | 9 | 12.49% |
| Wisconsin | 56,773 | 58,776 | -2,003 | -3.41% | -28 | -2.03% |
| **Region** | **497,106** | **499,042** | **-1,936** | **-0.39%** | **-4** | **1.72%** |

**Table 5-3.** Regional mean normalized differences in emissions inventories by month, as a regional aggregate and county-level average, PLUTO 2000 – NEI 2001. Normalized difference calculated with respect to NEI 2001.

**Figures**

| | NOx | | VOCs | | $PM_{2.5}$ | | CO | |
|---|---|---|---|---|---|---|---|---|
| Month | Regional | County | Regional | County | Regional | County | Regional | County |
| 1 | -2% | -18% | 77% | 89% | -6% | -35% | 45% | 55% |
| 2 | -3% | -20% | 65% | 73% | -6% | -35% | 37% | 44% |
| 3 | -6% | -23% | 49% | 57% | -6% | -35% | 25% | 32% |
| 4 | -3% | -22% | 22% | 32% | -6% | -35% | 21% | 28% |
| 5 | -4% | -24% | 37% | 43% | -6% | -35% | 31% | 36% |
| 6 | -10% | -31% | 23% | 23% | -9% | -37% | 17% | 16% |
| 7 | -10% | -31% | 23% | 23% | -6% | -35% | 15% | 15% |
| 8 | -9% | -30% | 23% | 23% | -6% | -35% | 16% | 15% |
| 9 | -6% | -27% | 35% | 37% | -4% | -34% | 22% | 22% |
| 10 | -6% | -26% | 36% | 40% | -4% | -34% | 22% | 23% |
| 11 | -2% | -21% | 41% | 47% | -4% | -34% | 37% | 41% |
| 12 | 0% | -17% | 78% | 90% | -3% | -33% | 49% | 59% |
| **Annual** | **-5%** | **-24%** | **42%** | **48%** | **-6%** | **-35%** | **30%** | **32%** |

**Figure 5-1.** CMAQ simulated annual mean $PM_{2.5}$ ($\mu g/m^3$) for a) the base case and the change for each emissions scenario: b) MSA+; c) MSA-; d) MSA_ONLY; e) O3+; f) O3- Note that the scales for a) and d) differ from the others.

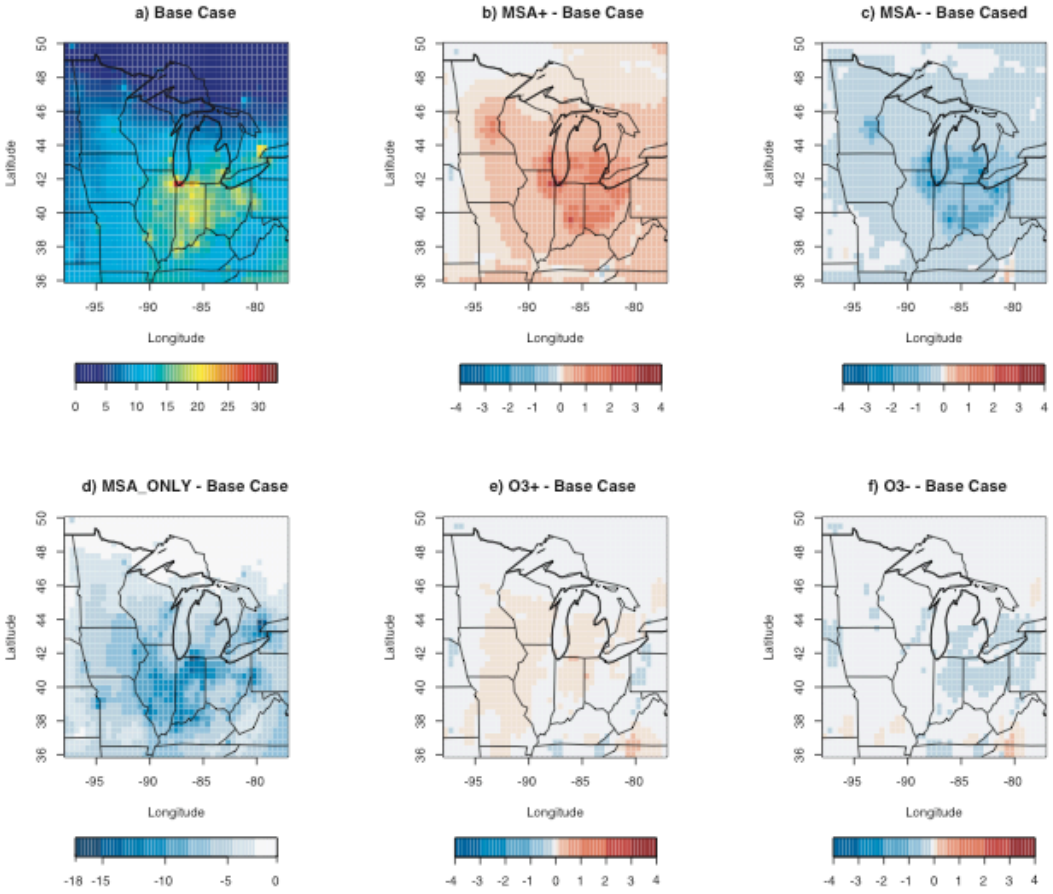

**Figure 5-2.** CMAQ simulated July mean $O_5$ (ppb) for a) the base case and the change for each emissions scenario: b) MSA+; c) MSA-; d) MSA_ONLY; e) O3+; f) O3-. Note that the scales for a) and d) differ from the others.

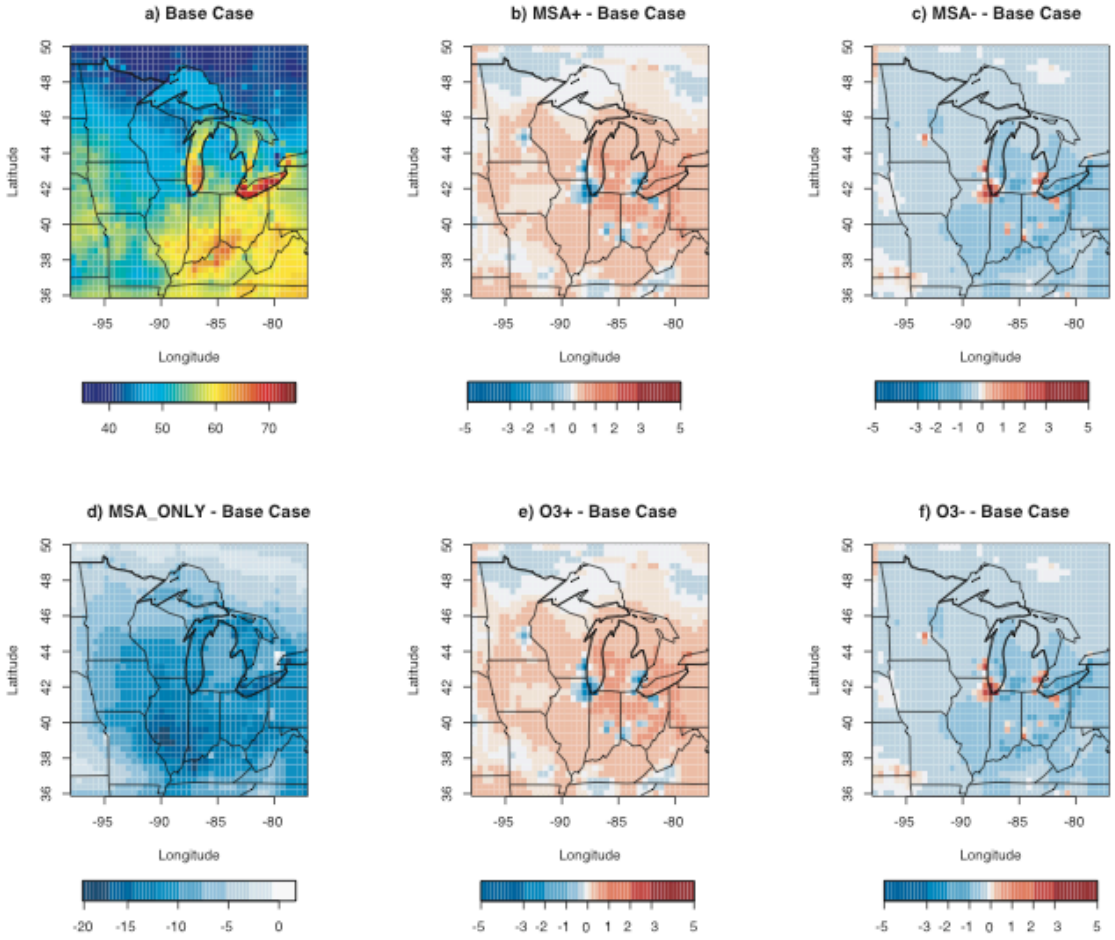

**Figure 5-3.** Differences in simulated 2002 July mean $O_3$ (ppb) between the O3+ and O3- emissions scenarios.

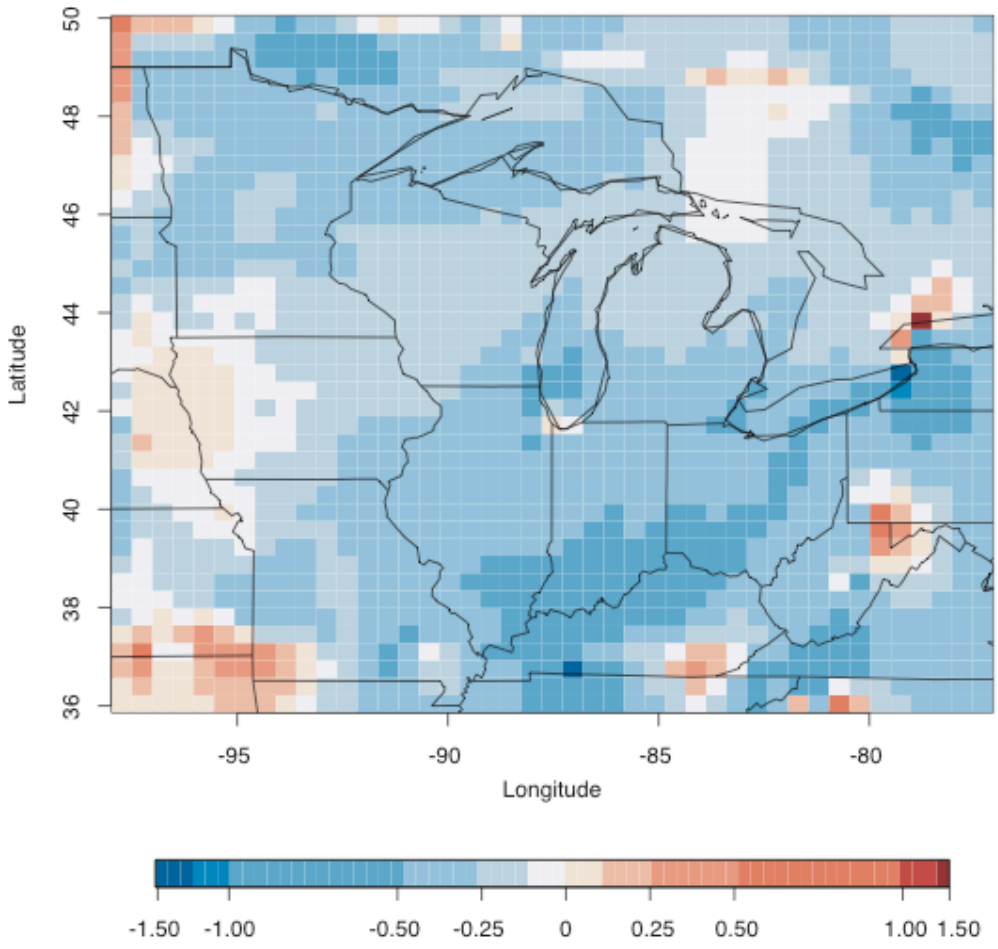

**Figure 5-4.** Differences in simulated 2002 annual mean $PM_{2.5}$ ($\mu g/m^3$) between the MSA+ and MSA- emissions scenarios.

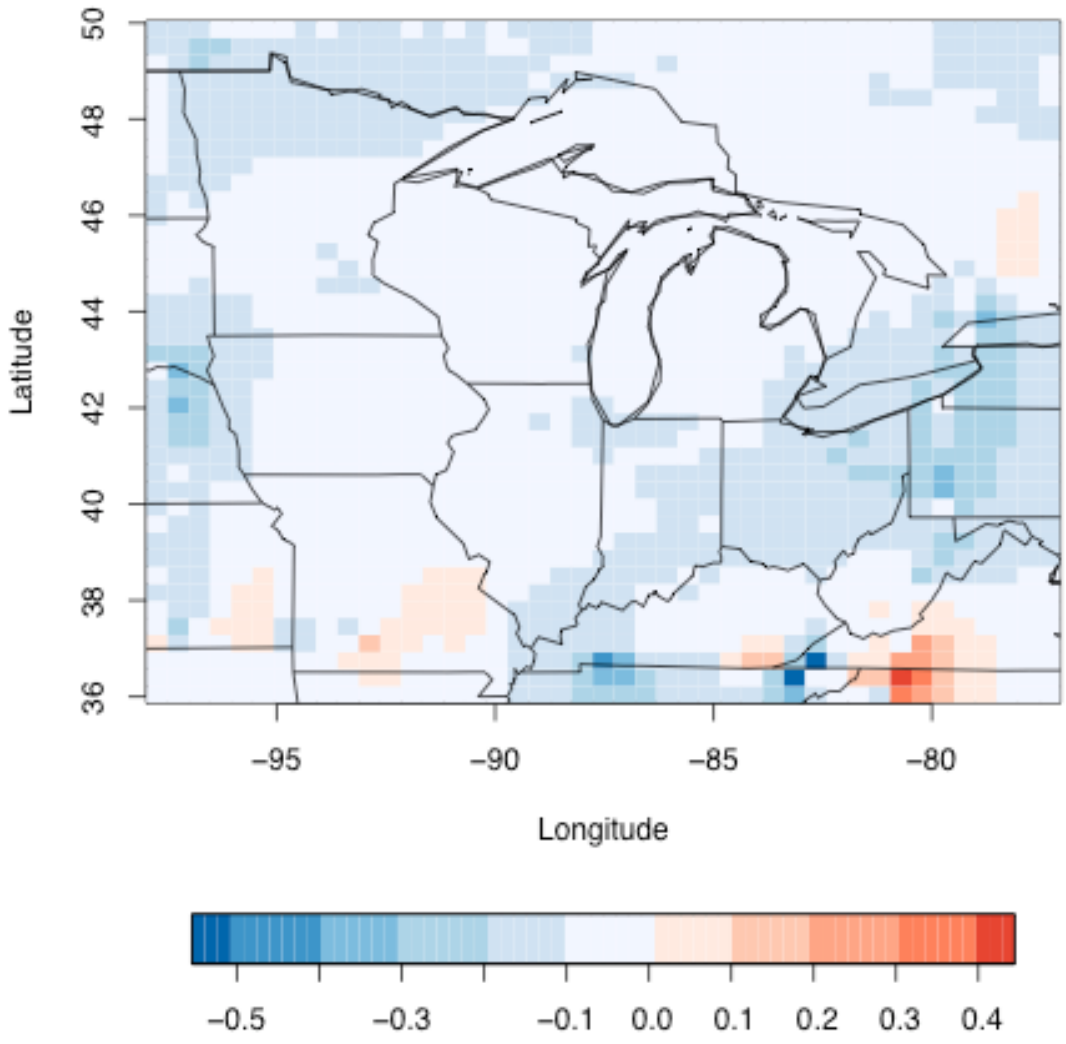

**Figure 5-5.** Simulated July 2002 mean 2 m temperature (K) in WRF_FNL, WRF_NARR, and NARR, and resultant differences from NARR. NARR values interpolated to the 12 km WRF regional grid from the NARR 40 km native grid.

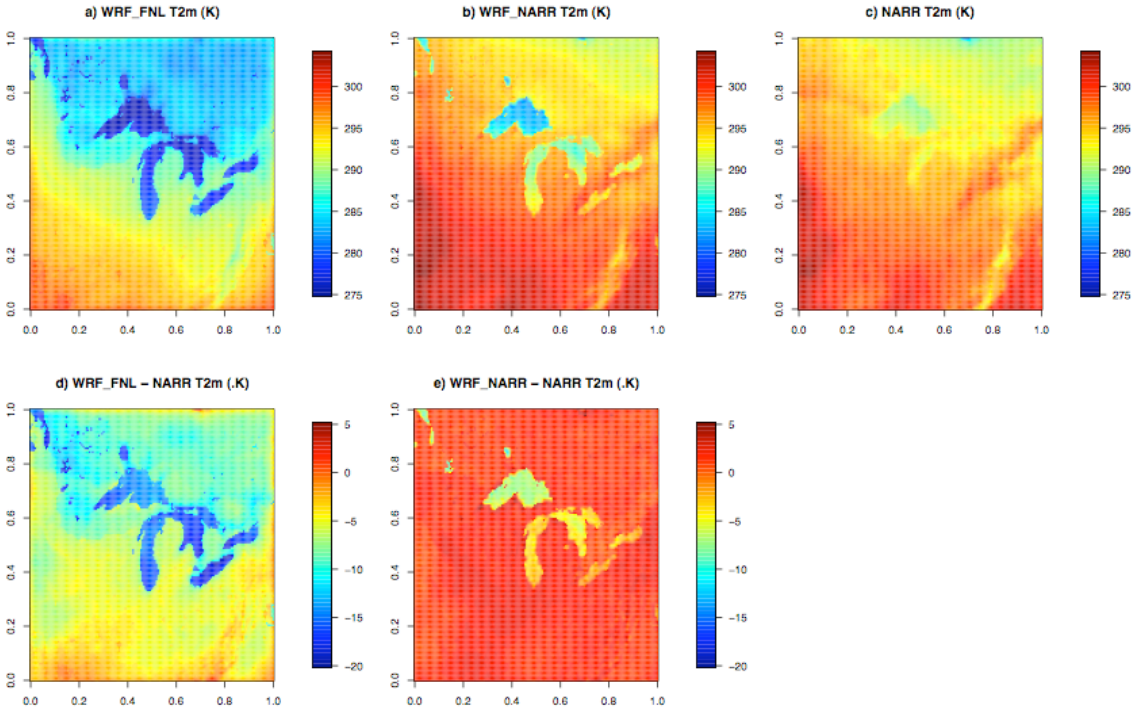

**Figure 5-6.** Simulated July 2002 mean 2 m water vapor mixing ratio in WRF_NARR and NARR, and their difference. NARR values interpolated to the 12 km WRF regional grid from the NARR 40 km native grid.

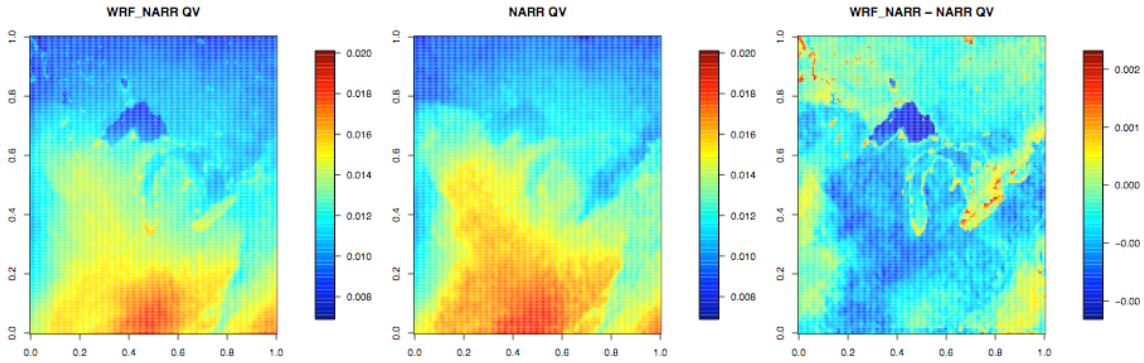

**Figure 5-7.** Simulated July 2002 mean $O_3$ (ppb) and $PM_{2.5}$ ($\mu g/m^3$) at 36 km (a and c) and 12 km (b and d) resolution.

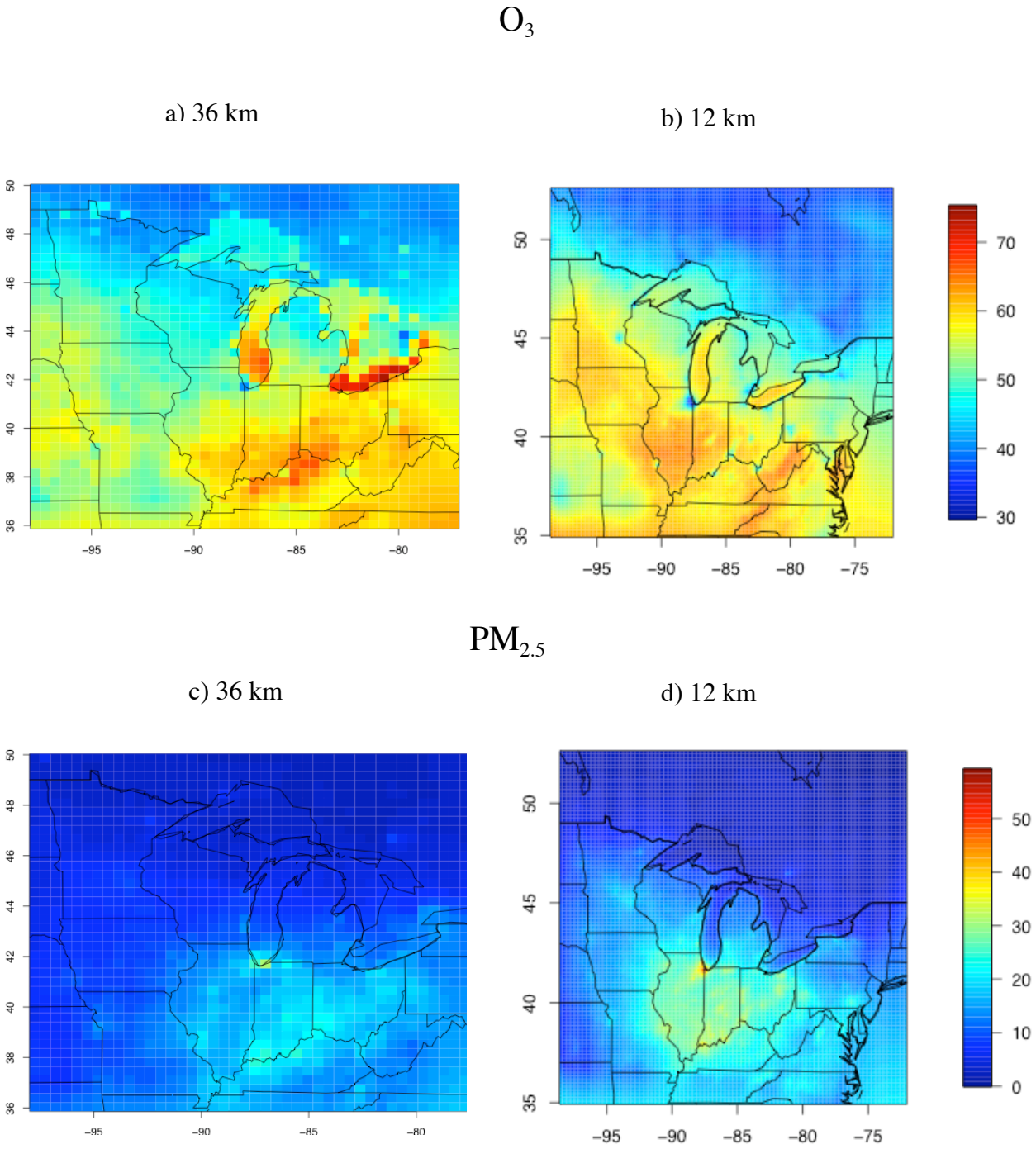

**Figure 5-8.** County-level differences in estimated annual vehicle miles of travel (millions of VMT/year), PLUTO 2000 – NEI 2001: a) raw difference; b) normalized difference (%) with respect to NEI 2001.

a)

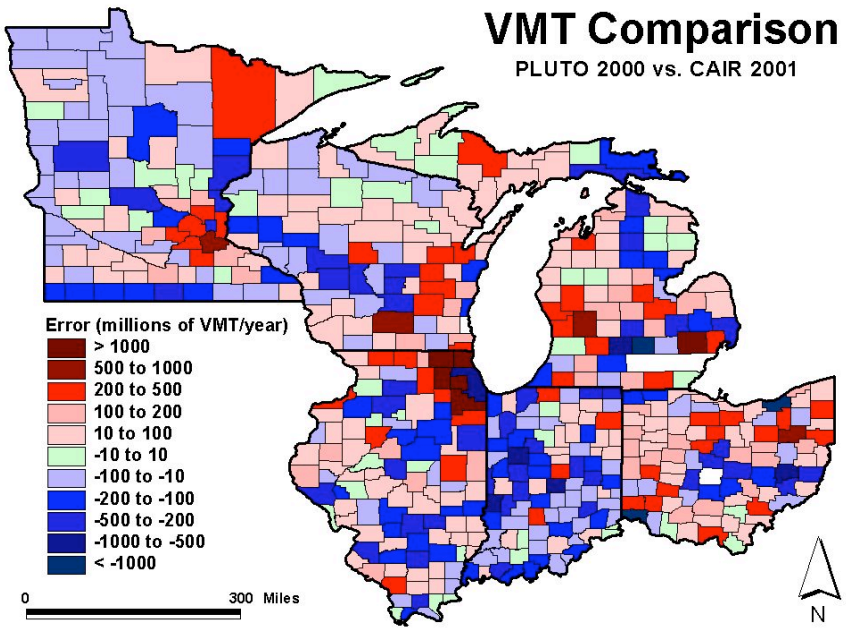


b)

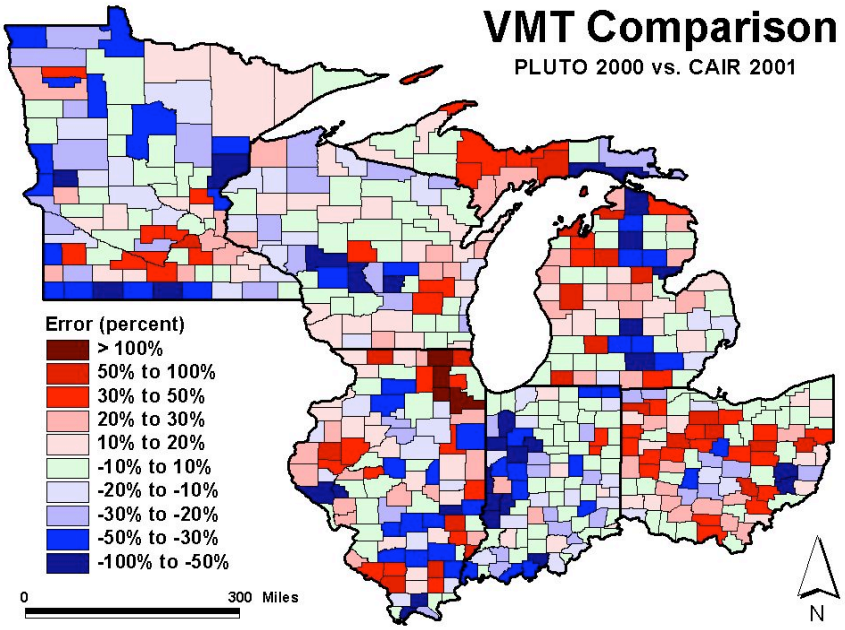

**Figure 5-9.** Sensitivity of CMAQ July mean surface-level pollutant concentrations to mobile emissions inventories, NEI 2001 – PLUTO 2000: a) $O_3$ (ppb); b) $PM_{2.5}$ ($\mu g/m^3$).

a)

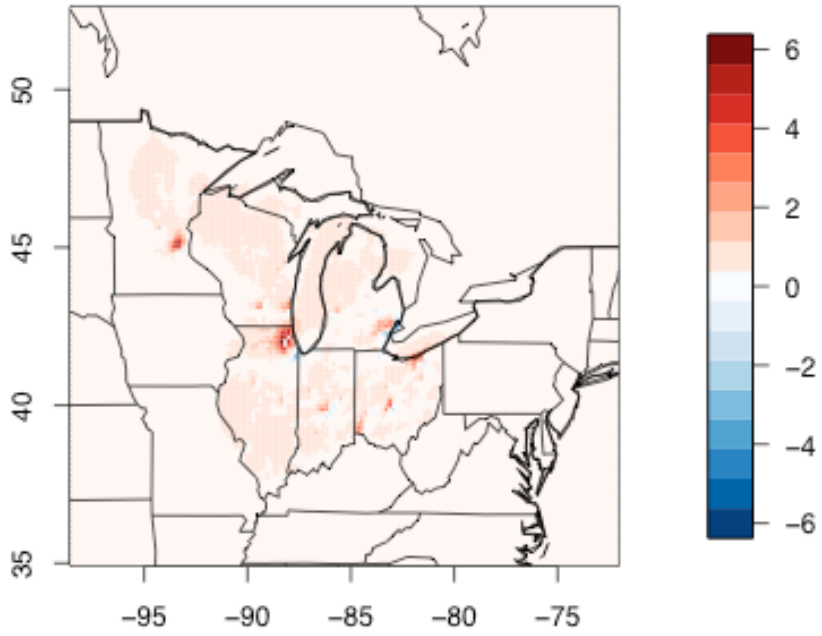


b)

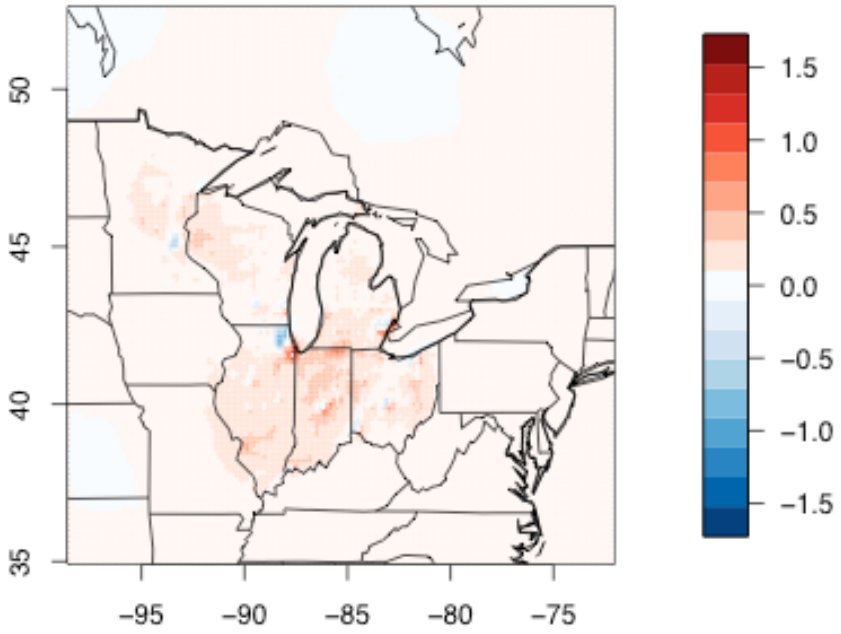

**Figure 5-10.** Changes in CMAQ July mean surface-level $O_3$ concentrations (ppb) with increases in population and travel over 50 years, PLUTO BAU 2050 – PLUTO 2000: a) 36 km grid; b) 12 km grid.

a)

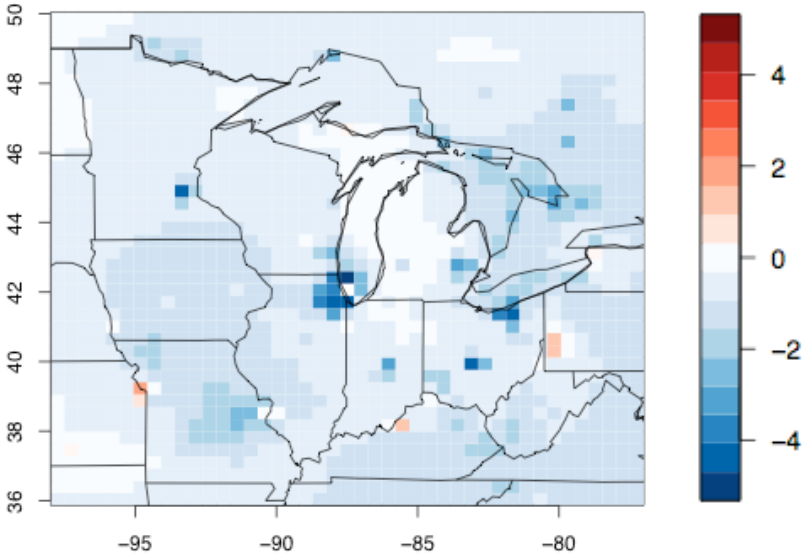


b)

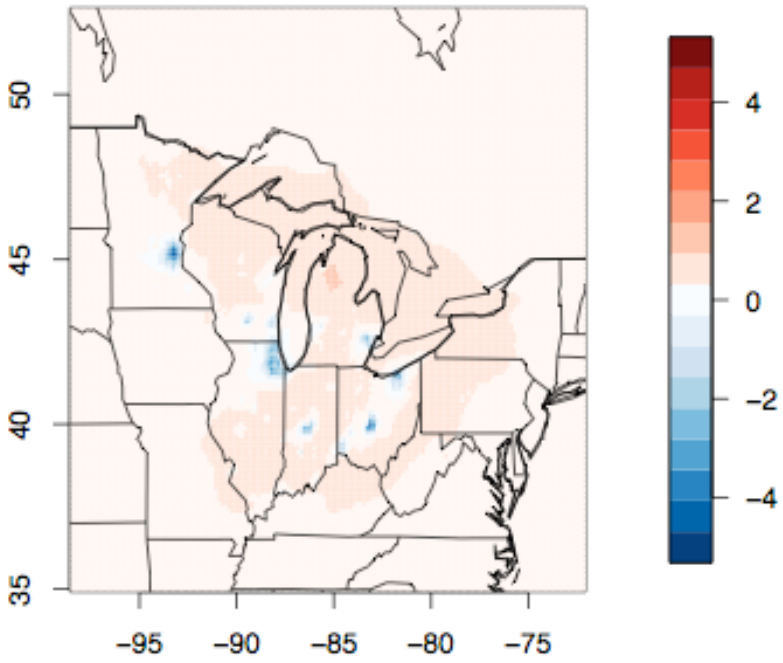

**Figure 5-11.** Changes in CMAQ July mean surface-level $PM_{2.5}$ concentrations ($\mu g/m^3$) with increases in population and travel over 50 years, PLUTO BAU 2050 – PLUTO 2000. 12 km grid resolution.

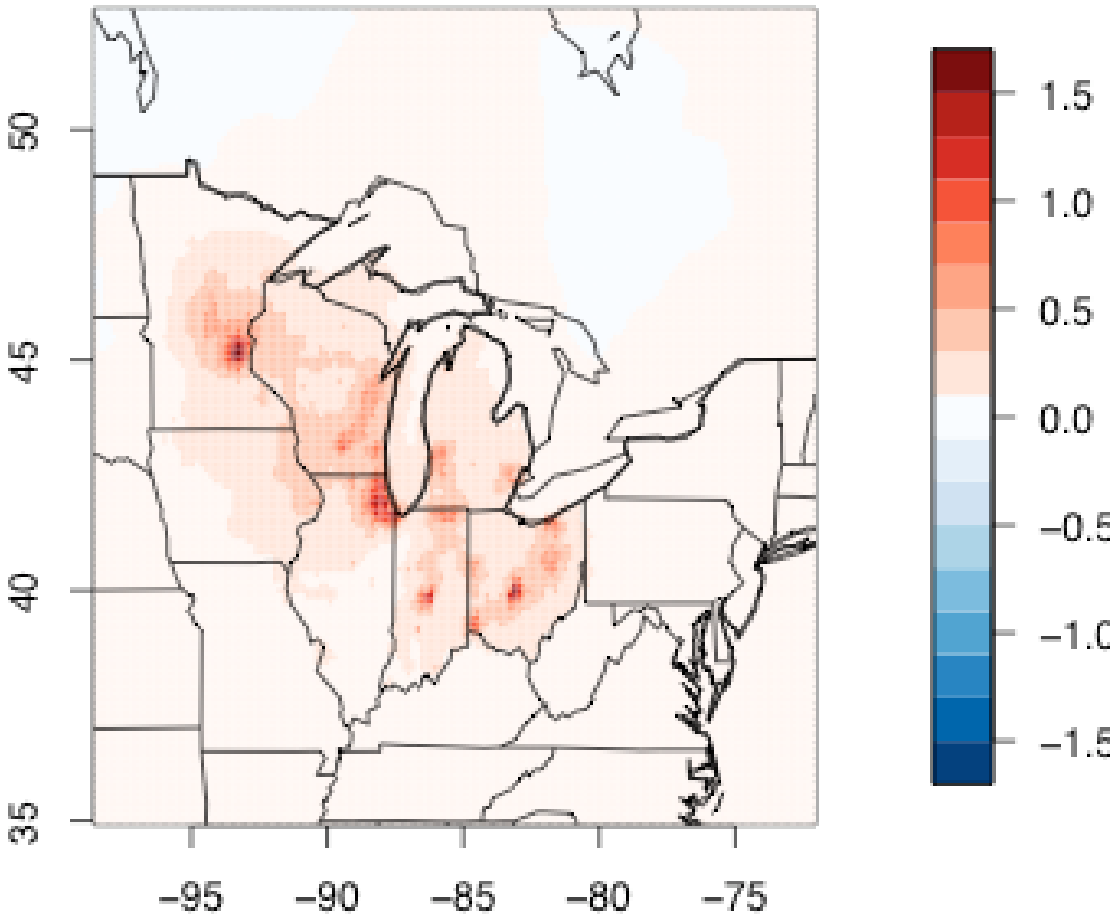

**Figure 5-12.** Sensitivity of CMAQ July mean surface-level pollutant concentrations to land use policy, PLUTO BAU 2050 – PLUTO SG2 2050: a) $O_3$ (ppb); b) $PM_{2.5}$ ($\mu g/m^3$).

a)

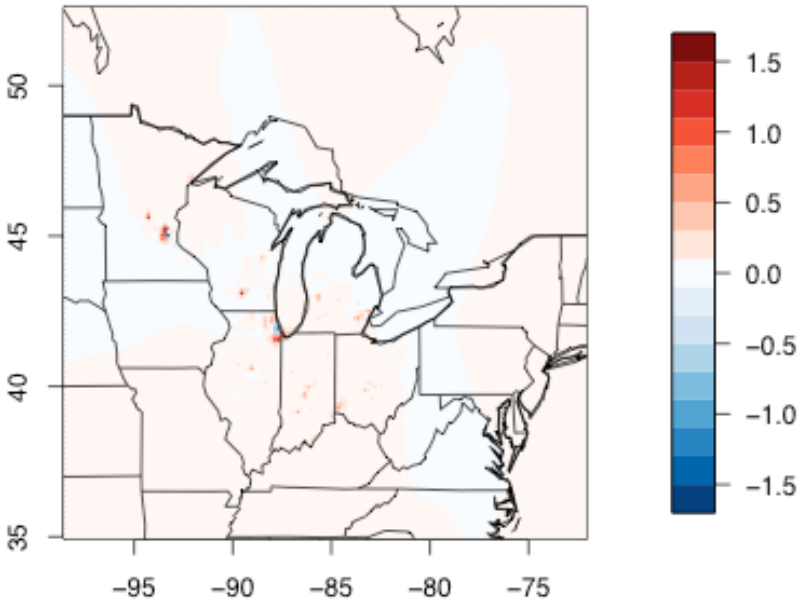


b)

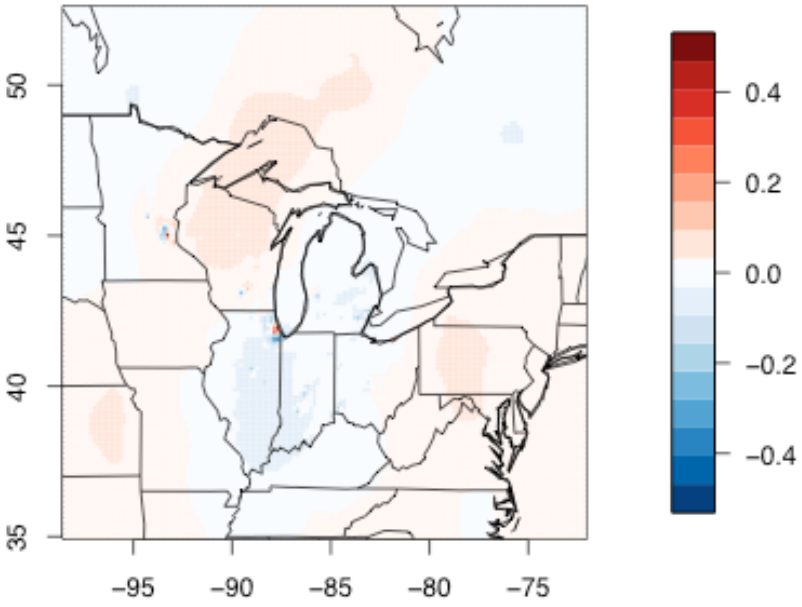

**Figure 5-13.** Sensitivity of CMAQ July mean surface-level pollutant concentrations to land use policy, PLUTO BAU 2050 Hybrid Plus – PLUTO SG2 2050: a) $O_3$ (ppb); b) $PM_{2.5}$ ($\mu g/m^3$).

a)

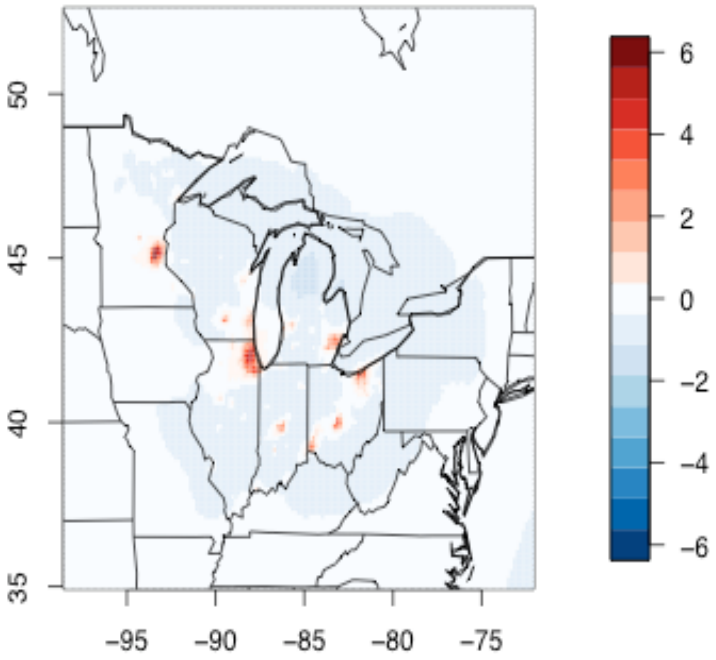


b)

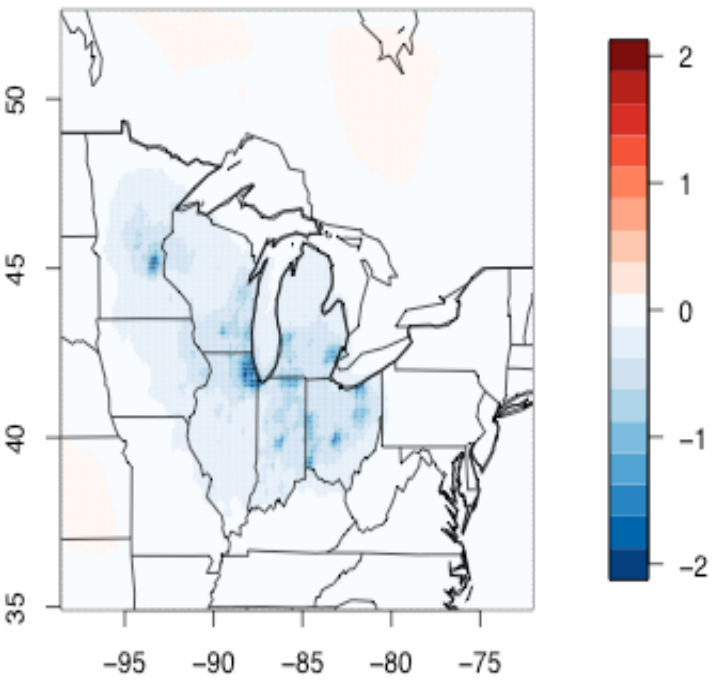

# Chapter 6. Climate Change and Air Pollution

## 6.1. Motivation

The 2007 report of the Intergovernmental Panel on Climate Change Working Group II refers to increases in surface $O_3$ as one of the top five global health impacts of climate change [*IPCC*, 2007a], and prior assessments focusing on regional air pollution impacts of climate change using CTMs have concluded that projected climate change is expected to increase $O_3$ mixing ratios in polluted areas of the U.S. [*Hogrefe et al.*, 2004; *Mickley et al.*, 2004; *Steiner et al.*, 2006; *Forkel and Knoche*, 2006; *Murazaki and Hess*, 2006; *Tao et al.*, 2007]. However, given the considerable expense of these simulations, these studies have all been limited to a single CTM, constrained by one or two emissions scenarios as realized in a single global climate model. Furthermore, projections from GCM simulations must be downscaled to the high spatial resolution needed for assessing local and regional impacts of climate change, but uncertainties in the downscaling process are difficult to quantify. This limited experimental framework exposes this type of assessment, whether for air pollution or any other potential impact of climate change, to considerable structural uncertainty inherent in the chosen model, as well as parametric uncertainty in how the model is configured. In fact, the parametric uncertainty alone can be very high: in the regional climate model simulations by *Lynn et al.* [2004, 2005] that drove the experiments by *Hogrefe et al.*, [2004], a single arbitrary choice of a parameterization for cumulus clouds greatly changed temperature and precipitation across the study domain.

If these kinds of assessments are to be trusted by policymakers as input to decisions on how to respond to future climatic changes, then they must provide a modicum of confidence that their arbitrary choices of scenarios, models, and parameters are representative of potential future states of global and regional climate and chemistry. At present, it remains too expensive—in both computation and human resources—for most regional assessments to run extended dynamical simulations with many climate and chemical transport models using multiple global climate models and emissions scenarios as inputs. However, statistical downscaling represents an alternative method for providing this expansive view of regional climate response to global changes.

This chapter describes my attempts to follow and further delineate best practices in statistical downscaling for regional climate and chemistry in support of integrated assessment, through my contributions to two such projects in which I participated. In section 6.2, I explore the response of statistical downscaling for temperature to changes in inputs and model parameters, presenting results from 96 different statistical model configurations. I then use the range of spatial and temporal differences in the statistical estimates to provide a context for assessing the representativeness of the two dynamical simulations by *Lynn et al.*, employed by the New York Climate and Health Project. In section 6.3, I then apply lessons learned from this experiment to directly projecting climate impacts on $O_3$, focusing on sensitivity to the choice of global climate models and emissions scenarios. This analysis contributed to the Chicago Climate Impacts Report,

which formed the scientific basis for the City of Chicago Climate Action Plan, and provides context for a CTM run using a single climate model and scenario.

### 6.2. Projecting Impacts of Global Climate Change on Local Climate

From: Spak, S., T. Holloway, B. Lynn, and R. Goldberg (2007), A comparison of statistical and dynamical downscaling for surface temperature in North America, *J. Geophys. Res.*, 112, D08101, doi:10.1029/2005JD006712.



We employed a multiple linear regression model and the MM5 dynamical model to downscale June, July and August monthly mean surface temperature over eastern North America under greenhouse gas-driven climate change simulation by the NASA GISS GCM. Here we examine potential sources of apparent agreement between the two classes of models and show that arbitrary parameters in a statistical model contribute significantly to the level of agreement with dynamical downscaling. We found that the two methods and all permutations of regression parameters generally exhibited comparable skill at simulating observations, although spatial patterns in temperature across the region differed. While the two methods projected similar regional mean warming over the period 2000-2087, they developed different spatial patterns of temperature across the region, which diverged further from historical differences. We

found that predictor domain size was a negligible factor for current conditions, but had a much greater influence on future surface temperature change than any other factor, including the data sources. The relative importance of SD model inputs to downscaled skill and domain-wide agreement with MM5 for summertime surface temperature over North America in descending order is: Predictor Domain; Training Data/Predictor Model; Predictor Variables; Predictor Grid Resolution. Our results illustrate how statistical downscaling may be used as a proxy for dynamical models in sensitivity analysis.

This experiment complements the New York Climate and Health Project (NYCHP), a funded health impacts assessment study based at Columbia University and funded by the U.S. Environmental Protection Agency. The NYCHP employs a multi-scale modeling framework for assessing the changes in heat- and ozone-related mortality in the 31-county New York City metropolitan area resulting from projected climate and land use change over the next 80 years. The NYCHP framework incorporates a global climate model, a regional climate model [*Lynn et al*., 2005], regional land use modeling [*Solecki and Oliveri*, 2004], and a regional air quality model [*Hogrefe et al*., 2004] to generate temperature and ozone projections for human health risk analysis [*Knowlton et al*., 2004].

Publications from the NYCHP [*Lynn et al*., 2004; *Hogrefe et al*., 2004] have highlighted uncertainty within the RCM regional temperature scenario and emphasized the importance of the regional temperature scenario as a primary influence on projected

changes in regional ozone and corresponding health impacts. A more thorough understanding of uncertainty in regional temperature resulting from the choice of climate downscaling procedure is a critical requirement if integrated assessment results are to be applied to inform policy decisions.

We employed regression techniques and a dynamical regional climate model to downscale June, July, and August monthly mean surface temperature over eastern North America under greenhouse gas-driven climate change simulations. We found that the two methods and all permutations of regression parameters generally exhibited comparable skill at simulating historical observations, although spatial patterns in temperature across the region differed. While the two methods projected similar regional mean warming over the period 2000-2087, they again developed vastly different spatial patterns of temperature across the region, which diverged greatly from their historical differences. We found that for statistical downscaling with multiple linear regressions, predictor domain size was a negligible factor for current conditions, but had a much greater influence on future surface temperature change than any other factor, including the source of predictor and training datasets. We found that employing a smaller predictor domain maintained stationarity and led to better agreement with the RCM, while continental-scale predictors simulated much greater warming than regional and local predictors.

### 6.3. Projecting Impacts of Global Climate Change on Local Climate

From: T. Holloway, S.N. Spak, D.J. Barker, M.P. Bretl, K. Hayhoe, J. Van Dorn, D. Wuebbles (2008), Change in Ozone Air Pollution over Chicago associated with Global Climate Change (*Journal of Geophysical Research – Atmospheres*, in press), doi:10.1029/2007JD009775.



While presenting a conference poster on the application of statistical downscaling to particulate matter in the Upper Midwest [*Woods et al.*, 2006], our group was approached to provide a similar statistical downscaling assessment of $O_3$ response to climate change in support of the City of Chicago Climate Action Plan, in order to provide context for a regional dynamical chemical transport modeling study that was already underway. At the time, only one recently published study [*Wilby*, 2007] had applied statistical downscaling to $O_3$, and at only one site. In contributing to up this task, I sought to apply knowledge gained from the experiments in section 6.2: to use multiple climate models and multiple emissions scenarios; to purposefully select a reliable statistical model with a limited range of model options; to eliminate the inclusion of spatial patterns in analysis, because the choice of predictor domain is unimportant in predicting present-day climate but has such a strong influence in future projections; and this time, to conduct downscaling with an off-the-shelf tool so that future analyses would have a model for how to apply best practices in statistical downscaling with a reproducible model. I then worked with my advisor, Tracey Holloway, and two undergraduates to conduct

downscaling in a clear, reproducible manner that applies and builds upon the best practices suggested by the IPCC [*Wilby et al.*, 2004].

Our analysis approach identifies key dependencies between 8-hour maximum surface $O_3$ and local near-surface weather variables. We then apply these observationally determined relationships to projected meteorological variables from three general circulation models over the 21$^{st}$ century. We employ the Statistical Downscaling Model (SDSM) 4.1 [*Wilby et al.*, 2002]. SDSM is a decision-support tool for the rapid development of single–site climate impacts analysis. Climate change is only one factor affecting future $O_3$. Economic growth, changing levels of background pollution, land cover change, and new energy technologies all reflect global changes with local effects, in Chicago and worldwide. Of these, we consider the meteorologically driven changes in $O_3$ associated with climate change alone.

We examine projected changes in ground-level $O_3$ over the City of Chicago based on climate projections from three global models, driven by a range of assumptions regarding future greenhouse gas emissions. All simulations predict that the Chicago area will get warmer over the next 100 years, with related changes in circulation, humidity, cloud cover, and precipitation. These meteorological changes alone are expected to increase ground-level $O_3$ by an average of 6.2 ± 3.7 s.d. ppb (low-growth) to 17.0 ± 6.2 s.d. (high growth) in the summer months by the end of the century, with an associated 3-

fold (low growth) to 8-fold (high growth) increase in the number of exceedances of the 84 ppb NAAQS for $O_3$ (Figure 1).

Our approach combines meteorological projections from the GCMs and historical measurements of ground-level $O_3$ from four sites in the Chicago area. This approach calculates historic relationships between meteorology and $O_3$, and considers how future meteorology would affect ground-level $O_3$ if these relationships remain constant. This assumption of stationarity introduces significant uncertainty, and ties projections directly to GCM model skill, which may exhibit particular errors over the Chicago region [*Kunkel et al.*, 2006; *Liang et al.,* 2006]. The outcome of a statistical downscaling analysis should therefore not be taken as a "forecast," but rather as an evaluation of future $O_3$ under a transparent set of assumptions: constant $O_3$-climate relationships, no change in precursor emissions, and global climate scenarios as represented by the selected GCM simulations.

Our results are comparable to those found by collaborators at the University of Illinois at Urbana-Champaign using chemical transport modeling [*J.-T. Lin, D. J. Wuebbles, et al., Effects of Future Climate and Emissions Changes on Surface Ozone Air Quality over the Chicago Area, paper in preparation*, 2008]. Preliminary results from this complementary study suggest that, between 1996–2000 and 2095–2099, climate change alone (including climate-induced changes in biogenic emissions) produces a 8 – 9 ppb increase in summertime maximum daily 8-hour averaged $O_3$ mixing ratios over the Chicago area under the A1FI scenario and 3 – 5 ppb under the B1 scenario [*J.-T. Lin,*

*personal communication, 7/16/07*]. These projections are somewhat lower than our projections, which – for the same 2095-2099 period – range from 12-25 ppb (A1FI and A2 scenarios) and 2-8 ppb (B1 scenario) for change relative to the 2002-2006 period. It is not obvious why the regional dynamic models used by *Lin et al.* and *Tao et al.* [2007] exhibit weaker $O_3$ responses to climate (the regional modeling system discussed in *Hogrefe et al.* [2004] yields only slightly lower projected $O_3$). The statistical downscaling algorithms may overestimate the sensitivity of $O_3$ to large-scale climate by ignoring feedback mechanisms such as changes in $O_3$-precursor emissions, chemistry, boundary layer height or lake-breezes that may damp out the direct effect of global climate change.

Despite these differences, it is critical to note the net result given to policymakers is identical for both studies—that climate alone leads to increases in $O_3$ on the order of 10% (low emissions scenario) to 25% (high emissions scenario) by the end of the 21st century. As with temperature in Section 6.2, dynamical and statistical modeling, despite complete different model approaches, yield highly consistent results. The fact that one approach is processed-based, driven by directly simulating atmospheric chemistry and physics, while the other is empirical, driven exclusively by observed local relationships independent of a causal mechanism, suggests that any agreement in outcomes between the two methods may indicate that both methods present a faithful downscaled projection of changes in the global climate system. Given the great uncertainty in forecasting anything 100 years in advance, this is strong support, which should allow policymakers greater confidence in accepting results and applying them to craft local responses for

mitigation and adaptation. Furthermore, if both methods provide similar results, faithfully downscaling GCM results, this then allows uncertainty analysis to be focused on the host GCMs themselves—in their structural and parametric uncertainties and their choices of emissions scenarios.

### 6.4 Conclusions

When applied in conjunction to study the same system, the combined evidence provided by two distinct downscaling approaches enhances their credibility as inputs to the decision-making process. Because both approaches reflect structural uncertainties and limitations, and because agreement between them leads to stronger conclusions than by employing either method alone, we argue that analyses of future air quality and climate change benefit from the application of both statistical and dynamical methods.

Downscaled projections provide an estimate of specific, localized response to climate change that raw GCM output cannot yet provide, but substitute the known limitations of GCMs, such as inadequate spatial resolution, with a different set of local uncertainties. The unique value of local projections in integrated assessment is contingent upon the bias and noise added in downscaling, as well as the transparency of the downscaling process. These studies highlights the advantages and relative ease for integrated assessments to take into account multiple sources of information, at all available scales, in order to quantify uncertainty and reduce the assessment's reliance on a few linkages and arbitrary settings. Regional scenarios, and the assessments to which

they contribute, can be improved by assessing multiple downscaling methods for the same GCM, ranging from state-of-the-science dynamical models to relatively simple statistical predictions; and by using multiple downscaling methods with an ensemble of GCMs and surface datasets to yield the most plausible projections and develop a comprehensive understanding of the physical and mathematical reasons behind apparent agreement among distinct regional downscaling techniques. Conversely, the divergence in projections in these shows how inappropriate it may be to pick just one statistical analysis for comparison with dynamical results, and especially when using statistical downscaling as a standalone tool.

These qualitative and quantitative comparisons and sensitivity analyses are a step toward the development of a comprehensive methodology for estimating the uncertainty added in the process of downscaling climate change scenarios.

**References**

Forkel, R., and R. Knoche (2006), Regional climate change and its impact on photooxidant concentrations in southern Germany: Simulations with a coupled regional climate-chemistry model, *J. Geophys. Res.*, 111, D12302, doi:10.1029/2005JD006748.

Hogrefe, C., B. Lynn, K. Civerolo, J.-Y. Ku, J. Rosenthal, C. Rosenzweig, R. Goldberg, S. Gaffin, K. Knowlton, and P. L. Kinney (2004), Simulating changes in regional air pollution over the eastern United States due to changes in global and regional climate and emissions, *J. Geophys. Res.,* **109**, D22301, doi:10.1029/2004JD004690.

Intergovernmental Panel on Climate Change, (2007a), Working Group II, Impacts, Adaptation and Vulnerability, Fourth Assessment Report, Summary for Policymakers, http://www.ipcc.ch/SPM13apr07.pdf.

Intergovernmental Panel on Climate Change (2007b), IPCC, Working Group I, The Physical Science Basis, Fourth Assessment Report, Chapter 10, http://ipcc-wg1.ucar.edu/wg1/wg1-report.html.

Knowlton, K., J.E. Rosenthal, C. Hogrefe, B.H. Lynn, S. Gaffin, R. Goldberg, C. Rosenzweig, K. Civerolo, J.Y. Ku, and P.L. Kinney (2004), Assessing ozone-related health impacts under a changing climate, *Env. Health Persp,* **112**(15), 1557-63, doi:10.1289/ehp.7163.

Kunkel, K.E., X.-Z. Liang, J. Zhu, and Y. Lin (2006), Can CGCMs simulate the Twentieth Century "warming hole" in the central United States? *J. Climate*, 19, 4137-4153.

Liang, X.-Z., J. Pan, J. Zhu, K.E. Kunkel, J.X.L. Wang, and A. Dai (2006), Regional climate model downscaling of the US. summer climate and future change. *J. Geophys. Res.*, 111, D10108, doi:101029/2005JD006685.

Lynn, B. H., L. Druyan, C. Hogrefe, J. Dudhia, C. Rosenzweig, R. Goldberg, D. Rind, R. Healy, J. Rosenthal, and P. Kinney (2004), Sensitivity of present and future surface temperatures to precipitation characteristics**,** *Clim. Res.,* **28**(1),53-65.

Lynn, B. H., C. Rosenzweig, R. Goldberg, C. Hogrefe, D. Rind, R. Healy, J. Dudhia, J. Biswas, L. Druyan, J. Rosenthal, and P. Kinney (2005), The GISS-MM5 regional climate modeling system: sensitivity of simulated current and future climate to model physics configuration and grid-resolution, *J. Clim.*, submitted.

Mickley, L. J., D. J. Jacob, B. D. Field, and D. Rind (2004), Effects of future climate change on regional air pollution episodes in the United States. *Geophys. Res. Lett.*, 31, doi:10.1029/2004GL021216.

Murazaki, K., and P. Hess (2006), How does climate change contribute to surface ozone change over the United States?, *J. Geophys. Res.*, 111, D05301, doi:10.1029/2005JD005873.

Solecki, W. D., and C. Oliveri (2004), Downscaling climate change scenarios in an urban land use change model, *J. Env. Management,* **72**, 105-115, doi:10.1016/j.jenvman.2004.03.014.

Steiner, A. L., S. Tonse, R. C. Cohen, A. H. Goldstein, and R. A. Harley (2006), Influence of future climate and emissions on regional air quality in California, *J. Geophys. Res.*, 111, D18303, doi:10.1029/2005JD006935.

Tao, Z., A. Williams, H.-C. Huang, M. Caughey, and X.-Z. Liang (2007), Sensitivity of U.S. surface ozone to future emissions and climate changes, *Geophys. Res. Lett.*, 34, L08811, doi:10.1029/2007GL029455.

Wilby, R. L., C. W. Dawson, and E. M. Barrow (2002), SDSM - a decision support tool for the assessment of regional climate change impacts, *Environ. Model. Software Environ. Data News*. 17 (2), 147-159.

Wilby, R.L., S.P. Charles, E. Zorita, B. Timbal, P. Whetton, and L.O. Mearns (2004), Guidelines for use of climate scenarios developed from statistical downscaling methods, IPCC Data Distribution Centre Report, UEA, Norwich, UK, 27 pp.

Wilby, R. L. (2007), Constructing climate change scenarios of urban heat island intensity and air quality, *Environment and Planning B*.

Woods, H.L., T. Holloway, S.N. Spak (2006). The Contribution of Regional Meteorology to Particulate Matter Variability in the Upper Midwestern United States, *Eos Trans. AGU*, 87(52), Fall Meet. Suppl.

## Figures

**Figure 1.** Days per summer (June, July, August) with $O_3$ above the NAAQS limit of 84 ppb. Colored, solid lines reflect the 10-year running mean of exceedances for each model (mean across SDSM ensembles, and across the study sites). Colored dotted lines reflect year-to-year exeedance values (mean across SDSM ensembles, and across the study sites).

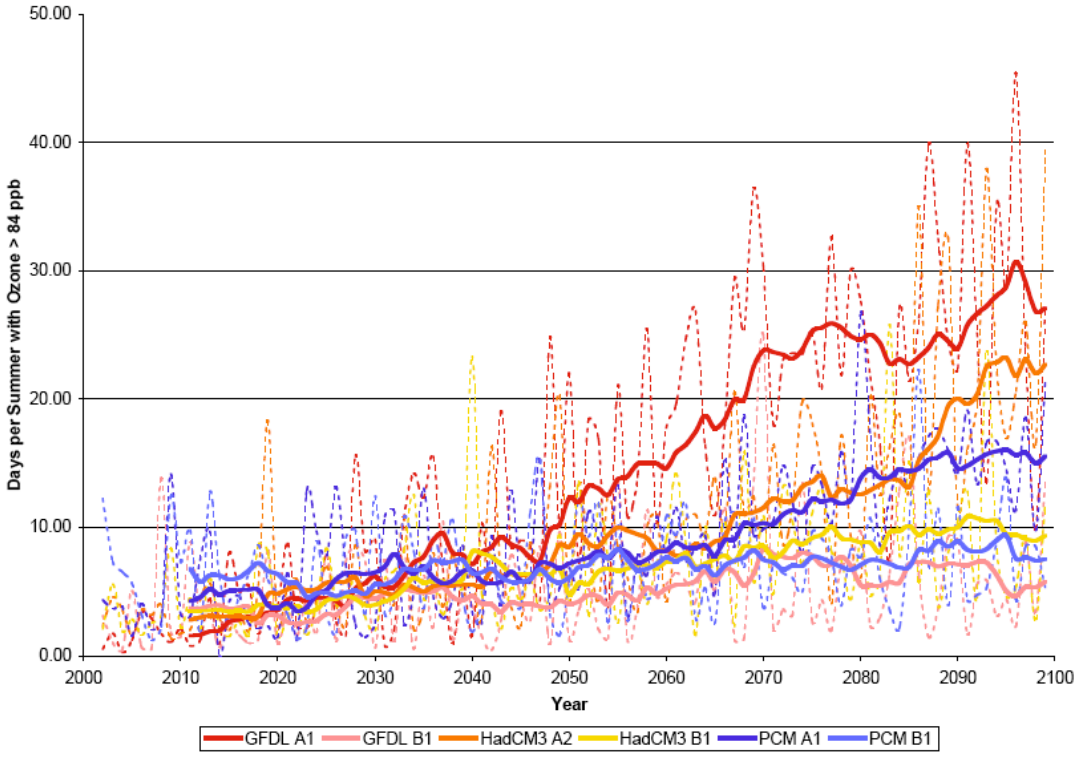

# Chapter 7. Conclusions and Policy Relevance

This concluding chapter integrates the results of my research into atmospheric chemical transport in the Great Lakes region: its current state, the underlying processes that give rise to observed conditions, and potential impacts of future changes in climate and land use. The studies that comprise this dissertation each provide unique contributions to: the *scientific documentation and understanding* of regional chemistry, climate, and their interactions in atmospheric chemical transport; *methodological innovations* designed to improve the process by which numerical modeling is conducted for air pollution and climate change science and policy analysis; and *policy-relevant implications* that stem from the results of these studies, their inherent limitations and uncertainties, and a meta-critique of their respective experimental designs. Conclusions based on these findings are clustered to highlight their implications for future policy and important comments on methods for air quality science and science-policy.

## 1. Policy Relevance

The Great Lakes have a strong impact on pollutant concentrations in lakeshore communities and, to a lesser degree, throughout the region. The lakes enhance surface level ozone concentrations throughout the year, and exert a seasonal influence on the chemistry, transport, and vertical distribution of fine particles. In the cool seasons in particular, polluted continental airmasses only cross the southern Great Lakes

episodically, reducing zonal particle transport. Thus, regardless of local activities and policies, a community's location and proximity to the lakes—particularly Lake Michigan and Lake Eerie—is a decisive "force majeure" in local air pollution. First, the lakes influence the extent to which a community will be subjected to unhealthy levels of pollution due to emissions originating hundred of kilometers away. Conversely, they also determine the pollution footprint of emissions from any particular location, and the extent to which an area's own emissions are ventilated away, limiting local problems at the expense of regional neighbors downwind. Although implicit in many regulatory analyses, such as regulatory dispersion modeling in siting emissions sources, these factors are not explicitly considered in the air quality management policies at the federal, state, and county levels. For instance, in $NO_x$ cap and trade under the $NO_x$ SIP Call and the Clean Air Interstate Rule, emissions credits are treated as a raw commodity, such that the location of each emissions source and the direct population-weighted $O_3$-related health impacts of emitting from that point at a particular time are not considered in the price it pays. Likewise, many counties in the region have never been in attainment for the $O_3$ NAAQS, which just became even more stringent. Over time, if current emissions control policies and those proposed in pending SIPs continue to be ineffective in ensuring local and regional compliance with the NAAQS, a more direct consideration of the role of the Great Lakes in air quality problems may be useful in designing new policy measures that reflect the unique pollution transport characteristics of the region.

In the Great Lakes region, nonlinear photochemical conditions make ambient ozone concentrations at current levels more sensitive to emissions controls than to increases in anthropogenic emissions. However, fine particle concentrations respond equally to increases and decreases in emissions. Thus, strategies for controlling ozone precursors are likely to be more successful for each gram of emissions prevented than controls on primary aerosols, and reductions in $NO_x$ emissions in $NO_x$-limited areas are more likely to reduce summertime ozone problems than wintertime nitrate aerosols.

The view of regional air pollution as being an urban problem that spills over to impact the "clean country air" is, in the Upper Midwest, outdated. Chemical transport modeling with and without rural anthropogenic emissions confirms observational evidence that fine particle concentrations in the Upper Midwest are defined by a regional background of rural origin with a localized excess near urban areas. Anthropogenic emissions from rural areas and small cities in the Great Lakes region dominate regional fine particle concentrations, are responsible for nearly half of the production of ozone in the region. As the 11 largest urban areas in the region are home to 65% of its residents, this means that rural citizens and emissions-intensive rural economic activities have greater regional air quality impact, per capita and per dollar of GDP, than urbanites and urban businesses.

Land use policies aimed at limiting urban sprawl lead to modest reductions in urban ozone and fine particle pollution. Pollutant concentrations are twice as responsive

to the widespread adoption of hybrid electric motor vehicles than to land use policies. However, hybrid vehicles represent a trade-off in air quality: their reduced emissions reduce urban and regional fine particle pollution and regional ozone, but paradoxically, increase ozone in the urban areas struggling to maintain compliance with the National Ambient Air Quality Standards. Whenever changes in the locations and rates of $NO_x$ emissions are likely—whether through purposeful policy, incremental technological changes, or the natural evolution of local and regional economies—chemical transport modeling should be applied to identify possible air pollution impacts in advance. As effective emissions controls for large stationary sources of $NO_x$ emissions continue to reduce their impact, new methods for estimating bottom-up changes in the spatial, temporal, and speciation profiles of area anthropogenic emissions become ever more critical for understanding the current state of regional air pollution; projecting its future evolution; and developing effective air quality management strategies.

That said, using chemical transport models for evaluating the impacts of changes due to long-range policy efforts is complicated by the parametric uncertainty in the many required model inputs. Results are found to be resolution-dependent: ozone concentrations over the surfaces of Great Lakes are highly sensitive to model spatial resolution, and spatial patterns in ozone and fine particles throughout the region change dramatically between simulations at 36 km, the standard resolution for continental-scale policy modeling and air quality forecasting, and the 12 km scale now employed in state regulatory modeling and academic research. In addition, the magnitude of the signal of

50-year land use policy changes is less than the parametric noise in a single model variable: the fraction of trips that begin with a cold start, a highly uncertain estimate even at present. Moreover, given the many compensating errors in model chemistry, meteorology, emissions, and boundary conditions, it is often impossible to determine conclusively which set of present-day inputs are correct, and which are merely fortuitous. Chemical transport modeling is essential to both short-term and long-term air quality planning and policy analysis. However, chemical transport modeling of policy changes stretches the limits not of the models themselves, but of the modeler's ability to ensure that the magnitude of the signal in the desired results is greater than the uncertainty inherent in a modeling system requiring so many exogenous and often coarsely estimated input data.

All methods of projection assume some sort of stationarity over time. Something has to stay the same to provide a foundation for detecting change. Statistical downscaling assumes that relationships between local phenomena and large scale climate patterns remain the same, while dynamical models assume that the rate constants and mechanisms that described observed systems will also apply under future climate. Even our method for projecting future vehicle travel patterns assumes that the relationships between Americans' income, population density, vehicle ownership, and household travel patterns that have emerged over the past 40 years will continue along the same path for the next 50 years. In any case, analysts must be cognizant of the conditions that their models assume will not change, should confirm that the relationships are truly stationary, and

must be upfront with stakeholders about potential changes that their methods do not incorporate.

Despite structural differences, statistical and dynamical methods for downscaling the impacts of global climate change on local climate and ozone yield remarkably similar results. Parametric uncertainty leads to substantial model variability in response to arbitrary changes in both dynamic and statistical models. In fact, statistical downscaling for surface temperature is more sensitive to most internal parameters than to the sources of local and global climate data.

The use of both statistical and dynamical downscaling methods is a foundational best practice for effective climate change impacts assessment**.** When employing such structurally different methods together, similar results provide additional confidence in the validity of the downscaled results, and results from both models provide more information about potential future conditions than either method alone. The use of both methods to study the same system has tangible benefits for all stakeholders and decision-makers: for the naïve, there is confirmation that whatever the technical process that went into generating the "number" of interest, the result is not erroneous or an outlier; for the sophisticated, the two methods combine to describe both the probability distribution of potential states and the particular climatic processes that lead to the changes manifest in the selected scenario(s).

**2. Methodological Innovations**

Inter-species time series correlation comparisons between observed and predicted values provide a process-sensitive means for evaluating chemical transport model performance. This method can offer novel information about which processes are being skillfully simulated, beyond what can be deduced from comparing concentrations alone. In Chapter 3, we demonstrate that correlations between organic matter, elemental carbon, and $PM_{2.5}$ are up to seven times stronger in CMAQ than in observations. Modeled relationships between ammonium and sulfate are weaker than observed, and model biases in the two species are highly correlated in space and time. I suggest that this technique may be useful for assessing and improving model chemical mechanisms and provide a new route for analyzing processes in chamber studies. Observed relationships between chemical species may also prove useful in variational data assimilation, to provide a strong systematic constraint on chemical transport without the mass discontinuities associated with directly assimilating concentrations.

Bottom-up area source emissions inventories provide a means to generate spatially-specific future conditions for scenario-based policy modeling of urban and regional air quality. By combining census socioeconomic data and land use projections based on alternative growth, a household vehicle trip modeling framework, and a mobile emissions factor model, we created and deployed the first census-tract level mobile emissions inventory. At the county level, results for the present day are consistent with contemporary top-down estimates, differing on average by less than 2%. In addition to

providing very high-resolution present-day emissions estimates, this method further provides a spatially-resolved alternative to linear growth estimates, an essential element for direct comparison between technology-based and policy-based air quality management strategies through chemical transport modeling.

Statistical and dynamical downscaling, when employed together, can provide greater confidence in projecting local impacts of global climate change for integrated assessments. Since the two techniques are so structurally different, agreement increases the likelihood that both methods downscale GCM data with fidelity. In this context, where both methods are employed together, dynamical downscaling provides a means for exploring processes that lead to localized changes, while statistical downscaling can efficiently provide sensitivity analysis for many scenarios and data sources to define an envelope of potential local change.